

Unimolecular Electrical Rectifiers

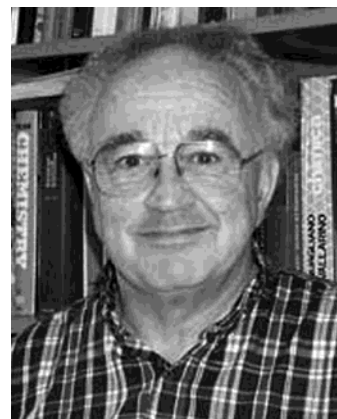
Robert M. Metzger*

Laboratory for Molecular Electronics, Department of Chemistry, Box 870336, The University of Alabama, Tuscaloosa, Alabama 35487-0336

Received September 3, 2002

Contents

1. Introduction	3803
2. Metal Contacts	3806
3. The AR Ansatz	3806
4. Marcus Electron Transfer Theory	3808
5. Three Processes for Rectification by Assemblies of Organic Molecules	3809
6. Current and Resistance across a Metal–Molecule–Metal System	3809
7. STM or AFM Information Storage	3810
8. Assembly: Physisorption versus Chemisorption	3810
9. Macroscopic Organic Rectifiers	3811
10. Langmuir–Blodgett Organic Multilayer Rectifiers	3812
11. Langmuir–Blodgett Monolayer Photodiode	3812
12. STM Studies of Rectifiers	3814
13. The Organic Rectifier Project	3814
14. Electrical Properties of Monolayers and Multilayers	3815
15. Rectification of C ₁₆ H ₃₃ Q-3CNO	3817
16. Molecular Properties of C ₁₆ H ₃₃ Q-3CNO	3818
17. Film Properties of C ₁₆ H ₃₃ Q-3CNO	3818
18. Metal–LB Film–Metal Sandwiches of C ₁₆ H ₃₃ Q-3CNO	3820
19. Unimolecular Rectification by C ₁₆ H ₃₃ Q-3CNO	3820
20. Failed Searches for New Rectifiers	3823
21. Two New Rectifiers	3824
22. Alternate Mechanism for Rectification by C ₁₆ H ₃₃ Q-3CNO	3825
23. “Tour Wires”: Self-Assembled Monolayer “S” Rectifier	3828
24. Tour Wire: Resistance of a Single Molecule Bound to Two Au Electrodes	3828
25. Tour Wires: Negative Differential Resistance	3828
26. Recent Rectifiers Studied Elsewhere	3828
27. Theory	3830
28. Challenges for the Near Future	3831
29. Opinions	3831
30. Conclusion	3831
31. Acknowledgments	3831
32. References	3831



Robert Melville Metzger was born in Yokohama, Japan, of Hungarian parents in 1940, moved to Paris, France, in 1946, to Merano, Italy, in 1948, and then to Los Angeles, CA, in 1959. After obtaining degrees in chemistry from UCLA (1962, research with W. F. Libby) and Caltech (1968, research with H. M. McConnell) and post-docs at Stanford (research with P. G. Simpson and M. Boudart), Metzger taught Italian at Stanford (1970–1971) and chemistry at the University of Mississippi (1971–1986) and the University of Alabama (1986 to present), where he is Professor of Chemistry and former Tricampus Director of the Materials Science Ph.D. Program. Metzger has published 188 papers, edited three books, obtained one patent, graduated 12 Ph.D.'s and 1 M.S., directed the research of 15 undergraduates, and gave talks or spent sabbatical or other leaves in 22 countries. In 1984, he became the first Coulter Professor of Chemistry at the University of Mississippi. In 1998, he received the Blackmon-Moody award of the University of Alabama for exceptional research.

processes measured or controlled on a molecular scale.¹ When results on single molecules were very sparse, molecular electronics, defined more widely (*sensu lato*), encompassed electronic processes by molecular assemblies of any scale, including crystals and conducting polymers.¹

This review concentrates on the former, narrower definition of the term; it focuses on processes that involve one molecule, or very few molecules. Molecular electronics, thusly defined, implies “reaching out and touching” individual molecules with electrodes or other probes, and exploiting their structure to control the flow of electrical signals from them and to them. Given the small size of molecules (about 0.5–3 nm), one may think of “unimolecular” electronics as the *reductio ad absurdum* of standard “inorganic” electronics.

In contrast, the electronic properties of single molecules have been studied by spectroscopy for almost a century, since photons can blithely interrogate molecules in the gas phase, in the solid state, or in solution without the need of electrical leads. This is the advantage of spectroscopy. The disadvan-

1. Introduction

“Molecular electronics” can be defined narrowly (*sensu stricto*) as the study of electrical and electronic

* Tel.: (205) 348-5952. Fax: (205) 348-9104. E-mail: rmetzger@bama.ua.edu.

tage of spectroscopic methods is that electrical circuits using photons as control elements cannot easily be reduced to nanometer-scale dimensions.

Unimolecular electronics, as described here, was first discussed in the United States Defense Department as a potentially promising area of research in the late 1950s; it was presaged by Richard P. Feynman's visionary comments ("there is plenty of room at the bottom"). Feynman's comments, which did not explicitly mention molecules, first given in a talk in 1959, were published in 1961.² Unimolecular electronics was launched in more seriousness in 1974, when Ari Aviram and Mark A. Ratner³ proposed electrical rectification, or diode behavior, by a single molecule with suitable electronic asymmetry.

The success in detecting unimolecular rectification will be the main subject of the present article, which will also review parallel developments in related areas and suggest how one might obtain power gain in unimolecular devices.

"Molecular electronics" was popularized by several conferences chaired by the late Forrest L. Carter in 1981, 1982, and 1985,^{4–6} which gathered not only some seminal ideas and results but also some other far-reaching, but less concrete ideas. As a reaction to exaggerated media propaganda about the latter ("biochips"), the area languished for several years, a victim of little interest, scarce funding, much scorn, and a trickle of results.

For several decades, researchers in intramolecular electron transfer and in artificial photosynthetic systems have been studying electron transfer within a large molecule. In the 1950s and 1960s, Henry Taube proved, by kinetic studies of redox reactions between metal ions bridged by ligands, that electron transfer across an organic bridge between two dissimilar metal ions occurs more slowly across aliphatic bridges than across conjugated aromatic bridges.⁷ This launched extensive studies of intramolecular electron transfer in molecules in solution, by fluorescence and time-decay spectroscopy.^{8,9} Intramolecular electron transfer (adiabatic or non-adiabatic, by direct exchange or by super-exchange) has been put under the theoretical "microscope", because of the pioneering work by Rudolph A. Marcus, Noel S. Hush, and others.¹⁰ There have been similar recent thrusts into "supramolecular chemistry",¹¹ and into "nanotechnology",¹² which may impact unimolecular electronics.

Given the ubiquity of inexpensive near-IR gallium arsenide lasers, and the need for greater information storage density, achievable, for instance, by halving the working wavelength, there had been a long search for "cheap" frequency-doubling devices (acentric organic crystals or poled polymers) as an alternative to expensive acentric inorganic crystals, such as lithium niobate.¹³ These frequency-doubling systems use the second-order nonlinear optical susceptibility of certain molecules, which arises from a large change in the static electric dipole moment between the ground state and the optically excited state. Much of the *elan* of this area was diminished by the appearance of gallium nitride as a powerful (but not yet inexpensive) blue or green laser.^{14,15} The need for

large changes in dipole moment between the ground state and the first optical excited state is shared, as we will show below, between nonlinear optics and good unimolecular rectifiers.

Since 1996, unimolecular electronics was rekindled by many direct measurements of the electronic behavior of single molecules, of Langmuir–Blodgett (LB) monolayers of molecules,^{16,17} or of "self-assembled monolayers" (typically, thiols on gold).¹⁸ Finally, we can "touch" molecules and measure their individual electrical behavior! We can touch a single molecule by a scanning tunneling microscopy (STM) tip, by a conducting-tip atomic force microscopy (AFM) tip, or between two Au tips, or touch a monolayer by making electrical contacts to sandwiches of organic monolayers placed between super-thin inorganic metal pads (with areas from $1 \mu\text{m}^2$ to 1cm^2). We can measure the current vs voltage ($I-V$) characteristics either of a single molecule, or of a monolayer of molecules, or many layers, either locally, by scanning tunneling spectroscopy (STS) or, as a macroscopic average, over a pad. The technical challenge is that the "metal | organic | metal" sandwiches must be made without "frying" the organic layer.

The reason that unimolecular electronics is receiving greater attention is the hope that molecules could become an alternate vehicle for technologically useful active electronic devices. These days, there are concerns about how much smaller silicon-based integrated circuits can be shrunk, to make components closer, and the speed of computing faster. There has been an empirical correlation, or plot, that since the mid 1960s the computing power has doubled, at first every two years and by now every 18 months or so (Gordon E. Moore's "law").¹⁹ This occurs as the "design rules" for integrated circuits (i.e., the smallest distance between adjacent components) get smaller and smaller.²⁰ However, this shrinkage cannot go on forever. There is a widely held opinion that, below design rules of 50 nm, huge technical hurdles may face silicon-based electronics, while molecules, with sizes 0.5–3 nm, can presumably do similar tasks with great facility. It has been said, for instance, that the insulating gates needed in field-effect transistors (FETs) must be made of materials quite different than silicon dioxide. One should always remember Yogi Berra's remark that "it is difficult to predict things, especially about the future". In other words, technology and science often register dramatic advances in areas, or in techniques, not predicted by prophets or scientific panels of "experts". The diligence of scientists and engineers advancing the field of silicon-based electronics may provide unexpected technical break-throughs that may be a "moving target" for the researchers trying to bring molecular electronics to maturity and usefulness. But it is fun to try to be both successful and useful.

Here is a brief and subjective list of recent advances in unimolecular electronics.

(1) STS showed that the currents across alkane-thiols and aromatic thiols bonded to a Au(111) surface are larger when the molecules are aromatic chains than if they are aliphatic.²¹ This result was

not surprising,⁷ but it has now been obtained by direct measurement.²¹

(2) By an innovative “break junction” technique, a thin gold film, deposited above a thinned-out silicon wafer, was broken reproducibly by restraining the silicon wafer between two static wedges and moving a piston by a piezoelectric scanner toward a thinned-out central area of the wafer. When the silicon cracked, so did the gold, and a very narrow gap between the gold shards could be controlled by the scanner to within 1 Å or less. When a benzene solution of 1,4-benzenedithiol was poured on this break junction, some bithiols bonded to one shard, and some to both shards; the latter provided a one-molecule conductive path. The resistance of 1,4-benzenedithiol between Au electrodes was measured as several megaohms,²² which is much larger than Landauer’s quantum of resistance ($h/2e^2$) = 12.91 kΩ,²³ possibly because of mismatch between the Fermi level of Au and the relevant molecular orbital of the molecule. This result has been duplicated recently.²⁴

(3) Molecules of 2'-amino-4-ethynylphenyl-4'-ethynylphenyl-5'-nitrobenzene-1-thiolate, attached to Au on one side and topped by a Ti electrode on the other, exhibit negative differential resistance (NDR);²⁵ this was also followed by STM.²⁶ The same molecules, attached covalently to a gold electrode, but with a second gold electrode on top, exhibit low- and high-conductivity states, with an exponential decay of the high-conductivity state (half-life of 800 s at 260 K). This molecule would be used as a molecular random-access memory cell.²⁷

(4) The Landauer quantum of resistance, 12.91 kΩ,²³ has been measured at room temperature between a multiple-walled carbon nanotube, glued to a conducting atomic force microscope (AFM) tip, and a pool of liquid Hg.²⁸

(5) FET behavior was observed by STM for a single-walled carbon nanotube curled over parallel Au lines, with the STM acting as a gate electrode; the power gain was only 0.33.²⁹ More recently, single-electron transistor effects were seen in metallic single-walled carbon nanotubes (SWCNTs), with kinks introduced into them by an AFM tip.³⁰ A single-walled semiconducting carbon nanotube (SWCNT), made to bridge a K-doped region (thus getting an n-type FET) and also an undoped region (forming a p-type FET), forms an intramolecular voltage inverter, with an output/input voltage gain of 1.6.³¹ The gain has been improved to 12.³² FET behavior in LB multilayers of conducting polymers had been seen a decade ago,³³ as has FET behavior in thin-film organic semiconductors, such as sexithiophene.^{34,35} It was claimed that a monolayer of bithiols, attached to an Au electrode (source), touching on one side an oxide-covered n-type Si gate region, and topped by another Au electrode (drain), also exhibited FET behavior;³⁶ this result proved to be fraudulent. A problem with using SWCNTs is that their assembly is still limited to Louis Pasteur’s impractical method of “picking” the one SWCNT that has, by luck, landed across the “correct” Au electrodes. What is needed is a SWCNT with chemically different terminations (A, B) at the

two ends (call it A-SWCNT-B), so that A-SWCNT-B can be separated chemically by exploiting its dipole and bonded selectively to electrodes as needed.

(6) An LB monolayer of a bistable [2]catenane closed-loop molecule, with a naphthalene group as one “station” and tetrathiafulvalene as the second “station”, and a tetracationic catenane hexafluorophosphate salt traveling on the catenane, like a “train” on a closed track, was deposited on poly-silicon as one electrode, and topped by a 5-nm Ti layer and a 100-nm Al electrode. The current–voltage plot is asymmetric as a function of bias (which moves the train on the track), and a succession of read–write cycles shows that the resistance changes stepwise as the train(s) move from the lower-conductivity station(s) to the higher-conductivity station(s).³⁷ The speed of a circuit derived from this result will be slow, since it depends on molecular translation.

(7) The organometallic equivalent of a single-electron transistor (SET) has been realized at 0.1 K with a Co(II) bis(tripyridyl); this structure has no power gain, but can be ascribed to the redox behavior (Co(II) ↔ Co(III)).³⁸ This has been labeled a “single-atom transistor” (SAT), but it is in reality an addressable Coulomb blockade device.³⁸

(8) Unimolecular rectification across an LB monolayer of hexadecylquinolinium tricyanoquinodimethanide was detected between Mg and Pt electrodes,^{39,40} and later thoroughly confirmed between Al electrodes^{41–43} and, most recently, even between oxide-free Au electrodes,^{44,45} to be a variant of the Aviram–Ratner (AR)³ mechanism. The AR proposal suggested a D–σ–A molecule connecting an electron donor moiety (D) to an electron acceptor moiety (A) through an insulating saturated sigma bridge σ; the mechanism of action involves inelastic tunneling through the molecule from its first electronic excited state D⁺–σ–A[−] to the less polar ground state D⁰–σ–A⁰.³ The first confirmed rectifier^{39–41,43–45} was a ground-state zwitterion D⁺–π–A[−], connected by a twisted pi bridge, rather than a sigma bridge, and used inelastic tunneling from the lower-polarity excited state D⁰–π–A⁰ to the higher-polarity ground state.⁴⁶ Most recently, two new LB monolayer rectifiers have been found, when sandwiched between gold electrodes.^{47,48} The first is a pyridinium salt, in which the rectification seems to be due to back charge transfer from the anion to the pyridinium ion.⁴⁷ The second is dimethylaminophenylazafullerene, which has a tremendous apparent rectification ratio (as high as 20 000).⁴⁸ Here, however, the bulk of the forward current seems to be due to the formation of stalagmites of gold, which do not pierce the monolayer totally but, once formed, behave ohmically;⁴⁸ the molecule itself rectifies, but not dramatically.⁴⁸

The progress toward organic rectifiers, since experimental study started in 1983, has been chronicled before.^{1,49–77} The first many years were dedicated to the study of D–σ–A systems and were plagued by a lack of good experimental techniques to measure rectification for a monolayer.^{49–66} The past few years have seen good rectification results from a ground-state D⁺–π–A[−] zwitterion system.^{67–77} The present review updates what was known and reviewed three

Table 1. Solution Cyclic Voltammetric Half-Wave Potentials $E_{1/2}$ (V vs SCE) and Gas-Phase Ionization Potentials I_D (eV) and Electron Affinities A_A (eV) for Donors D and Acceptors A^a

molecule	solvent/ reference ^b	solution-state data				ref	gas-phase data		ref
		oxidation		reduction			oxidation	reduction	
		(1) D→D ⁺ $E_{1/2}^{(1)}/V$	(2) D ⁺ →D ²⁺ $E_{1/2}^{(2)}/V$	(1) A→A ⁻ $E_{1/2}^{(1)}/V$	(2) A ⁻ →A ²⁻ $E_{1/2}^{(2)}/V$		D→D ⁺ I_D/eV	A→A ⁻ A_A/eV	
Donors D:									
TMPD (2)	a	0.10	0.66			82	6.25		111
TTF (3)	a	0.35	0.75			112	6.83		113
BEDT-TTF (4)	a	0.54	0.96			112	6.21		114
pyrene (9)	a	1.16				115	7.41	0.58	116
anthracene	a	1.09				115	7.55	0.60	117
benzene	a	2.30				115	9.38	-1.0	118, 119
Acceptors A:									
TCNQ (7)	a			0.127	-0.291	120		3.3	110
TCNaQ (10)	b			0.060	-0.425	121			
TCNE (11)	a			0.152	-0.568	120		2.3-2.9	122, 123
TCNQF ₄ (12)	b			0.53	0.02	124		3.72	125
DCNNaQI (13)	c			0.19	-0.35	126		~3.3	127
trinitrofluorenone (14)	a			-0.42	-0.67	128		2.2	129
<i>p</i> -benzoquinone (5)	a			-0.481	-1.030	130		1.95	117, 131
chloranil (15a)	a			0.01	-0.71	132		2.76	117
bromanil (15b)	a			0.00	-0.72	132			
fluoranil (15c)	a			-0.04	-0.82	132		2.92	117
DDQ (15d)	a			0.51	-0.30	130		3.13	129
anthraquinone (16)	a	1.21		-0.98	-1.50	133		1.59	131
C ₆₀ (6)	c			-0.18	-0.58, -1.07	134		2.6-2.8	135

^a $E_{1/2} = E_{ox,p} - 0.03$ or $E_{1/2} = E_{red,p} + 0.03$. The data for TCNQ¹⁰⁹ have been reinterpreted, shifting A_A from 2.8 eV¹⁰⁹ to 3.3 eV;¹¹⁰ this affects A_A for TCNQF₄ and DCNQL. Some of the I_D and A_A values are also shown in Figure 2. ^b (a) Solvent, CH₃CN; reference electrode, SCE. (b) Solvent, BuCN; reference electrode, SCE. (c) Solvent, CH₂Cl₂; reference electrode, Ag | AgCl; offset = 0.15 V.⁸⁹

years ago,⁷⁰⁻⁷³ with the new technique of “cold-gold” evaporation,^{44,45} the addition of two new rectifiers,^{47,48} and a thorough review of progress achieved elsewhere. The contributions from our laboratories have involved almost a score years.⁷⁸⁻¹⁰⁵ The rectification work by the Stuttgart group has been reviewed.^{106,107}

This review will first discuss why at present we still need metallic contacts. Then it focuses on the AR proposal, and on recent theoretical discussions of electron transport through monolayers. Next, it presents the assembly techniques needed to study the molecules of interest. Then it briefly reviews Marcus theory, presents three mechanisms that can cause rectification, and discusses what is known about electron transport through organic films. The attention then shifts to the main experimental results of asymmetric current-voltage plots for the three recently confirmed unimolecular rectifiers. Next, it reviews other work on photodiodes, rectifiers, and negative differential resistance devices, and recent theoretical efforts to explain these phenomena. Finally, it makes some guesses for future progress.

2. Metal Contacts

Many dreams of an all-organic computer may have been formulated, but at present the synthetic complexity of such a venture (making organic electronic components and also making organic or polymeric interconnects) may deter even the most optimistic visionaries. At the present time, only two-terminal devices, such as resistors, insulators, or rectifiers, have been studied; all these are interrogated by inorganic metal contacts (Au, Ti, Al, Mg, etc.).

Three-terminal molecular devices do not yet exist at present (excluding the recent fraudulent result³⁶ or the SAT³⁸). One can, of course, do some logic with two-terminal diodes, but the present semiconductor industry mostly uses three-terminal FET logic, with design rules down to 100 nm or so. This competition from industry suggests that somebody must first master how to bring three-terminal metal filaments within 1 nm of each other, without short circuits, then synthesize molecules with three terminations to bridge and connect across these gaps. The goal of bringing such electrodes together has interested several laboratories.^{38,108} When that goal is reached, and power gain is demonstrated through such three-terminal molecules, then all the necessary molecular electronic devices needed for unimolecular electronic circuits are present, and one can construct an all-organic computer by jettisoning the metal contacts and synthesizing all-organic backbones (using, for instance, conducting oligomers and polymers or single-walled carbon nanotubes (another nontrivial goal!)). It seems premature to worry about the organic backbones when the zoo of available molecular devices does not yet include molecules with gain.

Another design criterion is that we try to do with molecules what cannot easily be done with inorganic compounds. Otherwise, a me-too competition with proven commercial devices will always favor the existing device.

3. The AR Ansatz

The first concrete suggestion for unimolecular electronics was the 1974 AR proposal³ that a one-

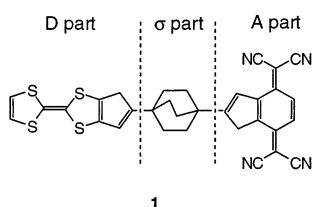
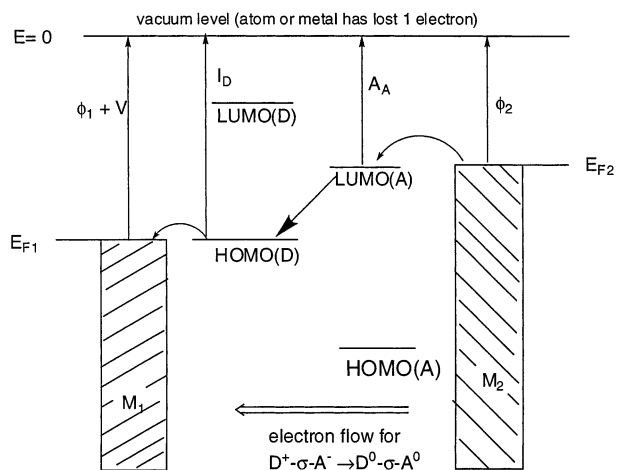


Figure 1. The AR Ansatz,³ showing a proposed D- σ -A molecule (or “Gedankenmolekül”) **1** (which was never synthesized) and the through-molecule electron flow from the excited zwitterion state $D^+-\sigma-A^-$ to the undissociated ground-state $D^0-\sigma-A^0$ when the molecule is placed between two metal electrodes M_1 and M_2 . Here, $E=0$ is the vacuum level, ϕ is the work function of the metal electrodes, V is the potential applied on the left electrode (the right electrode is grounded), I_D is the ionization potential of the donor moiety D, A_A is the electron affinity of the acceptor moiety A, E_{F1} and E_{F2} are the Fermi levels of the metal electrodes, and the HOMO and LUMO levels are the highest occupied molecular orbitals or lowest unoccupied molecular orbitals of the D and A moieties.

molecule rectifier could be achieved with a D- σ -A molecule, where D is a good one-electron donor with relatively low first ionization potential I_D , σ is some saturated covalent sigma bridge, and A is a good one-electron acceptor with relatively high electron affinity E_A , when this molecule is placed between two appropriate metal contacts M_1 and M_2 . The purpose of σ is to decouple the molecular orbitals of the donor moiety D from the molecular orbitals of the acceptor moiety A. Of course, this language is approximate: the molecular orbitals belong to the whole molecule, but they often are more localized on one moiety than the other.³ If the decoupling between D and A is complete, then intramolecular electron transfer becomes impossible. The molecular ground state of D- σ -A has a relatively lower dipole moment, and can be written as $D^0-\sigma-A^0$, while the first excited state is much more polar, has a higher dipole moment, and can be written as the zwitterionic or betaine state $D^+-\sigma-A^-$.³ Given what is known about organic molecules (see Table 1), it is likely that resonant transfer would be possible (Figures 1 and 2) when the Fermi energy E_F of M_2 is resonant with the LUMO of the A moiety or part (which is close to the negative of the electron affinity A_A of the A moiety), and the HOMO of the D moiety (which is

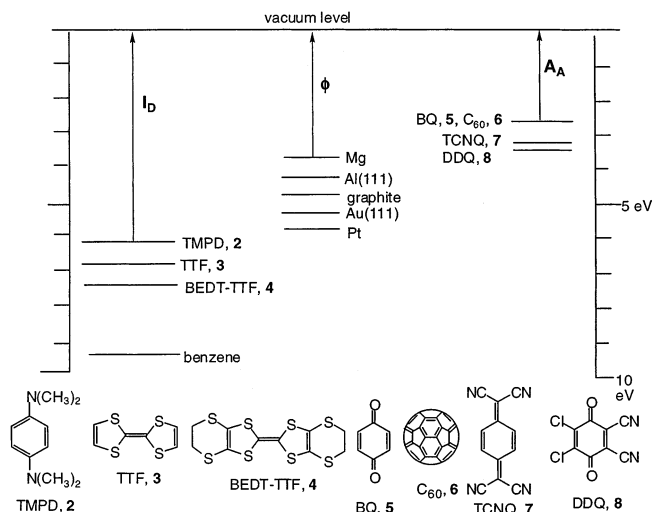


Figure 2. Energy levels: HOMOs of some donors (**2–4**; left), work functions ϕ of some metals (middle), and LUMOs of some acceptors (**5–8**, right).

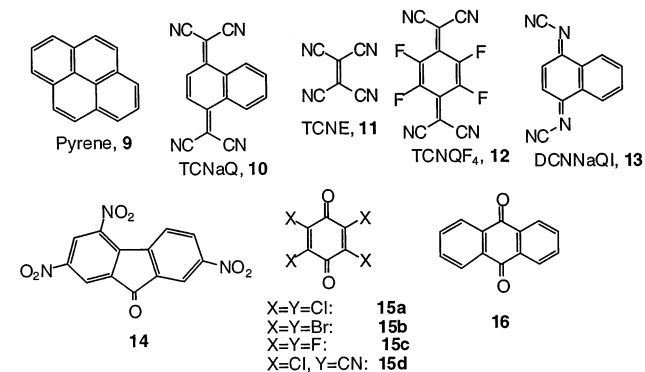
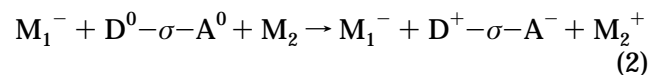
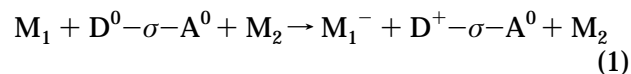
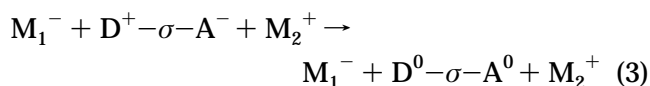


Figure 3. Structures of one more donor (**9**) and of several acceptors (**10–16**).

close to the negative of the ionization potential I_D of the D moiety) is in resonance with E_F of the metal M_1 (upon the application of a positive bias V onto M_1). The intramolecular electron transfer would be an inelastic tunneling from the excited electronic state $D^+-\sigma-A^-$ to the ground electronic state $D^0-\sigma-A^0$. The mechanism would consist of two resonant electron transfers across metal-organic interfaces,



followed by (or simultaneous with) an inelastic downhill intramolecular electron transfer,

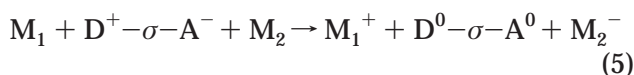


which achieves, overall, the migration of one electron from M_2 to M_1 .³

In the original formulation, a second, potentially competing process was considered and labeled as “autoionization”. If the molecule is first excited to its zwitterionic state,

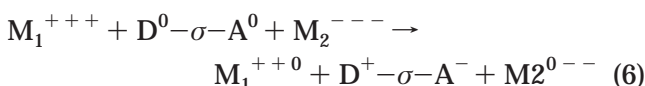


and the electron transfers occur across the molecule–electrode interfaces in a second step,

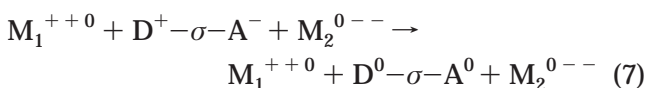


then, overall, the electron would be transferred in the opposite direction, from M_1 to M_2 . It was presumed³ that process (1), (2) \rightarrow (3) would be more likely than process (4) \rightarrow (5).

In light of what follows below, we should also consider whether molecular excitation can be induced (“pushed”) by an applied electric field. Assume that electrode M_1 is positively charged (call it M_1^{+++}) and M_2 is negatively charged (M_2^{---}), and that a resultant electric-field-induced excitation of the molecule to its zwitterionic excited state occurs by electron transfers across the two metal–molecule interfaces,

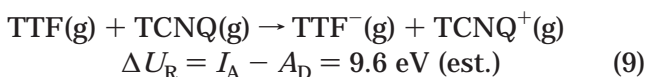
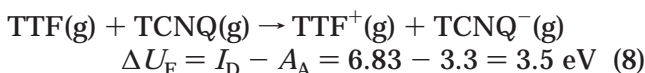


which is followed by de-excitation of the molecule by intervalence transfer (IVT):



This process, overall, moves an electron from M_2 to M_1 , as does the mechanism (1), (2) \rightarrow (3).

A minor semantic point: One should be careful about labeling D (electron-rich in its ground state) as “n-type” and A (electron-deficient in its ground state) as “p-type”, in analogy to inorganic semiconductors. Indeed, the electron flow within the AR molecule (to achieve overall electron transfer from M_2 to M_1) goes from A^- to D^+ , while in inorganic semiconductors the electron moves across the pn junction from the n-type region to the p-type region; however, the electron transfer is from the metal electrode closest to A to the electrode touching D. AR suggested for $D-\sigma-A$ to use D = tetrathiafulvalene (TTF, **3**) and A = tetracyanoquinodimethane (TCNQ, **7**) because these were respectively a good organic donor D and one of the best organic acceptors A, as evidenced by the following data (for the ions at infinite separation):



The AR proposal involves an electronic transition, which is inherently fast (picoseconds to nanoseconds) compared with translations,³⁷ conformational transitions, or molecular rearrangements (seconds to microseconds).

4. Marcus Electron Transfer Theory

Given that the speed of a unimolecular electronic device depends on the speed of charge separation

within the molecule, it is useful to review the electron transfer theory developed by Rudolph A. Marcus, because it can be used to study how fast an electron can move across a molecule, particularly a molecule of the donor–bridge–acceptor type. This speed is crucial if nanoscopic materials are chosen to compete with devices based on Si. We think that, if one makes nanometer-scale unimolecular devices, these should be as fast as practical (picoseconds to nanoseconds).

According to Marcus electron transfer theory,^{136–138} the rate k_{ET} of non-adiabatic electron transfer ($DA \rightarrow D^+A^-$) in weakly coupled DA pairs can be expressed by Enrico Fermi’s “Golden Rule” as

$$k_{\text{ET}} = 4\pi^2 h^{-1} |T_{\text{DA}}|^2 F_{\text{DA}} \quad (10)$$

where h is Planck’s constant, $|T_{\text{DA}}|^2$ is the electronic coupling between the electron donor moiety D and the electron acceptor moiety A, and F_{DA} is the Franck–Condon factor, representing the reorganization of bond lengths and bond angles required for the donor moiety D to lose its electron (and become a cation D^+ in its own equilibrium geometry) and for the acceptor moiety A to gain the electron (and become an anion A^- in its own equilibrium geometry). The dependence of this electronic coupling on increasing distance, R , between donor D and acceptor A is often approximated by a tunneling formula:¹⁰

$$T_{\text{DA}} = a \exp(-\beta R) \quad (11)$$

where β depends on the medium between the donor D and the acceptor A. For instance, β is larger when tunneling occurs through a vacuum ($\beta \approx 2.8 \text{ \AA}^{-1}$: “through-space tunneling”¹⁰) than in a structure where D and A are covalently bridged ($\beta \approx 0.27\text{--}0.70 \text{ \AA}^{-1}$: “through-bond tunneling”¹⁰).^{139,140} If, however, the electron transfer occurs by McConnell’s superexchange mechanism,¹⁴¹ i.e., by hopping, then the distance dependence becomes much weaker, β is smaller, and the electron can hop over much larger distances, with less attenuation. The Franck–Condon factor F_{DA} reflects the overlap between the nuclear wave functions of reactant (DA) and product (D^+A^-). From classical considerations, Marcus derived the expression

$$F_{\text{DA}} = (4\pi\lambda kT)^{-1/2} \exp[-(\Delta G^\circ + \lambda)^2/4\lambda kT] \quad (12)$$

where ΔG° is the standard free energy of reaction and λ is the reorganization energy. Here $\Delta G^\circ < 0$ for exergonic reactions. As illustrated in Figure 4, both the reactant DA and the product D^+A^- are modeled as similar harmonic oscillator potentials, with an identical dependence on the “reaction coordinate”, here taken as a distortion of the “relevant” chemical bond by a Hooke’s law harmonic potential. According to this classical analysis, electron transfer occurs only at the intersection of the two potentials (from the one for DA to the one for D^+A^-), which may be reached by thermal fluctuations of the nuclear coordinates. The horizontal displacement of the potential minima (“reaction coordinate x' ”) reflects the adjustment of the equilibrium nuclear coordinates from the electronic configuration of the reagent (DA) to the

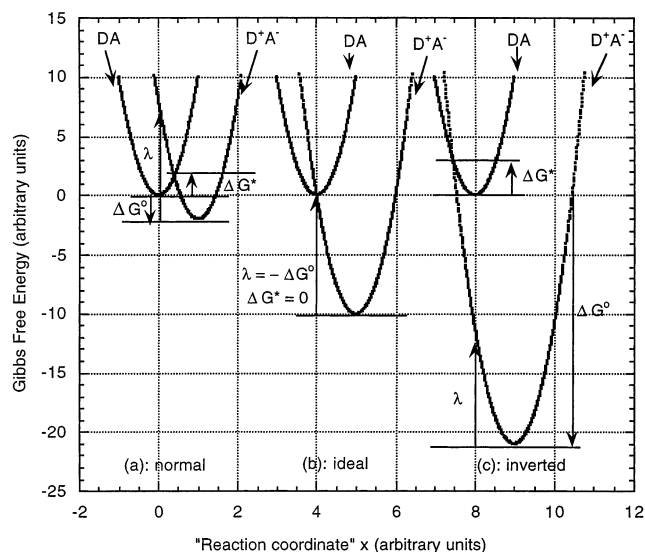


Figure 4. Simplified representation of three cases for Marcus electron transfer theory. The relevant Gibbs free energy surfaces are simply represented as parabolas centered around the equilibrium coordinate(s) of the reagent (DA), and as displaced parabolas of the same slope for the product (D^+A^-) after a one-electron electron transfer. In all three cases, the Gibbs free energy of reaction, ΔG° , is negative. The cases are (a) the “normal case”, where the free energy of activation ΔG^* is positive and the reorganization free energy λ is larger in absolute value than ΔG° ($\lambda > -\Delta G^\circ$); (b) the “ideal case”, where the free energy of activation is zero ($\Delta G^* = 0$) and the reorganization free energy λ is equal and opposite to the free energy of reaction ΔG° ($\lambda = -\Delta G^\circ$); and (c) the “inverted case”, where the reorganization free energy λ is smaller in absolute value than the free energy of reaction ($\lambda < -\Delta G^\circ$). In cases (a) and (c), one can obtain that $\Delta G^* = (\lambda + \Delta G^\circ)^2/4\lambda$.

electronic configuration of the product (D^+A^-). The reorganization energy λ is the energy, measured from the energy minimum of the product, required for the reagent to reach the product curve vertically, i.e., utilizing the equilibrium nuclear coordinates of the reagent. According to eq 12, the Franck–Condon factor F_{DA} (and hence the electron-transfer rate) increases with increasing driving force ($-\Delta G^\circ$) of the reaction (“normal case”, Figure 4a) up to a maximum when $-\Delta G^\circ = \lambda$ (“optimal case”, Figure 4b), but decreases when $-\Delta G^\circ$ exceeds λ (“inverted case”, Figure 4c). The experimental proof of this inverted region was obtained by Gerhard Closs, John R. Miller, and co-worker.¹⁴²

Experimental results from both the primary charge-transfer step in photosystem II, and also in model donor–bridge–acceptor systems, show that reaction rates are in the picoseconds to nanoseconds regime. Such numbers suggest that making unimolecular electronic components will not necessarily make them slow, *as long as electronic transitions are used*. For a chosen molecule A, Marcus theory suggests that one can empirically maximize the speed of electron transfer through a D–bridge–A molecule by varying the electron donor D appropriately.¹⁴² The reaction rate would increase indefinitely as the difference between Gibbs free energies of donor and acceptor increases, but must slow for the larger energy differences, because the Franck–Condon factors start to become much smaller than unity. One solution is

to use powerful, yet very rigid, electron donors and electron acceptors, so that the distortion in creating anions and cations of these molecules is minimized. For instance, buckminsterfullerene (C_{60} , **6**) is only a moderate acceptor (see Table 1^{111–135}), but its cage is quite rigid, so its Franck–Condon factor remains large (close to 1).

5. Three Processes for Rectification by Assemblies of Organic Molecules

There seem to be three distinct processes for asymmetrical conduction, i.e., rectification in “metal | organic | metal” assemblies. The first process is due to Schottky barriers¹⁴³ at the “metal | organic” interfaces. A surface dipole will be formed at this interface, and, if these dipoles are different in size, then the currents at positive bias will be different than those at negative bias.¹⁴³ We shall call molecules that rectify by this process “S” (for Schottky) rectifiers. Two recent works discuss Schottky diodes of this type.^{144,145}

The second process arises if the “chromophore” (i.e., the part of the molecule whose molecular orbital must be accessed during conduction) is placed asymmetrically within a “metal | molecule | metal” sandwich, e.g., because of the presence of a long alkyl “tail”.^{104,146} We shall call molecules that rectify by this process “A” (for “asymmetric”) rectifiers. This second process was recently confirmed experimentally¹⁴⁷ and was alluded to in earlier work.¹⁴⁸

The third process for rectification occurs when the current passing through a molecule, or a monolayer of molecules, involves electron transfers between molecular orbitals, whose significant probability amplitudes are asymmetrically placed within the chromophore. This third process we think of as true “unimolecular rectification”, and we shall call this process “U” (for unimolecular) rectification;¹⁰⁴ these “U” rectifiers are what we endeavor to achieve.

The practical requirements for assembling an ordered array of organic molecules between two inorganic metal electrodes may mean that the resulting monolayer may behave as an “A” or “S” rectifier, as well as a “U” rectifier. This is why true unimolecular rectification (“U” type only) is so rare.¹⁴⁶

6. Current and Resistance across a Metal–Molecule–Metal System

Landauer proved that a metal–tunnel barrier–metal sandwich allows a maximum current I :^{23,149,150}

$$I = (2e/h) \int_{-\infty}^{\infty} [f_L(\epsilon) - f_R(\epsilon)] \times \text{Tr} \{ G^a(\epsilon) \Gamma^R(\epsilon) G^r(\epsilon) \Gamma^L(\epsilon) \} d\epsilon \quad (13)$$

where the tunnel barrier can be a single molecule, e is the charge on one electron, h is Planck’s constant, ϵ is the energy, $f_L(\epsilon)$ and $f_R(\epsilon)$ are the Fermi–Dirac distributions in the left and right electrodes, respectively, $G^a(\epsilon)$ and $G^r(\epsilon)$ are the advanced (and retarded) Green’s function for the molecule, $\Gamma^R(\epsilon)$ and $\Gamma^L(\epsilon)$ are the matrices that describe the coupling between molecule and the metal electrodes, and $\text{Tr} \{ \}$ is the trace operator. From this formula, the quantum of

resistance R_0 and its reciprocal, the quantum of conductance, G_0 , are given by

$$R_0 = 1/G_0 = h/2e^2 = 12.91 \text{ k}\Omega \\ = 1/(7.75 \times 10^{-5} \text{ S}) \quad (14)$$

This is not to say that the resistance of a molecule is 12.91 k Ω , but that the resistance of the molecule plus the two electrodes is 12.91 k Ω .¹⁴⁹ The internal resistance of a molecule has not yet been measured. Recently, it was shown that a degenerate quasi-one-dimensional electron gas in a GaAs | GaAl_{1-x}As_x system, when interrogated in a four-probe geometry, has zero resistance drop between probes 2 and 3, in contrast to the expected 12.91 k Ω between probes 1 and 4, because the transport within the gas is ballistic;¹⁵¹ a similar result may be obtained in the future for a molecule.

The resistance of eq 14 must be divided by a factor N , if N elementary one-dimensional wires, or N molecules, bridge the gap in parallel between the two metal contacts:

$$R_N = h/2e^2 N = (12.91/N) \text{ k}\Omega \quad (15)$$

The electron transport from metal to organic material to metal has received much theoretical attention; we single out some of our recent contributions.^{102,104} First, asymmetries in current–voltage plots (usually ascribed to rectification) also occur if a chromophore is placed asymmetrically within the electrode gap¹⁰⁴ (“A” rectifiers). This has been seen in early STM experiments.¹⁵² Second, an analytic expression for elastic electron transfer between a metal and a single molecular orbital of a molecule is^{45,102,153}

$$I = I_0 \{ \tan^{-1}[\theta(E_0 + p e V)] - \\ \tan^{-1}[\theta(E_0 - (1 - p) e V)] \} \quad (16)$$

Here, E_0 is the energy of the molecular orbital, V is the applied potential, and p is the fractional distance of the molecule from, say, the left electrode (if the molecule is centered in the gap, $p = 1/2$). To obtain the efficiency of the current, the prefactor I_0 can be compared to $Q N_S$, where Q is the quantum of conductance (7.75×10^{-5} S) and N_S is the number of molecules sampled for conductance in parallel. There are many other formulas involving tunneling, which may be applicable depending on the details of the states accessible in the tunneling gap, the exact shape of the potential in the gap, etc.

In general, tunneling across molecules is expected to be approximately exponential to some power of the potential, so a sigmoidal curve is usually seen, symmetrical about $I = 0$ and $V = 0$. The various models have been discussed in some detail.⁴⁵ It is only when the connection across the metal electrodes is macroscopic, i.e., involves a very large number of channels ($N \rightarrow \infty$), or if scattering occurs during the electron transport¹⁵⁴ that Ohm’s law becomes applicable,¹⁵⁵

$$V = IR \quad (17)$$

and the current becomes linear with the applied voltage V .

In assessing rectification, one measures the rectification ratio (RR), defined as the current at a positive bias V divided by the absolute value of the current at the corresponding negative bias $-V$:

$$RR(V) = |I(V)|/I(-V) \quad (18)$$

There is also an interesting quantum limit: let an electron be confined to a small quantum dot (a two-dimensional confined region of capacitance C). When the ratio $e^2/2C$ is less than the thermal energy kT (where k is Boltzmann’s constant and T is the absolute temperature), then a Coulomb blockade ensues:¹⁵⁰ no more charges can be added until a threshold voltage V is exceeded, such that $eV > kT$. The “single-electron transistor” (SET) uses this Coulomb blockade¹⁵⁰ but, as discussed below, can have no power gain.

7. STM or AFM Information Storage

When it is said that for molecular device measurements one must “go out and touch a molecule”, the ideal tool seems to be STM. With STM,¹⁵⁶ one can select an atomically flat but conducting substrate (graphite, Au(111) on mica, MoS₂, silicon, and a few others), deposit the molecule of interest “somehow” on this substrate, and interrogate it with an atomically sharp Pt/Ir or W tip, to a precision of 0.1 nm in x and y , and 0.01 nm in z . Further, a silicon cantilever designed for AFM¹⁵⁷ can be coated with a metal, and thus can be used as a conducting-tip AFM (albeit with usually lower resolution than an STM). In the later 1980s, much hope existed that STM or AFM would prove to be the ultimate high-density information storage medium. However, the movement of the STM or AFM tip, controlled by a piezoelectric scanner, is inherently limited by the speed with which the piezoelectric scanner can move the tip across the medium to a prechosen location; this is the speed of sound. This relatively low speed would not match the speeds needed to make the medium practical, so the idea of STM or AFM on any surface as the ultimate high-density information storage medium was deemed unfeasible.¹⁵⁸ As a last resort, the “Millipede” was developed. This is an array of 1064 (32×32) closely spaced microfabricated AFM cantilevers that, as a multiplexed read-out or recording device, may compensate for the slow motion of a single probe.¹⁵⁹ A useful technique of STM is scanning tunneling spectroscopy (STS), where the scan over the surface is interrupted so that, at any given point, one or many I – V measurements are taken, hopefully with minimum tip drift.

8. Assembly: Physisorption versus Chemisorption

As one designs molecules for unimolecular rectifiers or, some day, for unimolecular transistors, one must decide how the designed molecules will be assembled and measured. One must somehow “go out and touch a molecule”. Control over the position of individual molecules on a surface during a measurement can be difficult. For putting a molecule on a

metal electrode, two choices are available: physisorption and chemisorption.

Physisorption, or physical adsorption, includes the random deposition from a vapor onto a solid substrate, or the transfer of an ordered monolayer (Langmuir film or "Pockels–Langmuir"⁸⁰ monolayer) from the air–water interface to a solid substrate, forming an LB monolayer or, if the transfer is repeated, an LB multilayer. LB physisorption has two advantages: one is that the percent coverage of the surface at the moment of transfer can be measured directly as the film transfer ratio; the other is that surface dipoles, that can form during chemisorption, are avoided. However, physisorption has two inherent limitations: the first is that, after transfer, the structure of the vapor-deposited film, or of the LB monolayer or multilayers, may change over time, as the film tends toward a thermodynamic steady state; the second is that any other adsorbates previously present on the metal electrode (e.g., the adsorbates that descend from air onto gold surfaces within 15 min after exposure to ambient air) are not displaced, but are merely covered by the physisorbed layers.

Chemisorption includes the formation of a covalent bond of thiols and similar compounds to gold and similar metals, or of chlorosilanes to hydroxyl-covered silicon surfaces; these have been labeled as "self-assembled monolayers" (SAMs). Chemisorption involves heats of bond formation (40–120 kJ/mol) and has two advantages. The first is that the chemical reaction displaces from the surface any previously formed physically attached adsorbates or impurities. The second advantage is that the adsorbed species, once bonded, is difficult to remove from the surface. There are three disadvantages to chemisorption: the uncertain degree of coverage, the possibility of further chemical reactions, and the formation of surface dipoles. One can hope that, by exposing a surface long enough (e.g., a few days) to the adsorbate, the heat of reaction will help drive the reaction to produce "full coverage" of a Langmuir, or monolayer, on the solid surface. There are spectroscopic techniques to monitor this deposition, but they are accurate to only maybe ± 0.1 Langmuir. Whereas physical rearrangement of the film is less of a problem, thiolates on gold slowly oxidize to sulfoxides in high-humidity areas. For either thiolates or sulfoxides, the bonding to gold is partially ionic, so one creates a surface dipole of maybe 1 or 2 D. This creates a Schottky barrier. The polarity of silane links on silicon is much less, but there is also less known about how ordered the silanes can be on silicon. A very useful table of which functional groups will adhere to which inorganic substrate by chemisorption has been published.¹⁶⁰

Before the work leading up to unimolecular rectifiers is discussed in detail, the earlier work on "macroscopic" organic rectifiers should be reviewed, along with studies on LB multilayers of insulators "doped" with donors and acceptors, on the first Langmuir–Blodgett monolayer photodiode, and on early uses of STM to detect asymmetries in through-molecule conduction.

9. Macroscopic Organic Rectifiers

Many reports of asymmetric conduction through molecules have been given in the literature over the past 40 years. Junctions of micrometers-thick layers of "n-doped" (electron donor) organic semiconductors with micrometers-thick layers of "p-doped" (electron acceptor) organic semiconductors act as rectifiers.

In a first study, "Pb | organic | Pb" sandwiches were achieved by evaporation,¹⁶¹ where the "organic" component was a two-layer evaporated film of either "indigo | chloranil", "indigo | (1:1)-(p-phenylenediamine:chloranil)", "chloranil:(1:1)-(p-phenylenediamine:chloranil)", or "phenazine | (1:1)-(p-phenylenediamine:chloranil)", both layers being several micrometers thick.¹⁶¹ The first-mentioned layer, accosted to the positive electrode, consisted of either indigo **17** (Figure 5) or phenazine **18**, both one-electron electron donors, while the second layer, accosted to the negative electrode, was either the electron acceptor chloranil, **15a**, or the (1:1) ionic donor–acceptor or charge-transfer complex, between the electron donor p-phenylenediamine, **19**, similar to TMPD, **2**, and the electron acceptor chloranil, **15a**.¹⁶¹

The second study involves a phthalocyanine sandwich "Au | Ni(Pc) (1–5 μm) | Cu(PcF₈) (1–5 μm) | Au", where forward bias sends electrons from the micrometers-thick layer of Ni(Pc), **20**, to the micrometers-thick layer of Cu(PcF₈), **21**.¹⁶² The rectification ratio increases when O₂ is present.¹⁶²

The third, very elegant study involves a macroscopic rectifying junction between a semiconducting anion radical salt of perylene (Per) and a semiconducting cation radical salt of Per.¹⁶³ A quartz substrate was furnished with pre-evaporated Au pads and cooled to 77 K; onto it, using suitable masks that

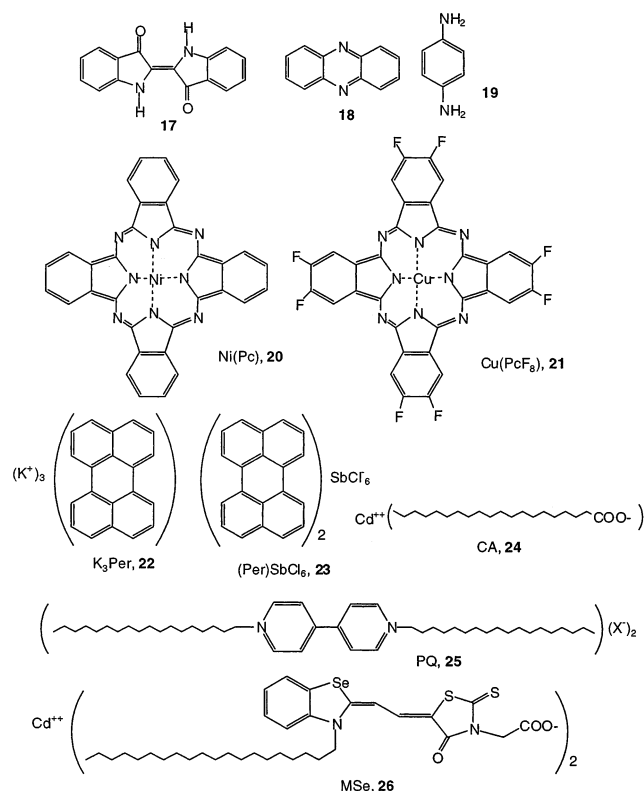


Figure 5. Structures 17–26.

were changed in situ, were evaporated first, potassium metal, second, perylene, and third, SbCl_5 .¹⁶³ By diffusion, the semiconducting anion radical salt K_3Per , **22**, was formed in the lower region, closest to the Au bottom electrode; the semiconducting cation radical salt $(\text{Per})_2\text{SbCl}_6$, **23**, was formed in the upper region.¹⁶³ (One may wonder whether perylene truly is a trianion in K_3Per , **22**, as it is claimed from the stoichiometry for maximum conductivity). Finally, 50-nm-thick Au contacts were evaporated on top.¹⁶³ At forward bias, high currents are seen at a forward bias of only 0.5 V, with rectification ratios of 10^5 and current densities of 300 A m^{-2} ; at reverse bias, Zener-type breakdown is seen at -19.4 V .¹⁶³ The perylene film thickness was not specified, but other data given suggest that it was probably a few hundred nanometers. The forward electron current goes from the electron-rich perylides in the K_3Per region to the electron-poor perylenium radical cations in $(\text{Per})_2\text{SbCl}_6$.¹⁶³

10. Langmuir–Blodgett Organic Multilayer Rectifiers

Hans Kuhn and co-workers studied photoconductivity within Langmuir–Blodgett (LB) multilayers, “doped” with electron donors, then covered by other LB multilayers “doped” with electron acceptors. In that work, a slight rectification effect was noted.¹⁶⁴

Michio Sugi et al. used (i) the electrically insulating LB amphiphile arachidic acid, $\text{C}_{19}\text{H}_{39}\text{COOH}$, which under the conditions of deposition (pH 6.1) is probably cadmium arachidate, CA, $\text{Cd}(\text{C}_{19}\text{H}_{39}\text{COO})_2$, **24**; (ii) a bis(octadecyl)viologen, or paraquat, PQ, **25**, with unspecified gegenion (counterion), and which should act as an electron acceptor; and finally (iii) a cyanine dye, MSe, **26**, which should act as an electron donor; all three molecules have one or two long and hydrophobic alkane “tails”.¹⁶⁵ Presumably because of poor order in the Pockels–Langmuir film at the air–water interface, or poor LB film transfer of pure PQ, **25**, or pure MSe, **26**, onto solid substrates, solid solutions of these compounds with “inert” cadmium arachidate, **24**, were used instead: either 1 part PQ, **25**, to 5 parts CA, **24**, or 1 part MSe, **26**, to 5 parts CA, **24**.¹⁶⁵ The resulting sandwich “Al | $(\text{CA}_5\text{PQ})_3$ | $(\text{CA}_5\text{MSe})_4$ | Ag”, consisting of an LB trilayer of CA_5PQ , which should be a “p-region”, and an LB quadrilayer of CA_5MSe , which should be an “n-region”, had a rectification ratio of about 6 at about 0.5 V.¹⁶⁵ The paraquat or viologen, without its gegenion, presumably orients so the dipyrindyl dication replaces one cadmium ion.

Siegmar Roth and co-workers at the Max Planck Institute for Solid State Research in Stuttgart^{166–168} put LB multilayer films of molecules PcPd, **27** (Figure 6), and PTCDI, **28a**, into a sandwich “Au | 6 LB monolayers of PcPd, **27** | 6 LB monolayers of PTCDI, **28a** | Au”, where the palladium phthalocyanine PcPd, **27**, should be a weak electron donor, and the *N,N*-bis(di(ethoxy)methyl)perylene-3,4,9,10-tetracarboxyldiimide, PTCDI, **28a**, should be a moderate electron acceptor. A “soft evaporation” was used for the top Au electrode;¹⁰⁶ this electrode was formed by evaporation of Au from a boat, but a rotating shutter

with an open sector was interposed between the source and the target LB film surface, so as to allow the heat from the depositing Au atoms to dissipate within the organic film.¹⁰⁶ As shown in energy level diagram **29**, the HOMO of **27** is estimated to be 0.5 eV higher than that of **28a** (i.e., **27** can be oxidized more easily); the LUMO of **27** is 0.4 eV higher than that of **28a**.¹⁶⁶ At 4.2 K, the sandwich had a slight I – V asymmetry: higher currents started at $V < -0.40 \text{ V}$ at negative bias, but only at $V > +0.91 \text{ V}$ at positive bias.^{166,167} When only 10 monolayers of PcPd, **27**, are placed between Au electrodes, then symmetric I – V curves with onsets at $\pm 0.27 \text{ V}$ are seen; when only 20 monolayers of PTCDI, **28a**, are placed between Au electrodes, a symmetric I – V curve with onset at $\pm 0.55 \text{ V}$ is seen. The results are interpreted by using only the two molecular HOMOs.¹⁴⁸ The HOMO energy of PcPd is estimated to be lower than that of the PTCDI derivative,^{148,166,167} and since the PcPd is placed asymmetrically in the “Au | film | Au” sandwich, this causes an asymmetry in I – V curves;¹⁴⁸ the LUMOs were not involved in the proposed mechanism **29**.¹⁴⁸ In other words, this is an “A” multilayer rectifier. There were also plateaus in the I – V curves, ascribable to Coulomb blockade effects, i.e., of quantum dot behavior.^{166,167} This work was repeated with a slightly different PTCDI derivative **28b**, with similar results.¹⁶⁹ In a final experiment, a D– σ –A molecule, $\text{T}_3\text{–V}^{++}$, **30**, was synthesized, where the terthiophene (T_3) is the electron donor and the alkyl viologen (V^{++}) is the electron acceptor; accordingly, the HOMO of the viologen is much lower than the HOMO of the terthiophene.¹⁰⁶ A sandwich “Au | 4 LB monolayers of **28b** | 1 LB monolayer of **30** | 4 LB monolayers of **28b** | Au” was constructed. Here, the monolayer of **30** functions as the rectifier, and at 4 K the first small current increase occurs at $+0.28 \text{ V}$ at positive bias, and at -0.53 V at negative bias; this current then increases dramatically and symmetrically at both $+0.68$ and -0.65 V , presumably because of resonance with the HOMO of PTCDI, **28b**. The proposed mechanism **31** again neglects the LUMOs of **30** or of **28b** as being too high in energy, and also the NHOMO of **30**, localized on the viologen, as being filled and too low in energy; the mechanism involves the HOMO of **30**, localized on the terthiophene (T_3). Once again, this is an “A” monolayer rectifier.¹⁰⁴

11. Langmuir–Blodgett Monolayer Photodiode

In an experiment of great elegance, Masamichi Fujihira and co-workers at the Tokyo Institute of Technology produced the first electrochemical LB photodiode based on an LB monolayer of **32** (which could be described as a donor–sensitizer–acceptor molecule, D–S–A, Figure 7).¹⁷⁰ An LB monolayer of **32** was deposited on an optically semitransparent Au electrode; the cell was filled with a potassium chloride electrolyte solution and fitted with a counter electrode. Under bias, an electron was transferred from the solution to the ferrocene (D) part, from which (scheme **33**) the electron moved downhill to the ground state of the sensitizer, pyrene (S). When light of wavelength 330 nm was shined onto the monolayer, promoting the electron to the first excited state of pyrene, then to the viologen (A), and from there to

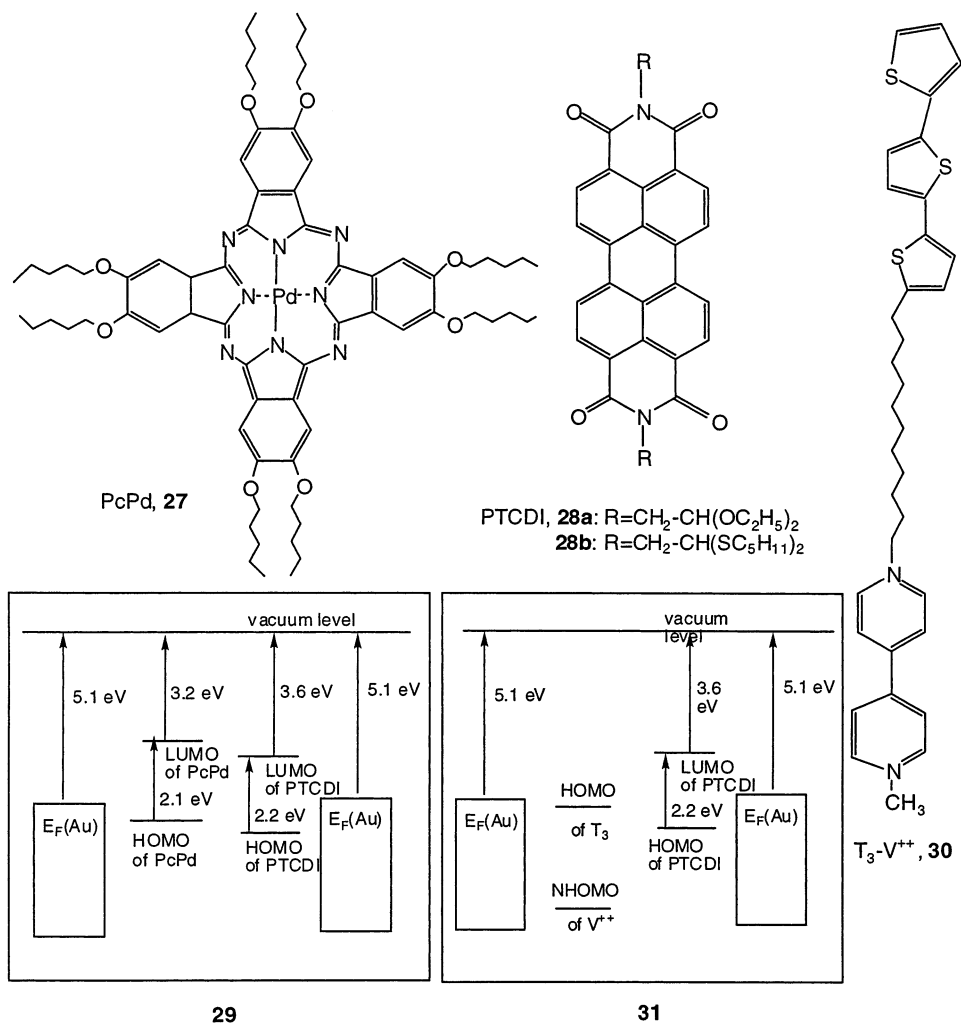


Figure 6. Structures **27**, **28**, and **30**, and energy level diagrams **29** and **31**.

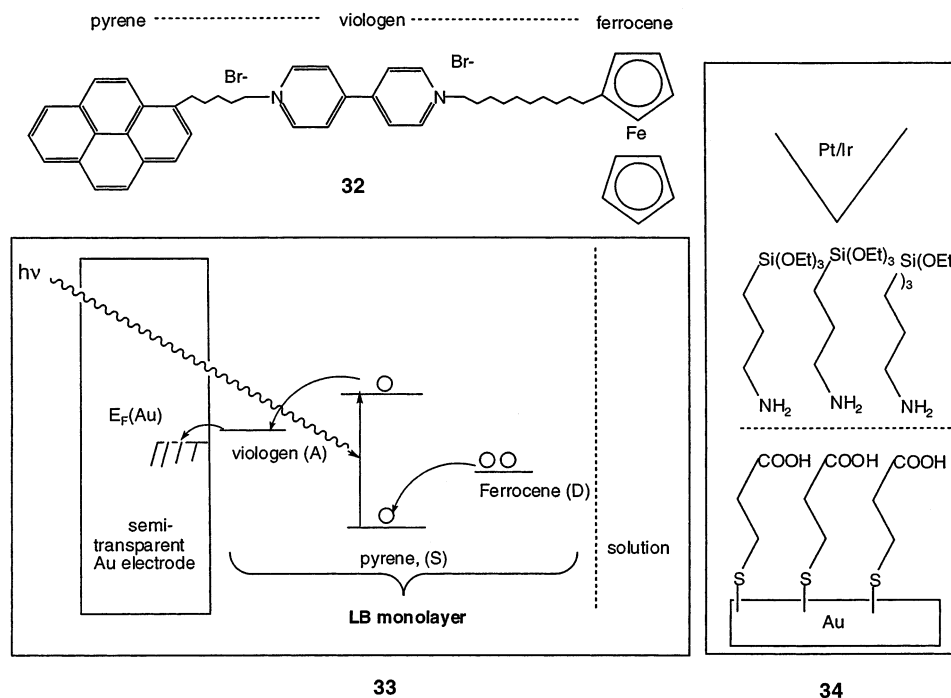


Figure 7. Structure **32**, and schemes **33** and **34**.

the Au electrode, the circuit was completed.¹⁷⁰ When the light was off, no current flowed.¹⁷⁰ The three

separate components (D, S, A) were also studied in mixed films.¹⁷⁰

This work, using three similar, separate components D, S, A, was repeated in Korea. The viologen acceptor was replaced by *N*-docosylquinolinium-TCNQ, gold was replaced by aluminum and indium-tin oxide electrodes, and LB multilayers were used.¹⁷¹ Similar results were obtained subsequently.^{172–177}

Electrochemical rectification at a monolayer-modified electrode has been reported.^{178,179} Electrochemical rectification at suitably modified electrode surfaces has had a long and illustrious history.^{180–188}

12. STM Studies of Rectifiers

Melvin Pomerantz and co-workers at IBM showed that a porphyrin covalently bonded to a carboxylated highly oriented pyrolytic graphite (HOPG) surface, and studied by STM, rectifies.¹⁸⁹ Jürgen Rabe and co-workers at the University of Mainz measured an unsymmetrical STM tunneling current through an alkylated hexabenzocoronene, deposited on graphite, probably because this molecule is asymmetrically placed between the electrodes.¹⁵² An unsymmetrical STS current was also seen in an oligo(phenylethynyl)-benzenethiol.¹⁹⁰ An STS study of the interaction of an amine-terminated monolayer touching a carboxyl-terminated silane (Figure 7, scheme 34) finds rectification at negative bias, which is ascribed to proton migration from the carboxylic end to the adjacent amine.¹⁹¹

13. The Organic Rectifier Project

As mentioned above, the AR proposal, or “Ansatz”, requires that one couple a strong donor D with a strong acceptor A in the same molecule by some covalent bridge, preferably saturated (see Figures 2 and 3 and Table 1). The synthesis requires that a strong oxidizing agent be coupled covalently to a strong reducing agent, not an easy synthetic challenge, but a challenge also met by researchers in artificial photosynthetic systems, e.g., by Devens Gust, Michael Paddon-Row, Noboru Mataga, and others. In addition, the synthetic plan for a rectifier must include appropriate terminations for the molecule, to allow its assembly between metal electrodes for electrical measurements.

The assembly technique chosen by the Organic Rectifier Project at the University of Mississippi (1982–1991) by Charles A. Panetta, Metzger, and collaborators was the LB method. Many molecules were made which did indeed form LB films (structures 35–43 in Figure 8, and Tables 2 and 3).^{49–66,78–91,93,94,192,195,200,208} They were all obtained by using the carbamate coupling reaction as the last synthetic step (it was not possible to convert a weak acceptor into a strong acceptor in the presence of a strong donor after the covalent bridge is already built; rather, the coupling reaction must strongly favor the bridge building over the competing formation of an ionic charge-transfer salt). An ester coupling was also successful.

Figure 9 shows three monofunctionalized donors, 44–46, and a set of monofunctionalized acceptors (47–49) used for the coupling reactions. The monofunctional TCNQ compounds CMTCNQ, 47a, and

CETCNQ, 47b, would not couple with TTF–CH₂–OH.¹⁹² The monofunctional TCNQ alcohol BHTCNQ, 47c,¹⁹³ was found to couple to TTF–NCO (generated from TTF–Li), to yield a TTF–carbamate–BHTCNQ (TTF–C–BHTCNQ), 35,^{49,50,78} and to TTF–COOH, to yield a TTF–ester–BHTCNQ (TTF–E–BHTCNQ).⁵⁰ Both of these products were obtained in low yield, and in two phases, one of which was ionic, the other neutral.⁵⁰ Then the attention turned to carbamates obtained by coupling BHTCNQ, 47c, to phenyl, 1-pyrenyl and *N,N*-dialkylaminophenyl isocyanates^{51–62,79–91} (the latter can be thought of as modifications of TMPD, 6). The synthesis of BHTCNQ, 47c,¹⁹³ contained a very inefficient, low-yield step. A new, monofunctionalized strong acceptor, prepared in somewhat higher yield, was HETCNQ, 47d.⁸³ Two other strong acceptors, HPTCNQ, 47e, and HBTCNQ, 47f, were prepared by similar routes.¹⁹⁴ An easily synthesized acceptor was HMTCAQ, 48, but both HMTCAQ and its underivatized parent molecule¹²¹ are weak two-electron acceptors; the peri hydrogens force them into a butterfly-shaped configuration. A final acceptor was HMTcNaQ, 49. Its crystal structure has been determined;¹⁹⁵ however, it decomposed instead of coupling with phenyl, 4-(dimethylamino)phenyl, or 1-pyrenyl isocyanates.¹⁹⁵

Carbamates and esters were thus obtained with BHTCNQ, 47c, HETCNQ, 47d, HPTCNQ, 47e, HBTCNQ, 47f, and HMTCAQ, 48, as acceptors. The various D– σ –A molecules that form LB films were the carbamates 35–43 mentioned above. Of these, 40–43 were “trial molecules” with the weak ethoxy-nitrophenyl (ENP) acceptor group.

The planned σ bridge length, equal to the number of C, O, or N atoms between D and A ends, was 4 (CMTCNQ, 47a; HMTCAQ, 48), 5 (CETCNQ, 47b), 6 (BHTCNQ, 47c; HETCNQ, 47d), 7 (HPTCNQ, 47e), and 8 (HBTCNQ, 47f). Since the carbonyl group provides partial conjugation within the bridge up to 2 atoms from the donor, one can surmise that, at least for the strong acceptor TCNQ, a 4–5-atom bridge length is too short for a coupling reaction to occur. Naturally, if the bridge is too long (say, >8 atoms) and flexible, then there is a danger that conformational freedom will allow the D and A ends to move to within intramolecular overlap, thereby creating a horseshoe-shaped molecule with internal charge transfer, which may not function as a rectifier. In addition, it is important that an IVT band be present. This will ensure that the electronic coupling T_{DA} between the ground state and the first excited state (eq 10) will be reasonably large; if the bridge is too long, then T_{DA} will become too small.

Of the molecules that formed Pockels–Langmuir monolayers at the air–water interface and LB films on a solid substrate, only 35 included the strong donor TTF and the strong acceptor TCNQ. There were two products for 35, one seemingly zwitterionic in the ground state, the other neutral, but both were difficult to purify.⁵⁰ Most molecules in Figure 8 were based on the strong monofunctionalized one-electron acceptors BHTCNQ, 47c, and HETCNQ, 47c, whose syntheses never gave very high yields. Two molecules

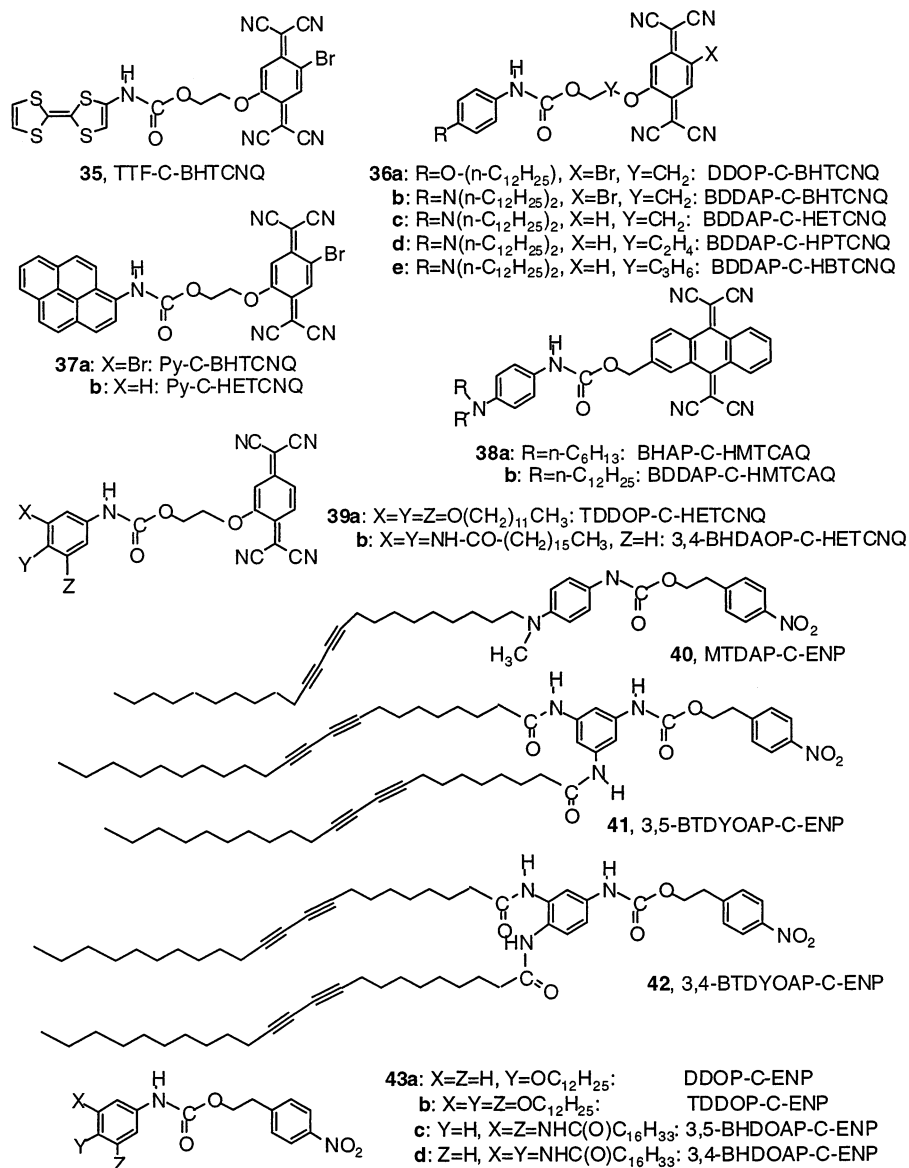


Figure 8. D- σ -A molecules **35**–**43** synthesized at the University of Mississippi (1982–1991).

(**38a** and **38b**) included the weak two-electron acceptor HMTCAQ. Several (**40**–**43**) used the weak acceptor ENP (ethylene-*p*-nitrophenol); they include a polymerizable diacetylene chain to aid in the rigidity of the eventual LB monolayer (an idea of the late Sukant K. Tripathy). All but two included a long “greasy tail” to aid in LB assembly. Two molecules (**37a** and **37b**) formed films with no alkyl chain (but it was not clear whether they were head-to-head assemblies or head-to-tail assemblies). The methods of testing for rectification used by the Metzger group in the period 1983–1990 were too crude,^{60,79} and no rectification was found.

Electrical rectification, measured by STS, was reported by Melvin Pomerantz at IBM in a molecule designed as an intramolecular H atom switch,¹⁹⁶ but the claim of rectification was withdrawn;¹⁹⁷ a similar claim of rectification by BDDAP-C-BHTCNQ, **36b**, measured with the same STM instrument,^{55,56} was also withdrawn; the “rectification” had been an instrumental artifact.^{55,56}

This does not say that all molecules in Figure 8 were “failures”. Now that better techniques have

become available,^{41,44,45} some of those molecules do deserve a second look. If the same research strategy is continued, then monosubstituted strong electron acceptors are necessary.^{60,65} So far, the ester and carbamate coupling reactions prevent the competing formation of charge-transfer anion radical-cation radical salts.^{60,65} The synthesis of monosubstituted strong acceptors needs vast improvement in yields. Indeed, from *p*-benzoquinones, a TCNQ-type acceptor can be made in low yields by reaction with malononitrile. But, starting from the same quinones, it is possible that the yield may be improved significantly if dicyanoquinodiimine (DCNQI) one-electron acceptors can be obtained by Hünig’s reaction.^{198,199} These should be equally strong acceptors.

14. Electrical Properties of Monolayers and Multilayers

It is easy enough to transfer an organic monolayer or multilayer atop a sufficiently flat metal layer by the LB method,^{16,17} or by chemisorption¹⁸ (the “self-assembly method”). It is much more difficult to then

Table 2. Oxidation Half-Wave Potentials ($E_{\text{ox}}^{(1)}$, $E_{\text{ox}}^{(2)}$) and Reduction Half-Wave Potentials ($E_{\text{red}}^{(1)}$, $E_{\text{red}}^{(2)}$), Measured by Cyclic Voltammetry (Volts vs SCE)

molecule ^a	no.	type	solvent/reference ^b	$E_{\text{ox}}^{(1)}$	$E_{\text{ox}}^{(2)}$	$E_{\text{red}}^{(1)}$	$E_{\text{red}}^{(2)}$	ref
TTF-C-BHTCNQ	35	strong D strong A	a	0.75i	0.99i	0.298	—	200
DDOP-C-BHTCNQ	36a	weak D strong A	b	1.2i		0.25	−0.07	54
BDDAP-C-HETCNQ	36c	medium D strong A	c	0.97i	1.4i	−0.08	−0.20i	60
Py-C-HETCNQ	37b	medium D strong A	c	1.0i	1.15	0.08	−0.35	60
BHAP-C-HMTCAQ	38a	medium D weak A	c	0.60			−0.36	60
TDDOP-C-HETCNQ	39a	weak D strong A	c	0.99i		0.07	−0.47	89
DDOP-C-ENP	43a	weak D weak A	c	1.39		−1.13		89
BDDOP-C-ENP	43b	weak D weak A	c	1.66i		−1.09		89
TDDOP-C-ENP	43c	weak D weak A	c	1.14i		−1.15		89
MTDAP-C-ENP	40	weak D weak A	c	0.54		−1.06		60

^a Acronyms: TTF, tetrathiafulvalene; TCNQ, 7,7,8,8-tetracyanoquinodimethane; C, carbamate linker; BHTCNQ, 2-bromo-5-hydroxyethoxyTCNQ; HETCNQ, 5-hydroxyTCNQ; Py, pyrene; BHAP, bis-hexylaminophenyl; HMTCAQ, hydroxymethyl-7,7,8,8-tetracyanoanthraquinodimethane; TDDOP, tris(dodecyloxy)phenyl; DDOP, dodecyloxyphenyl; ENP, 1-ethylene-4-nitrophenyl.^b (a) Solvent, CH₃CN; reference electrode, SCE. (b) Solvent, CH₃CN; reference electrode, Ag | AgCl; offset = 0.320 V.⁵⁴ (c) Solvent, CH₂ClCH₂Cl; reference electrode, Ag | AgCl; offset = 0.15 V.⁸⁹

Table 3. Pressure–Area Isotherm Data for Pockels–Langmuir Films^a

molecule	no.	type	<i>T</i> /K	Π_c / (mN/m)	$A_c/\text{\AA}^2$	ref
TTF-C-BHTCNQ	35	strong D strong A	292	12.7	134 ± 50	50
DDOP-C-BHTCNQ	36a	weak D strong A	292	20.2	50 ± 1	79
BDDAP-C-BHTCNQ	36b	medium D strong A	293	47.3	57 ± 1	80
Py-C-BHTCNQ	37a	medium D strong A	283	28.2	53 ± 1	79
BDDAP-C-HETCNQ	36c	medium D strong A	293	40.0	44 ± 1	60
Py-C-HETCNQ	37b	medium D strong A	293	46		60
BDDAP-C-HMTCAQ	38b	medium D weak A	293	22.3	58 ± 1	80
BHAP-C-HMTCAQ	38a	medium D weak A	293	35.8	42 ± 1	53
DDOP-C-ENP ^b	43a	weak D weak A	278	23.7	38 ± 1	89
TDDOP-C-ENP ^b	43b	weak D weak A	278	34.0	76 ± 1	89
TDDOP-C-HETCNQ ^b	39a	weak D strong A	283	47.5	54 ± 1	89
3,5-BHDOAP-C-ENP	43c	weak D weak A	299	49.6	39 ± 2	94
3,4-BHDOAP-C-ENP	43d	weak D weak A	300	54.5	35.8 ± 0.5	90
3,4-BHDOAP-C-HETCNQ	39b	weak D strong A	300	55.2	51 ± 1	90
MTDAP-C-ENP ^b	40	weak D weak A	278	16.5	63 ± 1	57
3,5-BTDYOAP-C-ENP	41	weak D weak A	298	18.7	58 ± 2	90
3,4-BTDYOAP-C-ENP	42	weak D weak A	300	49.4	50 ± 1	90

^a Π_c and A_c are the pressure and molecular area, respectively, at the collapse point. Acronyms are defined in Table 2. ^b The film makes Z-type LB multilayers (substrate at 22 °C, film at 5 °C).

deposit a second metal electrode atop the organic layer without damaging the organic layer. The electrical properties of LB monolayers and multilayers

had been studied for decades, e.g. by the groups of Kuhn,²⁰¹ Luciano C. Scala,²⁰² R. H. Tredgold,²⁰³ and Gareth G. Roberts.²⁰⁴

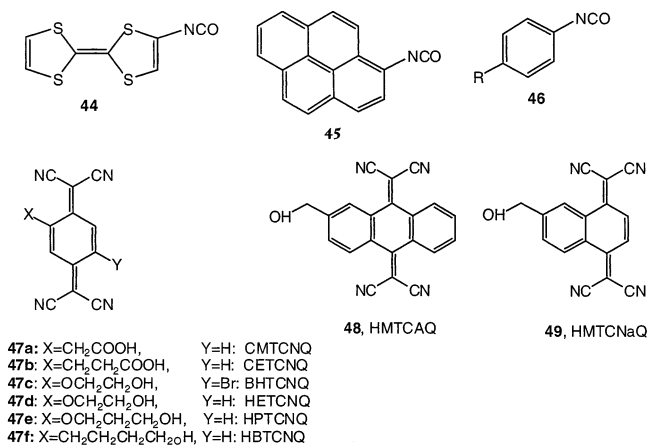


Figure 9. Monofunctionalized donors (**44–46**) and mono-functionalized acceptors (**47–49**).

A dramatic improvement in the method of making “metal–LB layers | metal” sandwiches was accomplished by J. Roy Sambles and co-workers at Exeter University, who found that Mg vapor and thin Mg films would damage the LB films least, and studied molecular rectification.^{39,205} The first molecule studied was DDOP–C–BHTCNQ, **36a**,⁷⁹ which had an asymmetric current–voltage curve.²⁰⁵ However, later work²⁰⁶ showed that a Schottky barrier between Mg and the BHTCNQ termination of **36a** (i.e., an interfacial Mg⁺⁺TCNQ⁻ or Mg⁺⁺(TCNQ⁻)₂ salt) was

probably responsible for the rectification, rather than asymmetric conduction through the molecule, as in the AR³ proposal. The LB multilayer of **36a** yielded an “S” rectifier.²⁰⁶

The second molecule studied by Sambles³⁹ was γ -hexadecylquinolinium tricyanoquinodimethanide, C₁₆H₃₃Q-3CNQ, **50** (Figure 10).³⁹ Molecule **50** is part of a series of zwitterionic molecules synthesized by the group of Geoffrey J. Ashwell at Cranfield University for their nonlinear optics;²⁰⁷ it resembles the first member of that series, α -picolinium tricyanoquinodimethanide or picolyl tricyanoquinodimethan, P-3CNQ, **51**, a crystalline ground-state zwitterion with a dihedral angle of 30° (between two least-squares planes of the pyridinium ring and the phenyl ring) and a calculated dipole moment of 26 D.²⁰⁸ The rectification measured for LB monolayers and multilayers of **50** sandwiched between a Pt electrode on one side and a Mg electrode on the other (with an overcoat of Ag)³⁹ was at first put into some doubt,^{62,64,65} but it was confirmed when insulating LB layers of tricosenoic acid were added between the electroactive layers of **50** and the electrodes,⁴⁰ and yet the rectification persisted.⁴⁰

15. Rectification of C₁₆H₃₃Q-3CNQ

The work at the University of Alabama by Michael P. Cava, Metzger, and co-workers aimed, since 1996,

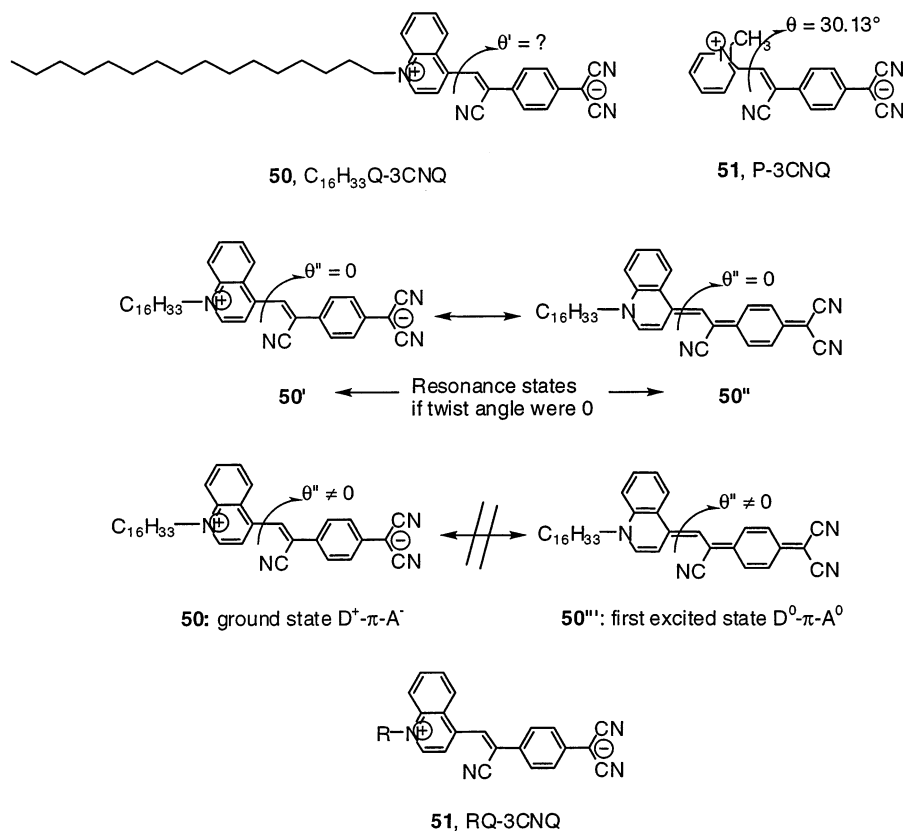


Figure 10. The first confirmed molecular rectifier, **50**,^{39–41,44,45} a related zwitterionic or betaine molecule **51**,²⁰⁸ and a generalized depiction **52** of analogues of **50** with different alkyl terminations. The very important twist angle $\theta = 30.13^\circ$ in the crystal structure of **51** is caused by steric hindrance between a hydrogen on the pyridinium ring and the N atom of the closest cyano group.²⁰⁸ A similar twist angle θ' must exist in **50** (for which no crystal structure is available). If this twist angle θ' were somehow reduced to zero, despite the steric hindrance, then structures **50'** and **50''** would be degenerate resonance states. Since the twist angle must be sufficiently far from zero, therefore either **50** is the ground state and **50'''** is the first electronic excited state, or vice versa.

at confirming unimolecular rectification by eliminating asymmetries in the current–voltage plots due to electrodes of dissimilar metals, and at clarifying the molecular mechanism for those asymmetries. This was done by studying molecule **50**, using the *same* metallic electrode on both sides on an LB monolayer or multilayer (at first Al,^{41–43} and more recently Au^{44,45,47,48}), by concentrating on “metal | LB monolayer | metal” sandwiches, rather than “metal | LB multilayer | metal” sandwiches, and by resorting to a thorough chemical and spectroscopic characterization of the molecular species responsible for rectification.^{46,47}

16. Molecular Properties of $C_{16}H_{33}Q-3CNQ$

The first improvement was a synthetic one: a 2-fold molar excess of the salt LiTCNQ afforded $C_{16}H_{33}Q-3CNQ$, **50**, in good yield.⁴¹ Molecule **50** is slightly soluble in polar solvents and insoluble in nonpolar solvents. It does crystallize, but it afforded crystal habits that were so intertwined that a unit cell could not be indexed.⁴¹ The cyclic voltammogram of **50** showed a reversible reduction at $E_{1/2} = -0.54$ vs SCE (this potential resembles that of *p*-benzoquinone, **5**); **50** has a second irreversible reduction, and a single irreversible oxidation.⁴¹ Therefore, **50** is a molecule quite dissimilar in design from the AR model D– σ –A molecule **1**, whose moieties TTF, **3**, and TCNQ, **7**, can be reversibly oxidized or reduced, respectively, two times. The molecular ground-state static electric dipole moment of **50** is $\mu_{GS} = 43 \pm 8$ D at infinite dilution in CH_2Cl_2 .⁴¹ The absorption spectrum in solution shows a relatively narrow band, peaked between 600 and 900 nm, which is strongly hypsochromic, with no vibrational structure in the more polar solvents; this band is an intervalence transfer (IVT) or internal charge-transfer band.^{41,46} This band fluoresces in the near-IR region.⁴⁶ From the Stokes shift, the experimental value of μ_{GS} , and also from a theoretical treatment of the solvation of ellipsoidal molecules in polar solvents, the excited-state dipole moment was estimated as $\mu_{ES} = 3-9$ D.⁴⁶ The molecule is clearly zwitterionic in the ground state ($D^+-\pi-A^-$) and less dissociated ($D^0-\pi-A^0$) in the first excited state. It is important to realize that the twist angle $\theta = 30^\circ$ in structure **51**, and a presumably similar twist angle θ' in structure **50**, are nonzero for steric reasons and prevent the π electron bridge in structures **50** or **51** from allowing complete mixing of the quinolinium or pyridinium electrons with the electrons on the 3CNQ part. If the twist angles in **50** were somehow reduced to zero (despite steric hindrance), then the two states **50'** and **50''** would be degenerate. Since the molecule is hypsochromic, the ground state must be **50** ($D^+-\pi-A^-$), and the first electronically excited state must be **50''** ($D^0-\pi-A^0$). The shortness of the π bridge in **50** allows for a strong IVT between the D and A ends of the molecule. We now turn to theoretical estimates of the molecular dipole moment μ_{GS} . If a full positive charge in **50** were placed on the quinolinium N atom and a full negative charge were localized on the central C atom of the dicyanomethylene bridge, this would yield $\mu_{GS} = 50$ D,⁴¹ which is reassuringly close to the

measured value. Molecular orbital analyses will yield such high dipole moments only if the phenyl ring is perpendicular to the quinolinium ring, i.e., if the twist angle $\theta' = 90^\circ$.^{101,212} For intermediate values of this twist angle, semiempirical molecular orbital theories provide lesser values of μ_{GS} , closer to 25 D,^{41,101} possibly because of the parametrization of the theoretical method.

An interesting recent study of the solvatochromism of a series of related monosubstituted trimethyl-2-methyleneindolinium tricyanoquinodimethanides allowed an estimate of the ionicity, or degree of charge transfer δ , in their ground states $D^{+\delta}-\pi-A^{-\delta}$.²⁰⁹

As shown below, the VUV spectrum of LB multilayers of **50** on quartz exhibits a strong peak at 570 nm;⁴¹ this peak was measured at 565 ± 5 nm for a monolayer at the air–water interface,²¹⁰ but there is a long absorbance tail that extends into the IR.^{41,210} A second peak can appear at the air–water interface, at 670 nm, which fades with time.²¹⁰ For **50** dissolved in low-polarity solvents, there are two peaks, which were interpreted as vibronic sub-bands⁴⁶ and which shift with solvent dielectric constant⁴⁶ but shift less when plotted against Reichardt's normalized solvent polarity parameter.^{210,211} In solvents of greater polarity, **50** exhibits only one peak, whose hypsochromic shift is pronounced.^{46,210} The earlier assignment was that two vibronic sub-bands are resolved in the lower-polarity solvents but not in the higher-polarity solvents;⁴⁶ the more recent assignment attributes the higher-energy sub-band in low-polarity solvents to the formation of centrosymmetric solvated association dimers,²¹⁰ which can survive for some time, even in a monolayer of **50** assembled at the air–water interface.²¹⁰

The HOMO of **50** shows a delocalized charge density, spread on both the D^+ part and the 3CNQ[−] part, while the LUMO is localized on the A^- part.⁴¹ The $S = 1/2$ anion radical of **50** was studied by electron paramagnetic resonance (EPR); it was obtained by holding a solution of **50** at -0.645 V vs the standard calomel electrode (SCE), i.e., at a potential more negative than the first reduction potential.⁴⁶ This anion radical yielded a well-resolved EPR hyperfine spectrum,⁴⁶ whose coupling constants can be simulated very well with significant spin densities localized on the 3CNQ part of the molecule,⁴¹ in agreement with theory. No experimental evidence was found within reasonable temperatures⁴¹ for a twisted internal charge-transfer transition, which had been suggested for **50**.²¹²

17. Film Properties of $C_{16}H_{33}Q-3CNQ$

Molecule **50** forms good amphiphilic Pockels–Langmuir monolayers at the air–water interface, with a collapse pressure of 34 mN m^{−1} and collapse areas of 43 Å² at 14 °C and 50 Å² at 20 °C, when measured in the dark.⁴¹ It transfers well on the upstroke, with transfer ratios around 100%, onto hydrophilic glass, quartz, or aluminum^{41,95} or fresh hydrophilic Au.^{44,45} It transfers poorly on the downstroke onto graphite, with a transfer ratio of about 50%.⁹⁵ Thereafter, the monolayers transfer only on the upstroke, with 100% transfer ratios onto all surfaces, forming Z-type LB multilayers^{41,95,207} (except

for that first poorly transferred layer on HOPG⁹⁵). Analogues **52**, with shorter aliphatic chains than the hexadecyl chain, also transfer well as LB films, provided that the chain is at least as long as $R = C_{12}H_{25}$. If the chain is shorter than that, then the monolayers assume a different structure, with imperfect side-by-side alignment of the dipoles, presumably because the van der Waals interactions of the long alkyl chains can no longer overcome the dipole–dipole repulsions, and the need to decrease the total moment within the monolayer starts to dominate.²¹³ An analogue of **50**, with only a methyl group (**52**, with $R = CH_3$) replacing the hexadecyl group, can be evaporated onto a substrate²¹⁴ but does not form an ordered film on it. Analogues **52**, with a terminal thiol group (e.g., **52** with $R = C_{12}H_{25}SH$), cannot be synthesized, because acids protonate the other end of the molecule; besides, a thiolate bonded to Au, being about 50% polar, would provide a surface dipole in addition to the dipole within **50**. Analogues of **52** with $R =$ alkyltriethoxysilyl could be covalently bonded to a silicon substrate, but the coverage was irregular.²¹⁵ More promise is shown by a recently prepared derivative of **50** with $R =$ alkylthioacetyl.²¹⁶

The LB monolayer thickness of **50** was determined by X-ray diffraction (23 Å⁴¹ and 29 Å⁴⁵), spectroscopic ellipsometry (23 Å),⁴⁵ surface plasmon resonance (22 Å),^{41,105} and X-ray photoelectron spectrometry (XPS) (25 Å).¹⁰⁵ Assuming an average monolayer thickness of 23 Å and a calculated molecular length of 33 Å (with an all-trans geometry for the $C_{16}H_{33}$ “tail”), one gets a tilt angle of $\cos^{-1}(23/33) = 46^\circ$ from the surface normal.⁴¹ The XPS spectrum of one monolayer of **50** on Au shows two N(1s) peaks, one at 401.7 eV (attributable to the quinolinium N) and one at 399.4 eV (attributable to the three CN species).¹⁰⁵ An earlier XPS spectrum of a multilayer of **50** on Al was deconvoluted into three peaks, one at 402.3 eV (quinolinium N), one at 400.3 (neutral CN), and one at 398.8 eV (negatively charged CN).⁴⁶ An angle-resolved XPS spectrum shows that, as the takeoff angle increases, the quinolinium N(1s) signal decreases, while the cyano N(1s) signal stays relatively constant; the cyano nitrogens lie closer to the Au substrate than does the quinolinium N atom.¹⁰⁵ The valence-band portion of the XPS spectrum agrees roughly with the density of molecular energy states.⁴⁶ The contact angle of a drop of water on “hydrophilic Au” is measured to be 40° (it should be zero if the gold were perfectly free of hydrophobic adsorbates from laboratory air); this angle increases to 92° if a monolayer of **50** is transferred atop fresh hydrophobic Au. Clearly, the hydrophobic alkyl chains are closest to the water surface.¹⁰⁵

What evolves is a picture of molecules of **50** that adhere somewhat by the two terminal CN groups onto a hydrophilic substrate, are tilted maybe 45° from the surface normal, and present alkyl chains to the air. This is confirmed by a grazing-angle FTIR study of **50** on Al⁴¹ or on Au.¹⁰⁵ Since a monolayer survives in the ultra-high vacuum of an XPS instrument, it must adhere rather well to it; i.e., it does not desorb very rapidly. The absorption spectrum of an 11-layer LB film of **50** is shown in Figure 11.

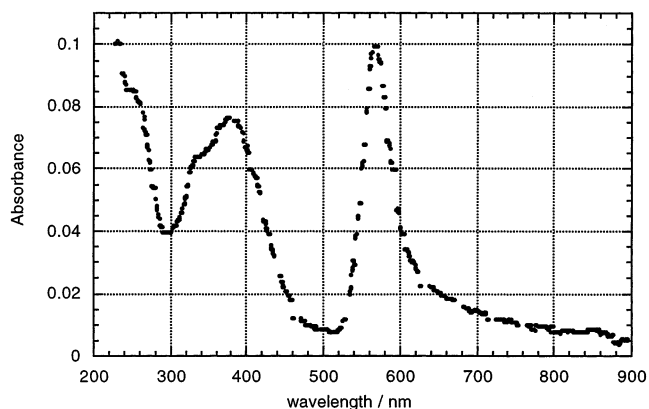


Figure 11. Absorption spectrum of an 11-layer LB film of $C_{16}H_{33}Q-3CNQ$, **50**, on quartz.⁴¹

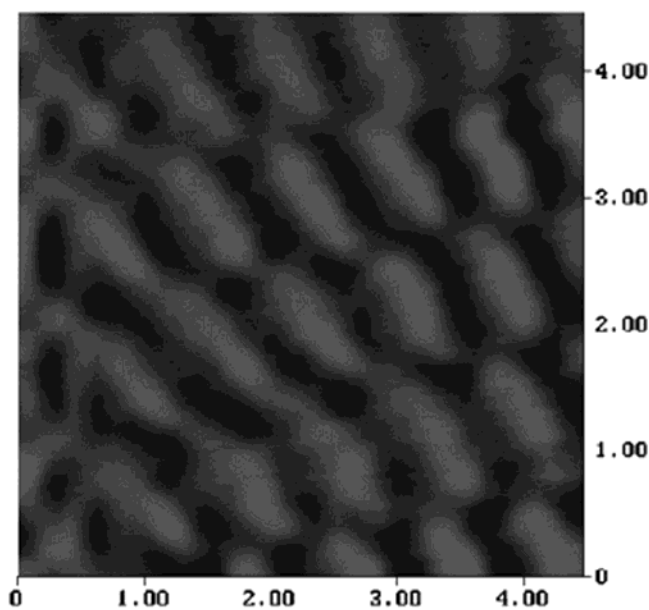


Figure 12. STM image of a LB monolayer of $C_{16}H_{33}Q-3CNQ$, **50**, on HOPG with a Pt/Ir tip (Nanoscope III). Scan size, 4.5 nm \times 4.5 nm; Z-range, 2.3 pA; bias, -316 mV; setpoint current, 3.2 pA.⁴¹

There is the intense IVT band at 570 nm or 2.17 eV.⁴¹ LB multilayers of **50** have a strong second harmonic signal $\chi_{zzz}^{(2)} = 180$ pm V^{-1} , whose strength is partly due to resonance enhancement at 532 nm from the tail of the absorption band.²¹⁷

The near-infrared fluorescence lifetime of the first excited state **50**^{'''} in solution has been measured to be as short as 1.4 ps,²¹⁸ which suggests that the speed of the rectification process for **50** may be very high (although the metal-to-molecule electron-transfer rates are as yet unknown). The STM image of **50** on HOPG has been measured (Figure 12).⁴¹ Since **50** adheres (poorly) with the alkyl chains closest to the graphite, one sees only an unresolved image of the molecule seen from the dicyanomethylene end, with a repeat distance of $6 \text{ \AA} \times 12 \text{ \AA}$,⁴¹ somewhat larger than the collapse area per molecule of 50 \AA^2 . The poor adhesion to graphite and the low coverage mean that the image seen in Figure 12 tends to migrate across the sample over time.⁴¹

18. Metal-LB Film-Metal Sandwiches of $C_{16}H_{33}Q-3CNQ$

To perform rectification measurements, LB monolayers and multilayers of $C_{16}H_{33}Q-3CNQ$, **50**, were sandwiched between macroscopic Al electrodes,⁴¹ and most recently between Au electrodes.^{44,45} First, the bottom electrode (either Al,⁴¹ or an adhesion layer of Cr followed by Au^{44,45}) is evaporated onto a glass, quartz, or Si substrate; second, the LB monolayer or multilayer of **50** is transferred above it; third, the

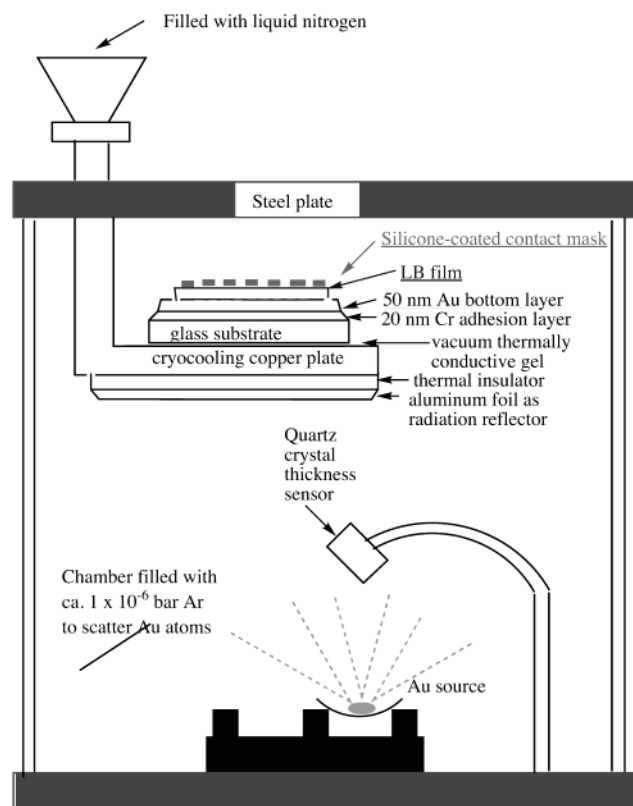


Figure 13. Geometry of "cold gold" evaporation.⁴⁵

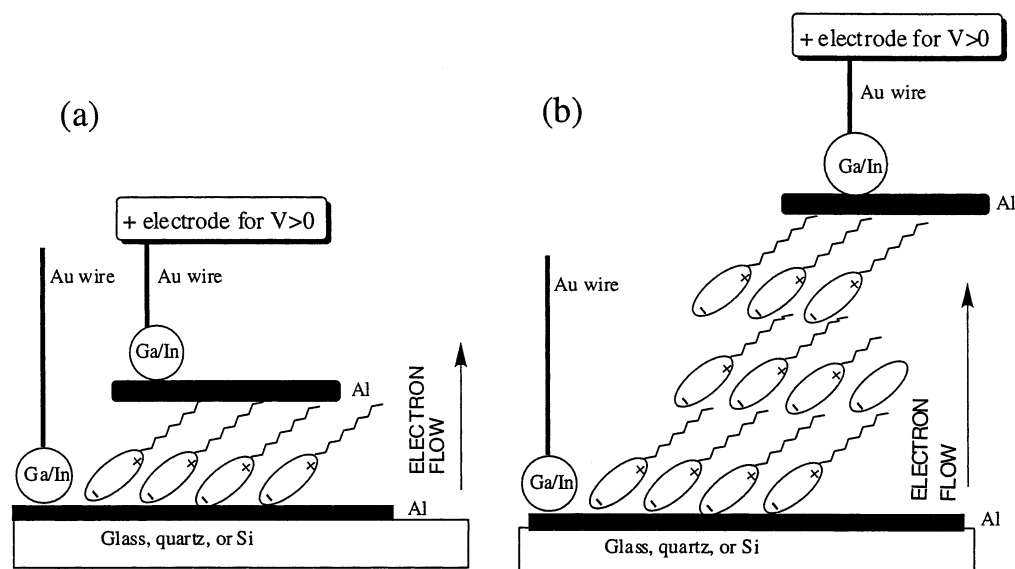


Figure 14. Geometry of (a) LB monolayer and (b) LB trilayer of $C_{16}H_{33}Q-3CNQ$, **50**, sandwiched between Al electrodes. The arrow shows the direction of enhanced electron flow under positive bias. The top Al electrode is 100–300 nm thick, depending on the run. A glass, quartz, or silicon substrate was covered by a bottom Al electrode of 25 mm × 75 mm × 100 nm, the LB film, and 12 top pads with thickness 100 nm and areas between 2.8, 4.5, and 6.6 mm², depending on the run.⁴¹

structure is dried for 2 days to remove any adventitious water; fourth, the second electrode is deposited through a shadow mask⁴¹ or a contact mask^{44,45} to make 30–48 pads per substrate (most recently of an area of 0.283 mm² each⁴⁵); fifth, a droplet of either Ag paste or Ga/In eutectic is put above the bottom electrode and (very gently) sequentially on one of the pads of the top electrode; and finally electrical measurements are made.

During the evaporation of the top electrode, a copper plate holding the sample is cooled by a liquid nitrogen bath; this suffices for an Al deposition⁴¹ but not for an Au deposition. For an Au deposition (Figure 13), two additional precautions are taken: one, to add 10⁻³ Torr of Ar gas to the evaporation chamber,²¹⁹ and the other, to protect the substrate from direct thermal radiance from the heated Au source by hiding the sample on the opposite side of the copper plate (always cooled to liquid nitrogen temperatures). This "cold gold" deposition²¹⁹ forces the Au atoms to undergo multiple scattering by Ar atoms before they reach the substrate.^{44,45} The final metal-LB film-metal geometry is shown in Figure 14 for Al⁴¹ and in Figure 15 for Au electrodes.^{44,45}

The Al layers are covered by its oxide, as is the Ga/In eutectic drop, while the Au electrodes have no oxide covering. This distinction becomes important in the discussion below.

19. Unimolecular Rectification by $C_{16}H_{33}Q-3CNQ$

A monolayer or multilayer of arachidic acid, $C_{19}H_{39}COOH$, sandwiched between Al electrodes as in Figure 14, has a sigmoidal and almost symmetrical curve under both positive bias and negative bias (as expected);⁴¹ the same results are seen when Au electrodes are used.⁴⁵ When a monolayer of $C_{16}H_{33}Q-3CNQ$, **50**, is placed between Al electrodes (with their inevitable patchy and defect-ridden covering of oxide), then a dramatically asymmetric current is seen

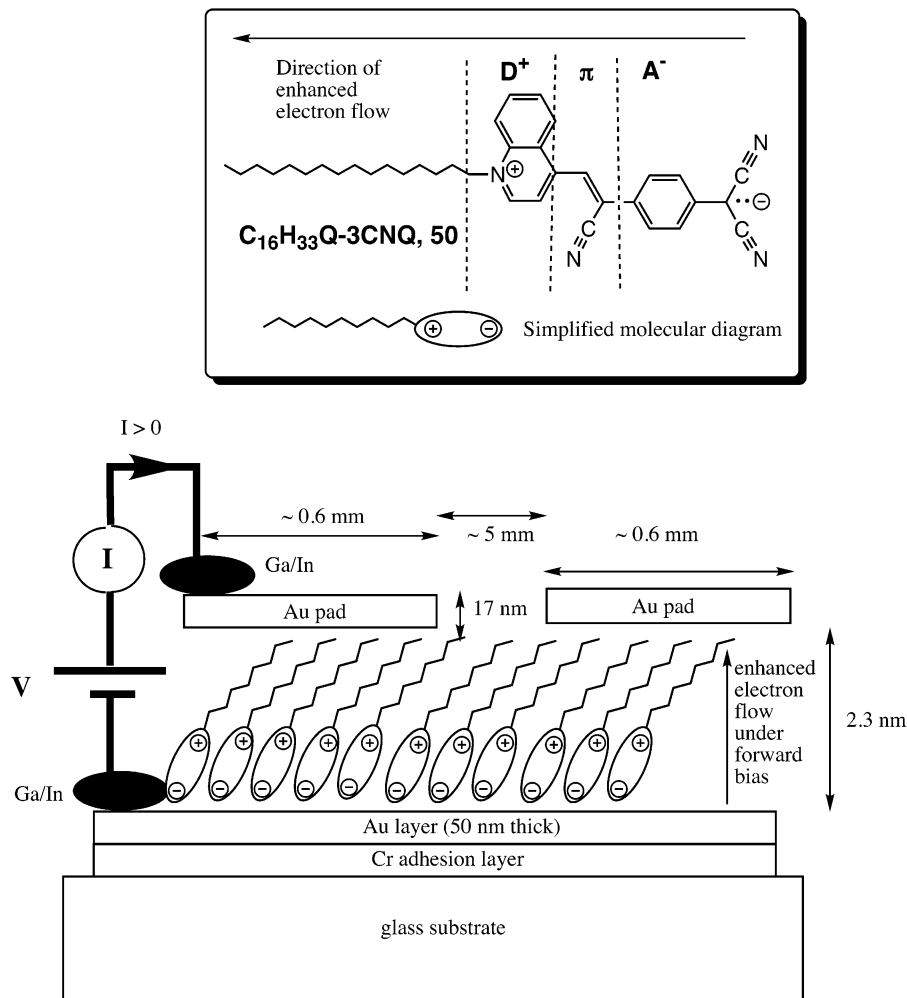


Figure 15. Molecular structure and geometry of LB monolayer of $C_{16}H_{33}Q-3CNQ$, **50**, sandwiched between Au electrodes, with an arrow showing the direction of enhanced electron flow under positive, or forward bias. The substrate was glass, $50\text{ mm} \times 50\text{ mm} \times 0.4\text{ mm}$, covered either by a Cr adhesion layer or by a hydrophobic xylene covering, followed by an evaporated Au film, $50\text{ mm} \times 50\text{ mm} \times 50\text{ nm}$, then the LB monolayer or multilayer, then 48 cylindrical Au pads, 17 nm thick and with an area of 0.283 mm^2 each.⁴⁵

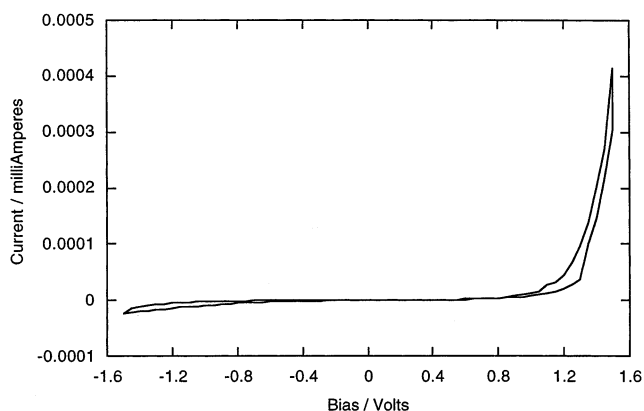


Figure 16. Plot of the DC current I versus the DC applied voltage V (I - V plot) through a single monolayer of $C_{16}H_{33}Q-3CNQ$, **50**, sandwiched between Al electrodes (top Al pad area 4.5 mm^2 , thickness 100 nm), using Ga/In eutectic and Au wires. The DC voltage is swept at a rate of 10 mV s^{-1} .⁴¹

(Figure 16). For **50**, the rectification ratio (eq 18) is $RR = 26$ at 1.5 V .⁴¹ Assuming a molecular area of 50 \AA^2 , the total current at 1.5 V corresponds to 0.33 electron molecule⁻¹ s⁻¹.⁴¹ The direction of enhanced electron flow is shown as an arrow in Figure 14. This

same asymmetry is seen also for multilayers of **50**, for a sample covered by Mg pads topped by Al pads⁴¹ (as in the Sambles experiment^{39,40}), for monolayers and multilayers of **50** on graphite studied by scanning tunneling spectroscopy,^{41,95} and even for a solution of **50** in dimethyl sulfoxide placed in the scanning tunneling microscope.⁴¹ The rectification ratios vary somewhat from pad to pad, as does the total current, in part because these are all two-probe measurements, with all electrical resistances (Al, Ga/In or Ag paste, wires, etc.) in series, and in part because any gentle pressure, put manually on the top pad through the drop of Ag paste or eutectic to make electrical contact, may vary from pad to pad. A thorough review of all data suggested that any molecule which exhibits $RR(V) < 2$ at maximum bias V should not be taken as a rectifier;⁴² some samples of **50** studied between Al electrodes have enhanced currents, albeit smaller, under negative bias instead of positive bias.⁴² As high potentials are scanned repeatedly, the I - V curves show progressively less asymmetry; the rectification ratios decrease gradually with measurement, i.e., with repeated cycling of the bias across the monolayer. One should remember

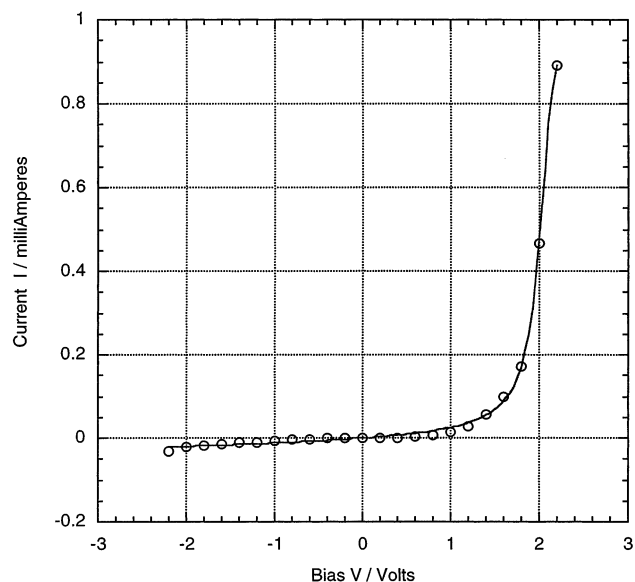


Figure 17. Current–voltage (I – V) plot for a cell “Au | monolayer of $C_{16}H_{33}Q$ -3CNQ, **50** | Au”. The resistance at 2.2 V is $R = 2.47$ k Ω ; the current at 2.2 V is $I = 9.83 \times 10^3$ electrons molecule $^{-1}$ s $^{-1}$. The rectification ratio at 2.2 V is $RR = 27.53$ in the first cycle (shown), but decreases to 10.1, 4.76, 2.44, and 1.86 in cycles 2, 3, 4, and 5, respectively (not shown).⁴⁵

that putting 1.5 V across a monolayer of thickness 2.3 nm creates an electrical field of 0.65 GV m $^{-1}$, which is very large; under such fields, many zwitterionic molecules in the monolayer may turn around, end over end, to minimize the total energy. The more “liquid”-like the monolayer, the easier this process would be. Measurements of the temperature dependence of rectification of **50** between Al electrodes, in the range 105 K < T < 390 K, established that the asymmetry is not temperature-dependent,⁴³ but that the currents increase with temperature; this may be due to temperature effects across the several metal–oxide–metal junctions.⁴³ A minor improvement in the geometry of Figure 14 was to laboriously polish the left edge of the bottom Al electrode to make it wedge-shaped, and thus move the top Al pad sideways, so it no longer rested above the bottom electrode but was just above the monolayer and the glass substrate. This increased the current from 0.33⁴¹ to 35 electrons molecule $^{-1}$ s $^{-1}$, and the rectification ratio rose to 53.⁷⁵

Although the experiments with Al electrodes measured the rectification of several molecules in parallel, or unimolecular rectification, this conclusion rested on the assumption that the oxide covering of the Al electrodes was sufficiently defective to allow “ohmic” contact with the molecules, or in other words, that no substantial electrical contact was made wherever the oxide coverage was thick, and that the current measured flowed mostly through those sites where the oxide coating was very thin or nonexistent. This conclusion may not have been completely convincing to all readers. With Au electrodes, the current through the pads increased dramatically, as expected, but the asymmetry persisted. This confirmed that the same asymmetric conduction through the molecules could be measured by using either Au or Al electrodes.^{44,45}

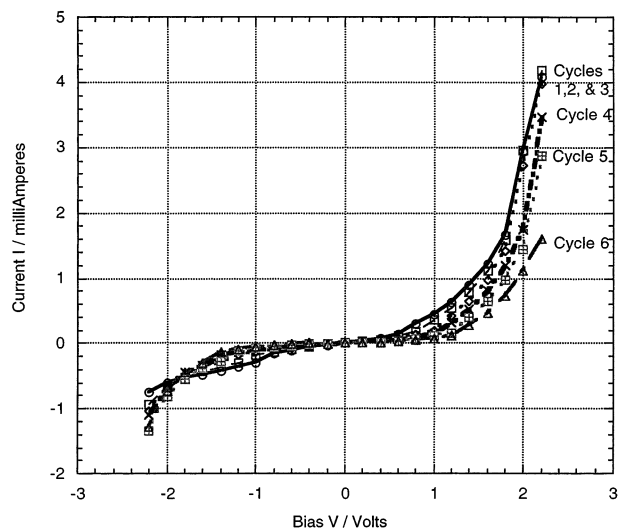


Figure 18. I – V plot for a cell “Au | monolayer of $C_{16}H_{33}Q$ -3CNQ, **50** | Au”, showing the decrease in rectification ratio. At 2.2 V in the first cycle, $R = 538$ Ω , $I = 4.09$ mA = 4.5×10^4 electrons molecule $^{-1}$ s $^{-1}$, and $RR = 5.39$. Cycle 1, \circ ; cycle 2, \square ; cycle 3, \diamond ; cycle 4, \times ; cycle 5, \equiv ; cycle 6, \triangle .⁴⁵

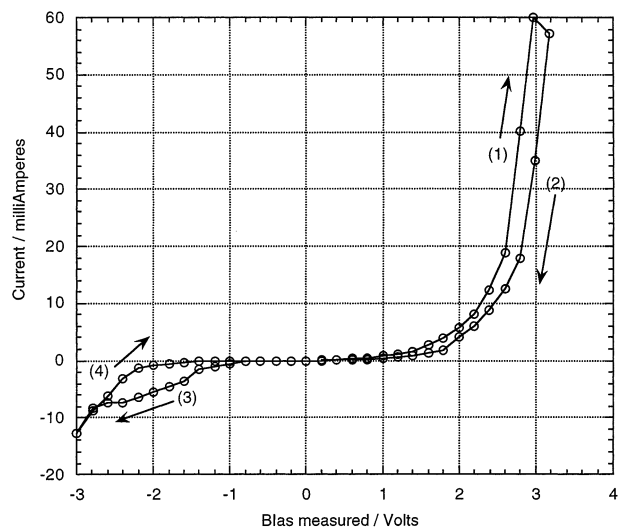


Figure 19. I – V plot for a cell “Au | monolayer of $C_{16}H_{33}Q$ -3CNQ, **50** | Au”, showing hysteresis in the first full measurement cycle. At 2.2 V in the first cycle, $R = 268$ Ω , $I = 8.20$ mA = 9.04×10^4 electrons molecule $^{-1}$ s $^{-1}$, and $RR = 6.62$.⁴⁵

Figures 17–21 give details of what was measured using Au electrodes. Figure 17 shows the best rectification ratio at 2.2 V ($RR = 27.53$). Figure 18 shows how the rectification ratio decreases from cycles 1 to 6. Figure 19 shows the highest current (90 400 electrons molecule $^{-1}$ s $^{-1}$). Some cells exhibit, as in Figure 20, a saturation in the forward current; this saturation is predicted by any physical model for conduction through a molecule (e.g., the AR model) or a set of molecules measured in parallel. For some other cells, as in Figure 21, the current increases until breakdown occurs; in some cells this happens at 5.0 V, i.e., the cells suffer dielectric breakdown only at a field close to 2 GV m $^{-1}$.⁴⁵ It is quite clear that rectification by a one-molecule-thick layer of $C_{16}H_{33}Q$ -3CNQ, **50**, is an established fact.

One plausible mechanism for rectification by $C_{16}H_{33}Q$ -3CNQ, **50**, is a minor change in the AR

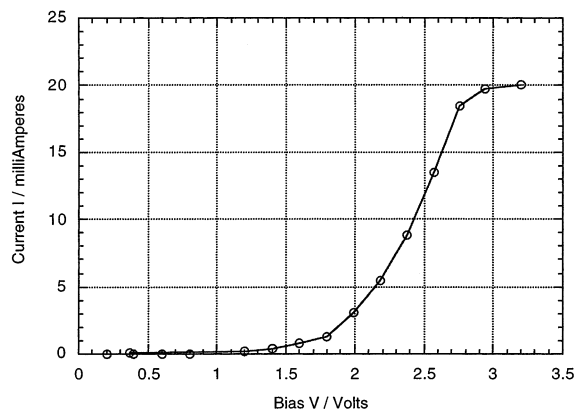


Figure 20. I – V plot for a cell “Au | monolayer of $C_{16}H_{33}Q$ -3CNQ, **50** | Au”, showing saturation in the forward current, $I = 20$ mA, at 3.2 V (this cell broke down at 3.4 V).⁴⁵

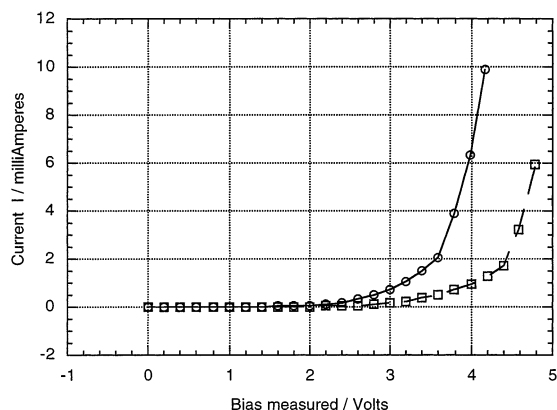
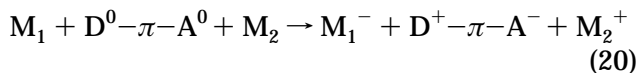
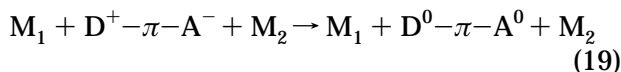


Figure 21. I – V plot for a cell “Au | monolayer of $C_{16}H_{33}Q$ -3CNQ, **50** | Au”, driven to breakdown, with no saturation. The cell was first measured to 4.2 V (with no breakdown), then again from 0 V until breakdown occurred at 5.0 V. No saturation in the forward current was found.⁴⁵

proposal, so that eqs 1, 2, and 3 are replaced by



where the first step is the electric field-driven excitation from the ground state to the excited state, followed by electron transfers across the two “molecule | metal” interfaces.⁴¹ A second plausible mechanism is given below.

Independently, Ashwell and co-worker confirmed that Z-type 30-layer films of **50** rectify between Au electrodes.²¹⁰ The thermal evaporation of the top Au electrode may have destroyed 20 of the 30 layers, as monitored by a decreased absorbance.²¹⁰ The currents for the multilayer²¹⁰ were 3 orders of magnitude smaller than those reported for the monolayer,⁴⁵ either because of inefficient electron transport between adjacent layers or because of current contributions from Au filaments within the LB monolayer.²¹⁰

Unorthodox results and a radical new interpretation of rectification were recently reported at the University of Exeter, when LB multilayers of $C_{16}H_{33}Q$ -

3CNQ, **50**, were studied to 8 K.²²⁰ In particular, 20 layers of $C_{16}H_{33}Q$ -3CNQ, **50**, were deposited atop an Au electrode and covered by a top Au electrode by the “cold gold” technique.²²⁰ At room temperature, rectification in the forward direction was seen.^{44,45,220} However, if a voltage (magnitude not specified) was applied to the film for 20 min, in either the forward or the reverse direction, then the rectification changed sign.²²⁰ The I – V characteristics of “what was left” were measured in the temperature range 8–295 K.²²⁰ Below a threshold voltage (between +5 and –3.5 V at 262 K, and between +8 and –8 V at 8 K), the conductivity was symmetric, characteristic of an insulator.²²⁰ the current was proportional to V at the lowest voltages but proportional to V^2 at intermediate voltages, temperature-independent, and due to space-charge-limited conduction.²²⁰ Beyond the threshold voltages, rectification began. The current was proportional to $V^{0.5}$ and seemed to be dominated by Poole–Frenkel hopping between trap sites. It was opined that **50** is a rectifying insulator.²²⁰ This interpretation runs counter to all previous work of the Exeter and the Alabama groups and may stimulate much further work and discussion.

20. Failed Searches for New Rectifiers

Some molecules tested at the University of Alabama, with structures related to **50**, did not rectify. In particular, a series of benzothiazolium tricyanoquinodimethanides (**53a**–**54b**) (Figure 22) were tested, and no rectification was found, maybe because the dipoles were lying in the plane of the film rather than normal to it.¹⁰⁰ Also, a di(decyl)ammonium tricyanoquinodimethanide (**55**) did not rectify, because the film was disordered.²²¹ FTIR and XPS evidence shows that the ordering within the monolayer was inferior to the order achieved by **50**.²²¹ There are decyl groups in **55** rather than the hexadecyl groups in **50**, and it is possible that in **55** the dipole–dipole forces, which would favor an antiparallel arrangement of molecules in the monolayer, was

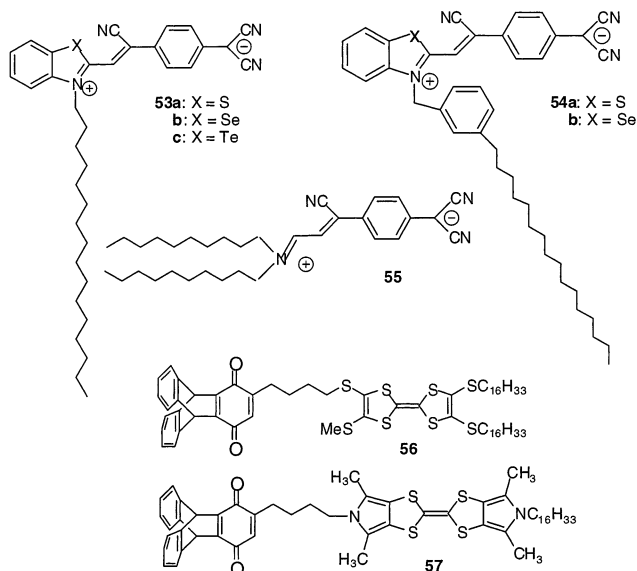


Figure 22. Zwitterionic molecules **53**–**55**, based on tricyanoquinodimethane,^{100,221} and structures **56** and **57**, based on trypticenequinone,^{96,99} which did not rectify.

of a strength comparable to the alkyl–alkyl interactions, which would favor a parallel arrangement.²²¹

Another disappointment was that two D– σ –A molecules **56** and **57**, based on the bulky acceptor triptycenequinone, did not form LB films, probably because the quinone end was not sufficiently hydrophilic.^{96,99} The synthetic design to convert the quinones into dicyanoquinodiimines by Hünig's reaction^{198,199} failed,^{96,99} because these conversions should be made before the donor and acceptor ends are coupled, not afterward.

21. Two New Rectifiers

Recently, two more molecules were studied at the University of Alabama, 2,6-di(dibutylamino-phenylvinyl)-1-butylpyridinium iodide, $(\text{Bu}_2\text{N}\varphi\text{V})_2\text{BuPy}^+\text{I}^-$, **58**,⁴⁷ and dimethylanilino-aza[C₆₀]fullerene, DMAn-NC₆₀, **59**⁴⁸ (Figure 23). Both are unimolecular rectifiers (the second one, barely).

$(\text{Bu}_2\text{N}\varphi\text{V})_2\text{BuPy}^+\text{I}^-$, **58**, forms a Pockels–Langmuir film at the air–water interface and transfers to hydrophilic substrates as a Z-type multilayer. The monolayer thickness was estimated as 0.7 nm by spectroscopic ellipsometry and 1.15 nm by surface plasmon resonance (at $\lambda = 532$ nm) or 1.18 nm (at $\lambda = 632.8$ nm); X-ray diffraction suggests a layer thickness of 1.3 nm.⁴⁷ The films exhibit an absorption maximum at 490 nm (which is slightly hypsochromic in solution), attributable to iodide-to-pyridinium back charge transfer, and a second harmonic signal $\chi^{(2)} = 50 \text{ pm V}^{-1}$ at normal incidence ($\lambda = 1064$ nm) and 150 pm V^{-1} at 45° .⁴⁷ X-ray photoelectron spectroscopy of a multilayer of **58** on a gold substrate finds only 30% of the expected signal from the iodide; it is likely that the iodide anion is partially replaced by a more abundant hydroxide anion during LB transfer.⁴⁷ The rectification is shown in Figure 24. Once again, there is a decrease of rectification upon successive cycles. Some cells have initial rectification ratios as high as 60. The measurements of the molecular area at film transfer (100 \AA^2) and of the monolayer thickness (1.1–1.3 nm) are consistent with the molecule sitting above the bottom gold electrode (Figure 15), as drawn in Figure 23, with the iodide (or other gegenion) closer to the bottom Au electrode and the pyridinium ion above it; the direction of enhanced electron flow is from the bottom Au electrode toward the top Au pad (as in Figure 15). Therefore, the favored direction of electron flow is from the gegenion to the pyridinium ion, i.e., in the direction of “back charge transfer”, and the rectification in $(\text{Bu}_2\text{N}\varphi\text{V})_2\text{BuPy}^+\text{I}^-$,

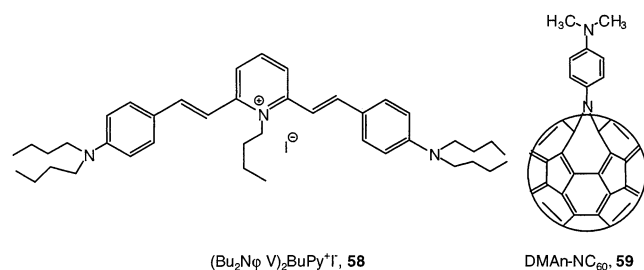


Figure 23. Two new rectifiers, molecules $(\text{Bu}_2\text{N}\varphi\text{V})_2\text{BuPy}^+\text{I}^-$, **58**, and DMAn-NC₆₀, **59**.

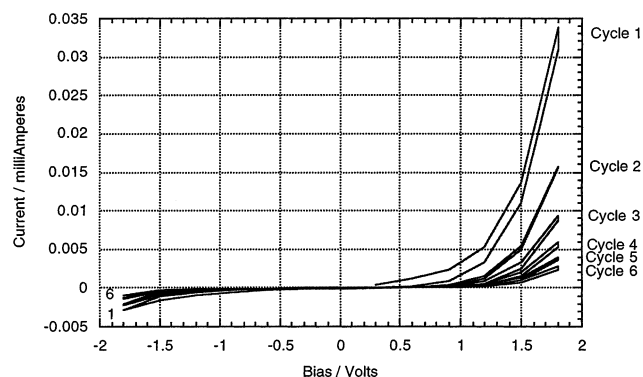


Figure 24. I – V plots for $(\text{Bu}_2\text{N}\varphi\text{V})_2\text{BuPy}^+\text{I}^-$, **58**, measured in a “Au | LB monolayer of **58** | Au” cell, for six successive cycles of measurement. The rectification ratios are RR = 12, 7, 5, 4, 3, and 3, for cycles 1–6, respectively.⁴⁷

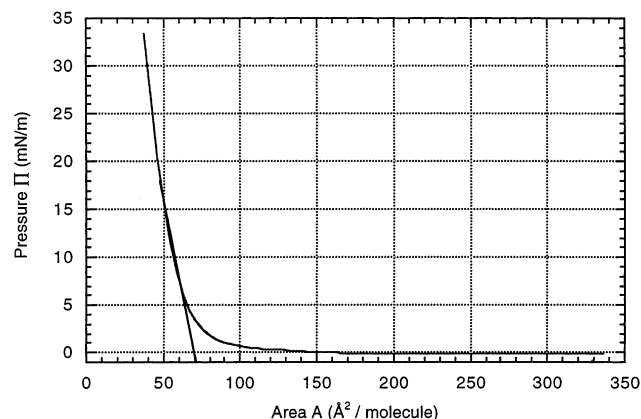


Figure 25. Pressure–area isotherm for DMAn-NC₆₀, **59**.⁴⁸

58, can be attributed to an interionic electron transfer rather than to an intramolecular electron transfer.⁴⁸

The azafullerene DMAn-NC₆₀, **59**, consists of a weak electron donor (dimethylaniline) bonded to a moderate electron acceptor (N-capped C₆₀). It is a blue compound, with a significant IVT peak at 720 nm.⁴⁸ The pressure–area isotherm⁴⁸ is shown in Figure 25. The Pockels–Langmuir film is very rigid; i.e., the slope of the isotherm is relatively large. However, the molecular areas are 70 \AA^2 at extrapolated zero pressure and 50 \AA^2 at the chosen LB film transfer pressure of 22 mN m^{-1} ,⁴⁸ whereas the true molecular area of C₆₀ is close to 100 \AA^2 . Therefore, it is thought that the molecules **59** transferred onto Au on the upstroke are somewhat staggered, as shown in Figure 26, with the more hydrophilic dimethylamino group closer to the bottom Au electrode. The film thickness is estimated by XPS to be 2.2 nm.⁴⁸ The monolayer is covered, as previously,^{44,45,47} with 17-nm-thick Au pads deposited by the “cold gold” technique. The dimethylamino groups in the LB film are probably not as closely packed as the azafullerenes. Angle-resolved N(1s) XPS spectra confirm that the two N atoms are closer to the bottom Au electrode than is the C₆₀ cage.⁴⁸ The current–voltage plot shown in Figure 27 is a dramatic but unwelcome surprise.⁴⁸

The top pads have an area of 0.283 mm^2 , as before,^{45,46} and the cell now supports 1 A of current across it! (Per molecule, that would be an absurdly large number, such as 5×10^{11} electrons molecule^{−1}

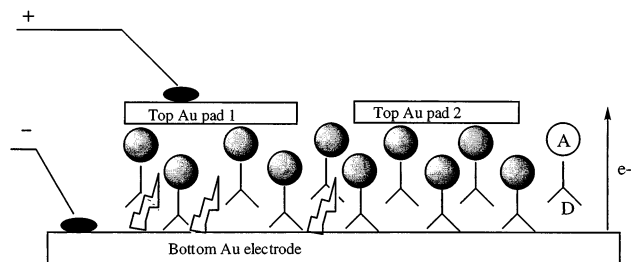


Figure 26. Schematic of LB monolayer of DMAn-NC₆₀, **59**, on gold substrate, including top Au pads and Au stalagmites. The direction of preferred electron flow under forward bias is also shown as an arrow from the bottom gold electrode to the top gold electrode pads.⁴⁸

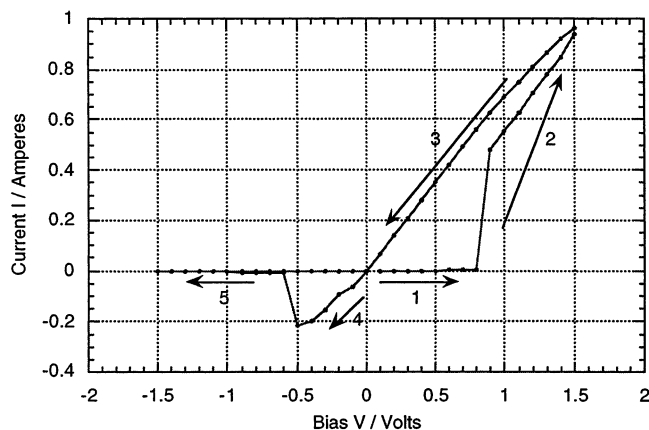


Figure 27. Current-voltage plots for DMAn-NC₆₀, **59**, measured in a "Au | LB monolayer of **59** | Au" cell, with numbers indicating the measuring sequence.⁴⁸

s⁻¹.) Moreover, the high current between 1.5 and -0.5 V in the "return" path (3 and 4 in Figure 27) is ohmic. The asymmetry decreases upon cycling (not shown here).⁴⁸ Probably, metallic Au filaments have formed within the monolayer, which do not pierce the fullerene ends of the monolayer, and are progressively destroyed by cycling the voltage; these Au stalagmites are shown in Figure 26 as jagged arrows or thunderbolts (see also ref 221a). In contrast, some cells show no such large current, but they do show a

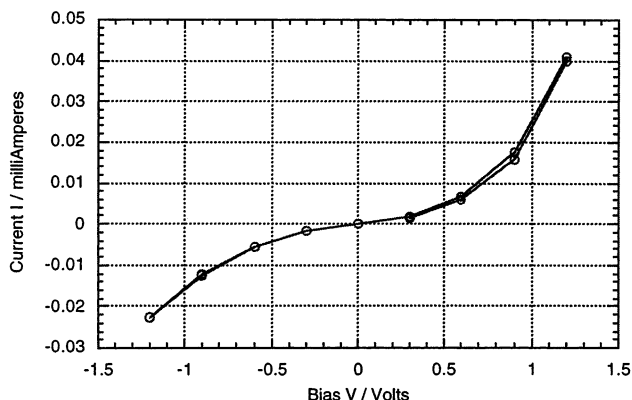


Figure 28. Current-voltage plots for DMAn-NC₆₀, **59**, measured in a "Au | LB monolayer of **59** | Au" cell, in which the current stays small. This should be the current due to the molecules **59** and not to the Au filaments.⁴⁸

much smaller current, which is "marginally" rectifying⁴² in the forward direction, with a rectification ratio RR of about 2 (Figure 28).⁴⁸

Table 4 collects relevant electrochemical data (oxidation and reduction potentials in solution) and spectroscopic information (intramolecular IVT peaks) for the D-σ-A and D⁺-π-A⁻ systems studied so far in our laboratory, including the three rectifiers **50**, **58**, and **59** discussed above.

22. Alternate Mechanism for Rectification by C16H33Q-3CNQ

In eqs 19 and 20, an explanation was given for the rectification of the zwitterion C₁₆H₃₃Q-3CNQ, **50**, in terms of a modified Avriam-Ratner mechanism. However, given that the molecule in solution only has a reversible first reduction (whereas the molecule conceived by AR had two reversible oxidations and two reversible reductions), therefore one could conceive of an alternate mechanism that involves only this reversible state. At forward bias, this mechanism consists of three consecutive steps.

(1) Electron donation from metal M₂ to the zwitterion, generating the radical anion D⁰-π-A⁻ (an

Table 4. Oxidation Half-Wave Potentials ($E_{\text{ox}}^{(1)}$, $E_{\text{ox}}^{(2)}$) and Reduction Half-Wave Potentials ($E_{\text{red}}^{(1)}$, $E_{\text{red}}^{(2)}$), Measured by Cyclic Voltammetry (Volts vs SCE) and Intramolecular Charge-Transfer Transition Energy $h\nu$ (eV)

molecule	no.	type	solvent/ reference ^a	$E_{\text{ox}}^{(1)}$	$E_{\text{ox}}^{(2)}$	$E_{\text{red}}^{(1)}$	$E_{\text{red}}^{(2)}$	$h\nu$	conditions ^b	ref
C ₁₆ H ₃₃ Q-3CNQ	50	weak D weak A	a	0.49i	—	-0.513	-1.16i	2.13	c	41
HDBzThz-3CNQ	53a	weak D weak A						1.67	d	100
BHDMTTF-Bu-TrQ	56	weak D strong A	a	0.51	0.85	-0.60				96
TMPyrTTF-Bu-TrQ	57	weak D strong A	a	0.69	1.23	-0.56				96
(Bu ₂ NφV) ₂ BuPy ⁺ I ⁻	58	weak D weak A	b	0.52	1.04	-1.08		2.46	e	47
DMAn-NC ₆₀	59	weak D weak A						1.66	f	48

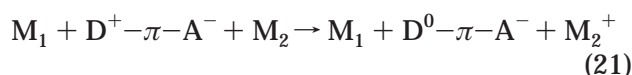
^a (a) Solvent, CH₂Cl₂; reference electrode, SCE. (b) Solvent, CH₃CN; reference electrode, SCE. ^b (c) In LB films on quartz; solutions are strongly hypsochromic.⁴⁶ (d) In DMSO solution; solutions are not solvatochromic.¹⁰⁰ (e) In THF solution. The absorption at 2.46 eV is probably due to an *interionic* CT band. (f) In CH₃CN solution. Solutions are weakly hypsochromic.

Table 5. Estimates of the Energy Level E_{LUMO} for **50 That Must Be Populated before Significant Through-Molecule Tunneling Can Occur^a**

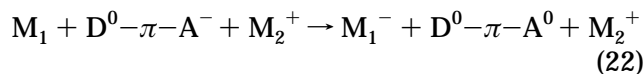
from ref, figure no.	LB layers	M_2	ϕ_2 / eV	M_1	V_t / V	E_{LUMO} / eV
41, Figure 14	15	HOPG	4.4	Pt	1.2	3.2
41, Figure 7	4	Al	4.2	Al	1.0	3.2
41, Figure 8	4	Mg	3.7	Al	1.0	2.7
41, Figure 9	1	Al	4.2	Al	1.5	2.8
41, Figure 11a	1	Al	4.2	Al	1.3	2.9
45, Figure 9	1	Au	5.1	Au	1.35	3.75

^a Relative to the vacuum level, using the work functions ϕ_2 of metal electrode M_2 . Obtained using estimates of the turn-on voltage V_t from ref 41, with additional data from ref 45. The linear average estimate of E_{LUMO} is 3.1 ± 0.4 eV. If one assumes the experimental value of the intervalence band energy $h\nu_{\text{CT}} = 2.17$ eV,⁴⁵ then $E_{\text{HOMO}} = 5.2 \pm 0.4$ eV.

electron is “pushed” from M_2 onto the LUMO of the molecule):

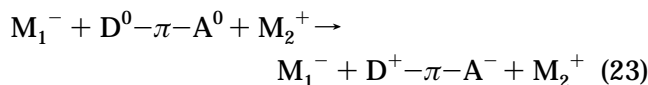


(2) Electron donation from the radical anion to metal M_1 (from the HOMO of the neutral molecule onto M_1), thus generating the low-polarity excited state $D^0 - \pi - A^0$:



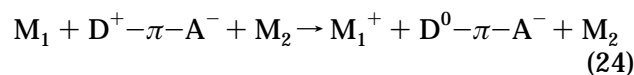
(3) De-excitation of the low-polarity excited state to the ground state $D^+ - \pi - A^-$ either by release of a

photon (IVT) or by radiationless (i.e., vibrational and thermal) de-excitation:

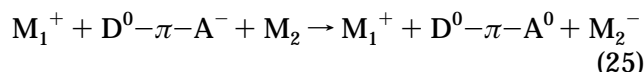


The steps under reverse bias are the following.

(4) Electron donation from metal M_1 to the zwitterion, generating the radical anion $D^0 - \pi - A^-$ (an electron is “pushed” from M_1 onto the LUMO of the molecule):



(5) Electron donation from the radical anion to metal M_2 (from the HOMO of the neutral molecule onto M_2), thus generating the low-polarity excited-state $D^0 - \pi - A^0$:



(6) De-excitation of the low-polarity excited state $D^0 - \pi - A^0$ to the high-polarity ground state $D^+ - \pi - A^-$, either by release of a photon (IVT) or by thermal radiation:

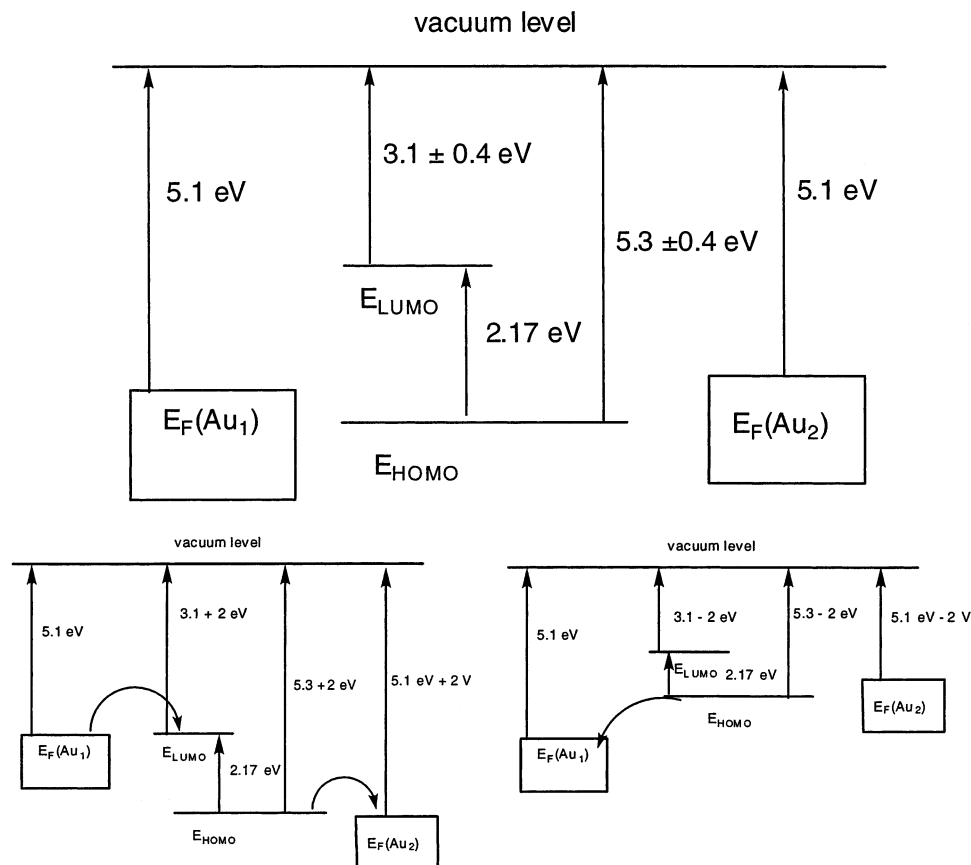
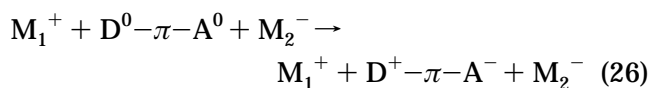


Figure 29. Flat-band energy diagrams for molecule **50** under zero bias between Au electrodes (top), under 2 V positive bias (bottom left) and under -2 V negative bias (bottom right).

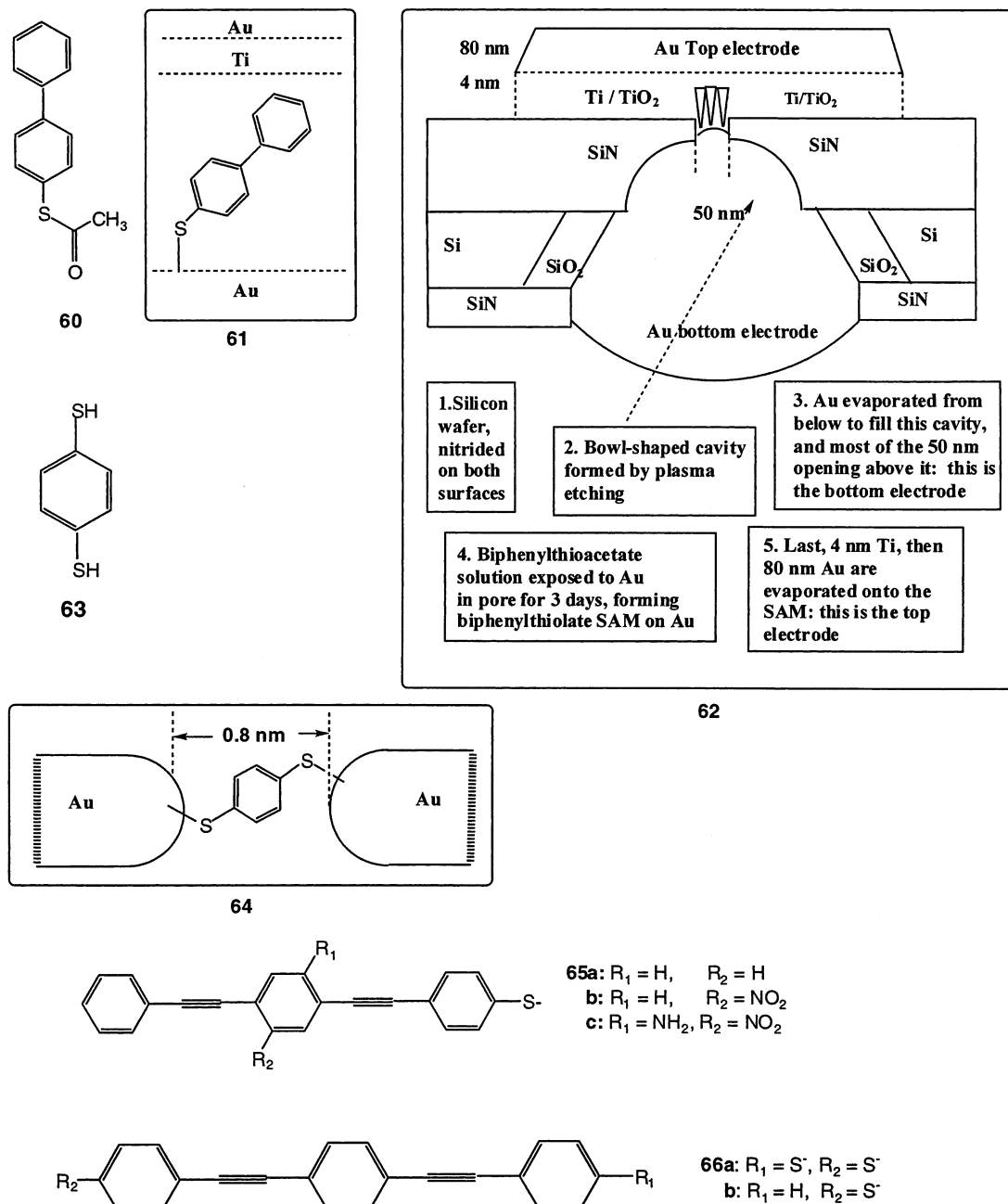


Figure 30. “Four wires”, structures **60**, **63**, **65**, and **66**, studied by Reed and co-workers in nanopore assembly **62** (**61** is the geometry of molecule **60** inside the nanopore assembly **62**), and break junction assembly **64**.

One should establish on theoretical grounds why the forward-bias reaction (eqs 21–23) is more likely than the reverse-bias reaction (eqs 24–26).

As shown in Figures 14 and 15, the observed direction of enhanced electron flow under forward bias^{41,45} is from the “bottom” electrode, closest to the negatively charged dicyanomethide end of the molecule (call it M₂), through the positively charged quinolinium moiety and the alkyl chain, to the “top” Au or Al pad (call this electrode M₁). The LUMO has significant molecular orbital coefficients only on the 3CNQ part of the molecule, and thus can be said to be physically “closer” to M₂ than to M₁, while the HOMO has coefficients spread throughout the aromatic part of the molecule.⁴¹ The alkyl chain places the aromatic chromophore asymmetrically in the gap, closer to M₂ than to M₁. Thus, the preference for eq

22 over eq 25 is due to the greater proximity of the LUMO to electrode M₂ than to electrode M₁. The removal of the electron from the radical anion in eqs 22 or 25 may be of comparable likelihood, since the HOMO is delocalized throughout the aromatic part of the molecule.

Table 5 updates the experimental estimate of the LUMO level,⁴¹ from which one can construct in Figure 29 a flat-band energy diagram for **50**, as an update of Figure 19 of ref 41. Under 2 V positive bias, the electron flow involves both HOMO and LUMO levels (Figure 29, lower left). If the bias is negative (Figure 29, lower right), then only the HOMO can be involved; it can first send one electron to the Au electrode on the left, then an electron can come from the right electrode to reset the molecule. Under reverse bias, the LUMO is too high in energy to get

involved. This qualitative description differs from the one-level description,^{45,102} which placed the LUMO responsible for rectification at 1.32 ± 0.25 eV above the Fermi level of Au, i.e., at 3.78 eV below the vacuum level, if $E_F(\text{Au}) = 5.1$ eV.⁴⁵ The one-level and two-level descriptions of rectification are quite different, and only future work will tell which one is more correct.

23. "Tour Wires": Self-Assembled Monolayer "S" Rectifier

Mark A. Reed at Yale University, James M. Tour at the University of South Carolina and now at Rice University, and their collaborators took thioacetyl-biphenyl, **60**, bonded it covalently to Au (forming biphenylthiolate, **62**, on the Au surface), and placed this self-assembled monolayer in contact with a 4-nm thin Ti electrode, using the elegant nanopore arrangement **61**.²²² What ensued is a dissymmetrical "Au | biphenylthiolate | Ti, TiO₂ | Au" sandwich, for which a very asymmetric current was observed, with a rectification ratio of about 500 at ± 1 V. Most likely, a small Schottky barrier formed at the "Au | molecule" interface, but a much larger Schottky barrier formed at the "molecule | Ti" interface (whose size would also depend on exactly how close the "Ti, TiO₂" layer got to the molecule).²²² This is the first of many studies involving "Tour wires", i.e., molecules with aromatic, alkene, and alkyne bridges, terminated in thiols at one or both ends.

24. Tour Wire: Resistance of a Single Molecule Bound to Two Au Electrodes

Later, a "break junction" technique **64** enabled Reed and co-workers to bond a symmetrical 1,4-benzenedithiol, **63**, to two Au shards, whose distance was carefully controlled by a piezoelectric piston pushing on the Si substrate onto which the Au had been evaporated.²² Here the molecule, dropped from a dilute solution, formed two symmetrical bithiolate bonds to Au (which are partly ionic), with two small but symmetrically opposite Schottky barriers, so no rectification was seen.²² Since the Fermi energy of the substituted benzene is not close to the work function of the Au, the Landauer quantum of resistance was not seen; a much higher resistance of 22 M Ω was measured.²² When more bithiolates bridged the same gap, then the resistance dropped, as expected, to integer submultiples of 22 M Ω , as befits molecular resistances measured in parallel.²²

25. Tour Wires: Negative Differential Resistance

The work on thiolates attached to nanopores similar to **61** took an unexpected turn. When molecule **65a** was used in a "Au | SAM **65a** | Ti, TiO₂ | Au" sandwich, symmetrical I - V curves were seen.²²³ However, when **65c** was used in the same geometry at 60 K, a region of "negative resistance" was seen. At intermediate positive values of V , as V increased, the current decreased, i.e., a negative differential resistance (NDR) device was obtained, with peak-to-

valley ratios of 1030.²²³ For compound **65b**, NDR was seen at 300 K and, more dramatically, at 190 K.²²³

26. Recent Rectifiers Studied Elsewhere

The interest in unimolecular rectification has spread. In a collaboration between the University of Mississippi and Exeter University, Panetta, Sambles, and co-workers studied the D- σ -A molecule **67** (Figure 31), where D is pyrene (a medium donor) and A is dinitrobenzene (a weak acceptor). This molecule was transferred as a Z-type LB multilayer onto an Ag electrode; the top electrode was Mg, overcoated by Ag.²²⁴ A five-layer film of **67** rectifies in the forward direction, with a rectification ratio $RR = 130$ at 2.5 V (i.e., just before breakdown).²²⁴ The forward direction is for facile electron flow from Mg to pyrene (D) to dinitrobenzene (A) to Ag; this direction is opposite to that predicted by the AR model.²²⁴

At Cranfield University, Ashwell and co-workers found that a Z-type LB multilayer of **68** rectified when 100 layers of **68**, co-deposited in a 1:1 ratio with octadecanoic acid, **69**, were placed between Au electrodes. The rectification ratio was about 70 at ± 1 V.²²⁵ When, however, the alkyl "tail" was shortened from octadecyl in **68** to dodecyl in molecule **70**, the relatively longer alkylsulfonate counterion presumably migrated, so that its negative charge moved closer to the dibutylamino end of the molecule, the structure changed from the benzenoid structure akin to **68** to the quinonoid structure in **70**, and the direction of rectification in multilayers reversed;²²⁶ this conclusion was buttressed by monitoring the

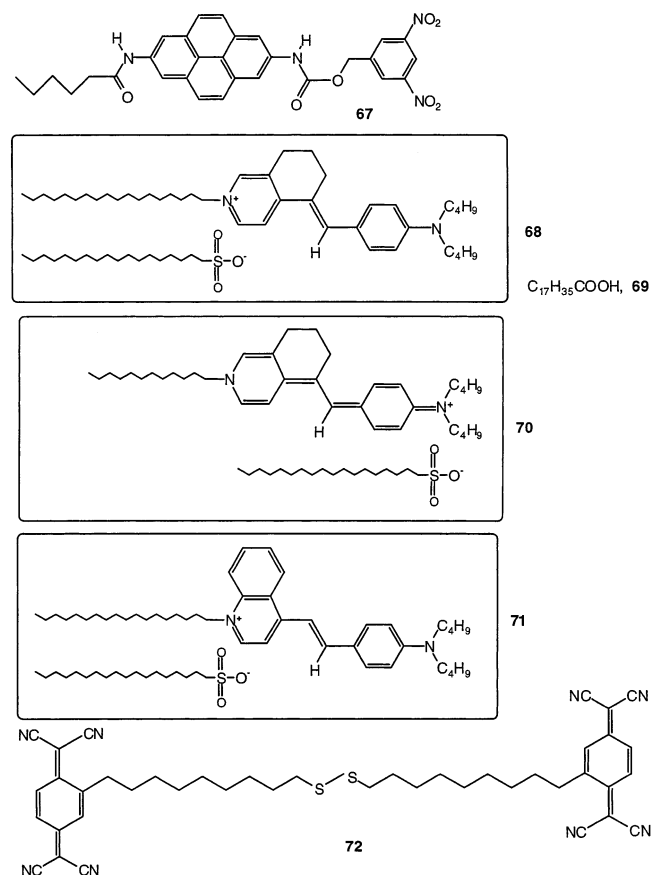


Figure 31. Structures 67–72.

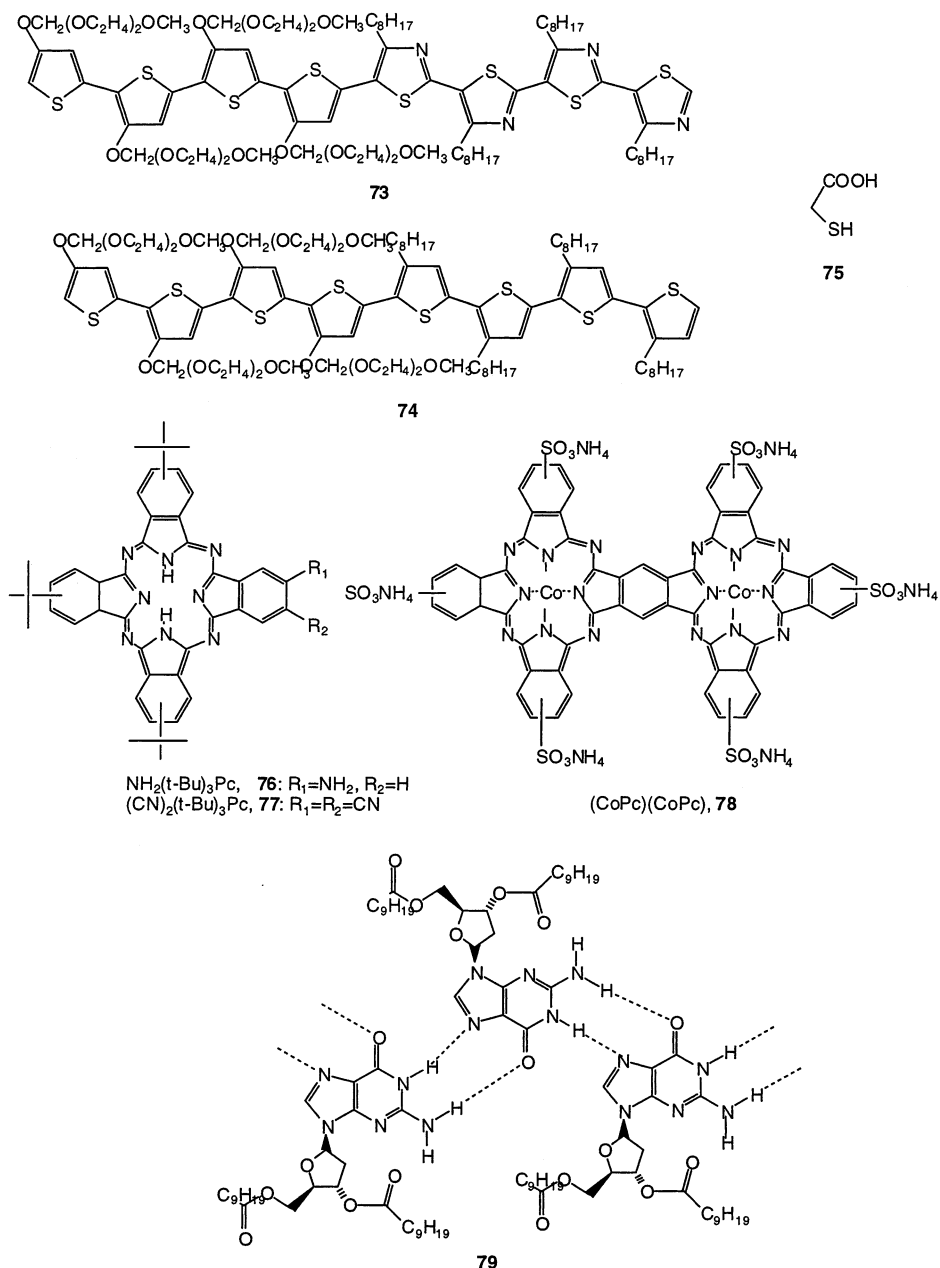


Figure 32. Structures 73–79.

second harmonic generation from the multilayer and also by theoretical calculations.²²⁶ A Z-type LB multilayer of **71** also rectifies when 40 of these layers are placed between two Al electrodes, or between Au electrodes (5 layers).²²⁷

At Harvard University and the University of Ferrara, George Whitesides, Maria Anita Rampi, and their co-workers chemisorbed a SAM of the bisulfide **72** on an Ag electrode, while monolayers of *n*-alkanethiols $n\text{-CH}_3(\text{CH}_2)_p\text{SH}$ of different lengths were attached to a mercury drop electrode.¹⁴⁷ When the two monolayers are brought into contact, the bilayer assembly “Ag | $-\text{S}-(\text{CH}_2)_{10}\text{TCNQ} | \text{CH}_3(\text{CH}_2)_p\text{S} | \text{Hg}$ ”, is formed, and an asymmetric $I-V$ curve is observed (increased electron flow from Ag through the monolayer to the Hg electrode).¹⁴⁷ The magnitude of the current at both positive and negative bias decreases, as expected, as p increases.¹⁴⁷ Since Hg and Ag have about the same work function (4.5 eV), and since

replacing the Ag electrode by an Au electrode makes no change in the observed properties, the asymmetry is not due to differences in the work functions of the two electrodes.¹⁴⁷ The rectification may be caused by an asymmetric placement of the chromophore in the gap,¹⁰⁴ but, surprisingly, the rectification ratio at ± 1 V decreases with increasing alkanethiol chain length: $\text{RR} = 15 \pm 3$ for $p = 11$, $\text{RR} = 9 \pm 2$ for $p = 15$, and $\text{RR} = 4.0 \pm 0.8$ for $p = 17$;¹⁴⁷ i.e., RR decreases with increasing asymmetry by about a factor of 2 per methylene unit added.¹⁴⁷

At the University of Chicago, Luping Yu and co-worker found, by STS, that a monolayer of **73** (see Figure 32), which contains four electron-donating thiophenes and four electron-accepting thiazoles, rectifies, while a monolayer of **74**, which contains only electron donors, does not.²²⁸ In detail, a hydrophilic Au surface was first covered by a 5-Å-thick layer of thioglycolic acid, **75**, then by a monolayer of **73** (22.5

Å thick) or by a monolayer of **74**. Although no STM images were shown to display the order within the monolayer, the STS curves show a rectification ratio of about 6 or 7.²²⁸ The electron flow under forward bias is from the Pt/Ir atomically sharp tip to the acceptor moiety (tetrathiazole), and from there to the donor moiety (tetrathiophene), and from the donor, through the thioglycolic acid, to the Au substrate.²²⁸

At the Academia Sinica in Beijing, Yunqi Liu, Daoben Zhu, and collaborators transferred a LB seven-layer Z-type multilayer film of the amino-*tert*-butylphthalocyanine, **76**, onto Au, and then covered it by Al. This “hamburger”²²⁹ “Al | 7 LB layers of **76** | Au” had a rectification ratio of 60 at ± 3.2 V.²²⁹ An organic field-effect transistor (Au gate electrode, poly(methyl methacrylate) insulator, seven Z-type LB monolayers of **76**, and Au source and drain electrodes) was also fabricated and tested.²²⁹ An LB seven-layer Z-type film multilayer film of the dicyano-*tert*-butylphthalocyanine, **77**, was transferred onto highly oriented pyrolytic graphite (HOPG) and probed by an atomically sharp W tip. It was shown by STS to rectify; the rectification ratio at ± 1 V was about 4.²³⁰ This rectification is ascribed to an AR transfer of an electron from the Fermi level of graphite to the LUMO of the molecule, and of an electron from the HOMO of the molecule to the Fermi level of W, thus creating an excited state $D^+ - Pc - A^-$, which then decays to the ground state of the molecule $D - Pc - A$. Physical organic chemistry tradition does indeed consider the cyano group as an “acceptor” group²³⁰ and a *tert*-butyl group as a very weak “donor” group, but this interpretation of the STS results²³⁰ is an extremely liberal interpretation of the AR model.

A very elegant STS study at Jilin University, Academia Sinica Beijing, and Northeast Normal University in China dealt with the binuclear phthalocyanine complex CoPc-CoPc, **78**,²³¹ for which an STM image was provided. Both Co X-ray photoelectron spectroscopy (two Co(2p) core peaks) and semi-empirical molecular orbital theory (INDO/S) indicate that the ground state is Co(I)Pc-Co(III)Pc, rather than Co(II)Pc-Co(II)Pc; one can then consider the molecule as $D - B - A$, where Co(I) is the electron donor moiety (D), and Co(III) is the electron acceptor moiety A.²³¹ The molecule stacks edge-on over HOPG.²³¹ A strong STS asymmetry (higher current at negative bias) is ascribed to easier electron flow from the Pt/Ir nanotip to Co(III), to create $D - B - A^-$ [Co(I)Pc-Co(II)Pc]; then the electron moves from the Co(I) site to graphite, creating the excited state $D^+ - B - A^-$ [Co(II)Pc-Co(II)Pc], which then relaxes to the ground state $D - B - A$ [Co(I)Pc-Co(III)Pc] by intramolecular intervalence transfer.²³¹

At the University of Lecce, Roberto Cingolani and collaborators grew a very small crystal of a derivatized deoxyguanosine, **79**, between between two Au electrodes.²³² The hydrogen-bonded network between three molecules is shown in **79**. A definite asymmetry in the $I - V$ curves (measured in the dark) is observed and is ascribed to the alignment of the molecular dipoles along the direction of intermolecular hydrogen bonding.²³²

27. Theory

Several theoretical efforts tried to explain the rectification by **50**. It was first posited that unimolecular rectification by **50** was caused by a twisted internal charge-transfer transition,²¹² but no experimental proof of this was found.⁴¹ It was next suggested that the ground-state conformation of **50** was not zwitterionic;²³³ the experimental evidence that the ground state was a zwitterion, or a betaine, was, however, overwhelming.^{41,46} Theoretical efforts to explain the large experimental dipole moment μ_{GS} in the ground state of **50**⁴¹ were only partially successful,^{41,101} if the phenyl ring is strictly perpendicular to the quinolinium ring (twist angle = 90°), then $\mu_{GS} = 50$ D can be obtained;^{101,212,234} for intermediate twist angles, $\mu_{GS} \approx 25$ D is usually obtained.^{41,234} For the case of only one energy level in the gap dominating the conduction, eq 16 was derived independently by two groups,^{102,153} but, as discussed above, it is not clear at present whether one or two molecular orbitals of the chromophore in the gap must be involved in the rectification. The experimental data can be fitted to eq 16, or to several other simple equations with equal ease.⁴⁵ A theory, using the Landauer approach, explained why a single molecule **50** rectifies between Au electrodes in the experimentally observed direction,¹⁰⁴ but gets the forward current flowing the wrong way for the Al electrode case.¹⁰⁴ If one could center the chromophore in the molecular gap, one would observe unimolecular rectification of the type “U”, with no contribution from “A” rectification.^{104,146}

Electron-transfer rates can be formally connected with electrical currents, and one can distinguish between a fully diabatic, sequential electron-transfer process, applicable when molecule and electrode(s) are weakly coupled, and the adiabatic, coherent, and resonant transfers, which becomes possible when molecule and electrodes are strongly coupled.²³⁴

Most other theoretical work^{233–243} focused on the experiments of Reed and co-workers at Yale University.^{22,222,223} Steady-state Hartree–Fock or Kohn–Sham methods for molecular devices cannot formally include currents traveling through the device,²³⁵ a new formalism circumvented this limitation²³⁵ and recovered the Landauer formula, eq 13.²³

The calculated currents across 1,4-benzenedithiol bonded simultaneously to two Au electrodes were too large,²³⁶ compared with experiment,²² maybe because peculiar energy levels were posited.²³⁶

Whether a “Tour wire” can rectify was studied, using the Landauer formalism and Green’s function techniques, to calculate the current across the ter-(phenylethynyl)bithiolate, **66a**, bonded to two Au electrodes, and across the ter-(phenylethynyl)monothiolate, **65a**, bonded to only one Au electrode, as a function of the distance of **65a** from a second Au electrode.²³⁷ High transmission resonance amplitudes, high conductance, and absence of rectification were seen for **66a**; low transmission amplitudes, low conductance, and rectification were seen for **66b**, and the coupling decreased for **65a** as the nonbonded electrode was moved farther away.²³⁷ This suggests that **65a** is an “A” or an “S” rectifier.

One explanation for NDR in **65c** was that the middle phenyl ring of **65c** can twist in and out of coplanarity with the other two phenyl rings, and that the current is locally higher when the rings are all coplanar.²²⁹ In contrast to this plausible theory, when a monolayer of **65c** on Au is studied by STM,²⁶ the current through some of the molecules increases dramatically, as the longest molecular axis changes tilt, relative to the surface.²⁶ The resultant increase in the STS current was ascribed to a changed coupling of the surface Au 4d orbitals with the thiolate 2p orbitals.²⁶

A different, and maybe more plausible explanation was found in a study of shifting of molecular levels in an electric field. The molecule had five phenyl rings, Ph-C-C-Ph-CH₂CH₂-Ph-CH₂CH₂-Ph-CC-Ph, with the central phenyl ring (underlined) separated from its neighbors by an ethylene linker (tunnel barrier) in an electric field; the two outer phenyl rings were coupled by an acetylenic linker.²⁴³ The field effects were reasonable: about 1 eV energy level shift for a field of 1 GV/m.²⁴³ Four possible channels for resonance were found, but two involving very large wave function amplitudes in the central benzene ring, and reasonable amplitudes in the adjacent benzene rings (LUMO+4 and LUMO+5), were considered the most likely candidates for an NDR peak.²⁴³

28. Challenges for the Near Future

Although unimolecular rectification has been fully confirmed, and discussed in several patents,^{244–247} there are still open questions for the near term.

(1) Can inelastic electron tunneling spectroscopy confirm that the electron really does go through the molecule (instead of tunneling through space)?

(2) How fast is the rectification process?

(3) Can the device be made sturdier, e.g., by anchoring the molecules covalently to both metal electrodes? Will this eliminate the decrease of RR over several cycles of measurement?

(4) What is the role of the metal electrodes during the measuring process? Do they indeed form stalagmites and stalagmites within the monolayer? Can this process be controlled?

(5) Can one merge the complementary advantages of LB methods (better order) and self-assembly methods (sturdier bonds to the metal electrodes)?

(6) Can one investigate optically what occurs during the electrical measurements? Can we “peek” under the monolayer?

(7) What is the role of image dipoles induced in the metal electrodes by the molecular dipole moments in either the ground state or the excited state?

(8) Can rectifiers and bridges and strands of conducting polymers be grafted together to form a molecular transistor with power gain?^{248–250}

29. Opinions

The molecular devices discussed here have been measured in two-terminal devices, and therefore cannot exhibit power gain. It is difficult to fabricate three or four metal electrodes with a molecular-size

gap (1–3 nm) between them; if these become possible, then one can conceive of a single molecule that might exhibit power gain.²⁵⁰

The work discussed here has been based rather strongly on molecules which undergo large dipole moment changes as they move between the ground state and the first electronic excited state. This property has also been exploited for nonlinear optics, and this intramolecular electron transfer is also of great interest to artificial photosynthesis. The advantage of such electronic transitions is that they are fast (from picoseconds to nanoseconds), and therefore may be able to compete in speed with Si-based or GaAs-based inorganic components. The disadvantage is that the organic synthesis that links strong donors to strong acceptors is nontrivial, and that, if excitation is accompanied by radiationless decay rather than by photon emission, then much heat will have to be dissipated (a serious problem also for inorganic electronics).

In the quest for electronic devices on the molecular scale, an alternate paradigm has been presented that depends on massively parallel architecture and fault-tolerant or fault-correcting algorithms,²⁵¹ and which may allow much slower translational³⁷ or conformational transitions. Here there are a plethora of chemical possibilities and fewer synthetic nightmares, and heat dissipation is much less problematic. Mother Nature of course, over billions of years, has pursued this slower course and learned how to over-wire the human brain.

The next few years of hard work may decide which course of action will lead faster to molecular computers.

30. Conclusion

We have presented here a review of unimolecular rectification, which, a quarter century after it was first proposed, has now become an established reality. May this progress guide all of us to many new ideas for molecular devices to power the ultimate computers of the future.

31. Acknowledgments

This work was generously supported by the United States National Science Foundation (grants NSF-DMR-FRG-00-95215 and DMR-00-99674) and was made possible by the help, the ideas, the patience, and the friendship of many colleagues, students, and postdoctoral fellows.

32. References

- (1) Metzger, R. M. *NATO ASI Ser.* **1991**, B248, 659.
- (2) Feynman, R. P. In *Miniaturization*; Gilbert, H. D., Ed.; Reinhold: New York, 1961; p 282 (see also <http://www.zyvex.com/nanotech/feynman.html>).
- (3) Aviram, A.; Ratner, M. A. *Chem. Phys. Lett.* **1974**, 29, 277.
- (4) Carter, F. L., Ed. *Molecular Electronic Devices*; Dekker: New York, 1982.
- (5) Carter, F. L., Ed. *Molecular Electronic Devices II*; Dekker: New York, 1987.
- (6) Carter, F. L.; Siatkowski, R. E.; Wohltjen, H., Eds. *Molecular Electronic Devices, Proceedings of the 3rd International Symposium*; North-Holland: Amsterdam, 1988.
- (7) Taube, H. *Angew. Chem., Int. Ed. Engl.* **1984**, 23, 329.

- (8) Balzani, V.; Scandola, F. *Supramolecular Photochemistry*; Ellis Harwood: New York, 1991.
- (9) Balzani, V., Ed. *Electron Transfer in Chemistry*; Wiley-VCH: New York, 2001; Vols. 1–5.
- (10) Ratner, M. A.; Jortner, J. In *Molecular Electronics*; Jortner, J., Ratner, M., Eds.; Blackwell Science: Oxford, UK, 1997; pp 5–72.
- (11) Lehn, J.-M. *Supramolecular Chemistry: Concepts and Perspectives*; VCH: Weinheim, Germany, 1995.
- (12) Roco, M. C.; Williams, R. S.; Alivisatos, P., Eds. *Nanotechnology Research Directions—Vision for Nanotechnology R&D in the Next Decade*; Kluwer: Dordrecht, The Netherlands, 2000.
- (13) Prasad, P. N.; Williams, D. J. *Introduction to Nonlinear Optical Effects in Molecules and Polymers*; Wiley-Interscience: New York, 1991.
- (14) Nakamura, S.; Mukai, T.; Sengh, M. *Appl. Phys. Lett.* **1994**, *64*, 1687.
- (15) Nakamura, S.; Fasol, G. *The Blue Laser Diode—GaN based Light Emitters and Lasers*; Springer: Heidelberg, Germany, 1997.
- (16) Blodgett, K. B. *J. Am. Chem. Soc.* **1935**, *57*, 1007.
- (17) Blodgett, K. B.; Langmuir, I. *Phys. Rev.* **1937**, *51*, 964.
- (18) Bigelow, W. C.; Pickett, D. L.; Zisman, W. A. *J. Colloid Sci.* **1946**, *1*, 513.
- (19) Moore, G. E. *Electronics* **1965**, *38* (8), 114.
- (20) International Technology Roadmap for Semiconductors, 2001 (<http://public.itrs.net/Files/2001ITRS/Home.htm>).
- (21) Bumm, L. A.; Arnold, J. J.; Cygan, M. T.; Dunbar, T. D.; Burgin, T. P.; Jones, L. H.; Allara, D. L.; Tour, J. M.; Weiss, P. S. *Science* **1996**, *271*, 1705.
- (22) Reed, M. A.; Zhou, C.; Muller, C. J.; Burgin, T. P.; Tour, J. M. *Science* **1997**, *278*, 252.
- (23) Landauer, R. *IBM J. Res. Dev.* **1957**, *1*, 223.
- (24) Reichert, J.; Ochs, R.; Beckmann, D.; Weber, H. B.; Mayor, M.; v. Löhneysen, H. *Phys. Rev. Lett.* **2002**, *88*, 176804.
- (25) Chen, J.; Reed, M. A.; Rawlett, A. M.; Tour, J. M. *Science* **1999**, *286*, 1550.
- (26) Donhauser, Z. J.; Mantooth, B. A.; Kelly, K. F.; Bumm, L. A.; Monnell, J. D.; Stapleton, J. J.; Price, D. W., Jr.; Rawlett, A. M.; Allara, D. L.; Tour, J. M.; Weiss, P. S. *Science* **2001**, *292*, 2303.
- (27) Reed, M. A.; Chen, J.; Rawlett, A. M.; Price, D. W.; Tour, J. M. *Appl. Phys. Lett.* **2001**, *78*, 3735.
- (28) Frank, S.; Poncharal, P.; Wang, Z. L.; de Heer, W. A. *Science* **1999**, *280*, 1744.
- (29) Tans, S. J.; Devoret, M. H.; Dai, H.; Thess, A.; Smalley, R. E.; Geerligs, L. J.; Dekker, C. *Nature* **1997**, *386*, 474.
- (30) Postma, H. W. Ch.; Teepe, T.; Yao, Z.; Grifoni, M.; Dekker, C. *Science* **2001**, *293*, 76.
- (31) Derycke, V.; Martel, R.; Appenzeller, J.; Avouris, Ph. *Nano Lett.* **2001**, *1*, 453.
- (32) Bachtold, A.; Hadley, P.; Nakanishi, T.; Dekker, C. *Science* **2001**, *294*, 1317.
- (33) Paloheimo, J.; Kuivalainen, P.; Stubb, H.; Vuorimaa, E.; Yli-Lahti, P. *Phys. Lett.* **1990**, *56*, 1157.
- (34) Garnier, F.; Horowitz, G.; Peng, X.; Fichou, D. *Adv. Mater.* **1990**, *2*, 592.
- (35) Turner-Jones, E. T.; Chyan, O. M.; Wrighton, M. S. *J. Am. Chem. Soc.* **1987**, *109*, 5526.
- (36) Schön, J. H.; Meng, H.; Bao, Z. *Nature* **2001**, *413*, 713.
- (37) Collier, C. P.; Mattern, D. L.; Wong, E. W.; Beverly, K.; Sampaio, J.; Raymo, F. M.; Stoddart, J. F.; Heath, J. R. *Science* **2000**, *289*, 1172.
- (38) Park, J.; Pasupathy, A. N.; Goldsmith, J. I.; Chang, C.; Yaish, Y.; Petta, J. R.; Rinkoski, M.; Sethna, J. P.; Abruña, H. D.; McEuen, P. L.; Ralph, D. C. *Nature* **2002**, *417*, 722.
- (39) Ashwell, G. J.; Sambles, J. R.; Martin, A. S.; Parker, W. G.; Szablewski, M. *J. Chem. Soc., Chem. Commun.* **1990**, 1374.
- (40) Martin, A. S.; Sambles, J. R.; Ashwell, G. J. *Phys. Rev. Lett.* **1993**, *70*, 218.
- (41) Metzger, R. M.; Chen, B.; Höpfner, U.; Lakshminantham, M. V.; Vuillaume, D.; Kawai, T.; Wu, X.; Tachibana, H.; Hughes, T. V.; Sakurai, H.; Baldwin, J. W.; Hosch, C.; Cava, M. P.; Brehmer, L.; Ashwell, G. J. *J. Am. Chem. Soc.* **1997**, *119*, 10455.
- (42) Vuillaume, D.; Chen, B.; Metzger, R. M. *Langmuir* **1999**, *15*, 4011.
- (43) Chen, B.; Metzger, R. M. *J. Phys. Chem. B* **1999**, *103*, 4447.
- (44) Xu, T.; Peterson, I. R.; Lakshminantham, M. V.; Metzger, R. M. *Angew. Chem., Intl. Ed.* **2001**, *40*, 1749.
- (45) Metzger, R. M.; Xu, T.; Peterson, I. R. *J. Phys. Chem. B* **2001**, *105*, 7280.
- (46) Baldwin, J. W.; Chen, B.; Street, S. C.; Konovalov, V. V.; Sakurai, H.; Hughes, T. V.; Simpson, C. S.; Lakshminantham, M. V.; Cava, M. P.; Kispert, L. D.; Metzger, R. M. *J. Phys. Chem. B* **1999**, *103*, 4269.
- (47) Baldwin, J. W.; Amaresh, R. R.; Peterson, I. R.; Shumate, W. J.; Cava, M. P.; Amiri, M. A.; Hamilton, R.; Ashwell, G. J.; Metzger, R. M. *J. Phys. Chem. B* **2002**, *106*, 12158.
- (48) Metzger, R. M.; Baldwin, J. W.; Shumate, W. J.; Peterson, I. R.; Mani, P.; Mankey, G. J.; Morris, T.; Szulcowski, G.; Bosi, S.; Prato, M.; Comito, A.; Rubin, Y. *J. Phys. Chem. B* **2003**, *107*, 1021.
- (49) Metzger, R. M.; Panetta, C. A. *J. Phys. (Paris)* **1983**, *44* (Colloque C3), 1605.
- (50) Metzger, R. M.; Panetta, C. A. In *Molecular Electronic Devices*; Carter, F. L., Ed.; Dekker: New York, 1987; Vol. II, pp 5–25.
- (51) Metzger, R. M.; Panetta, C. A.; Miura, Y.; Torres, E. *Synth. Met.* **1987**, *18*, 797.
- (52) Metzger, R. M.; Panetta, C. A. In *Proceedings of the Eighth Winter Meeting on Low-Temperature Physics*; Heiras, J. L., Akachi, T., Eds.; UNAM: Mexico City, 1987; pp 81–100.
- (53) Metzger, R. M.; Panetta, C. A. *NATO ASI Ser.* **1988**, *B168*, 271.
- (54) Metzger, R. M.; Panetta, C. A. *J. Mol. Electron.* **1989**, *5*, 1.
- (55) Metzger, R. M.; Panetta, C. A. *J. Chim. Phys.* **1988**, *85*, 1125.
- (56) Metzger, R. M.; Panetta, C. A. *Synth. Met.* **1989**, *28*, C807.
- (57) Metzger, R. M.; Panetta, C. A. In *Molecular Electronics—Science and Technology*; Aviram, A., Ed.; New York Engineering Foundation: New York, 1990; pp 293–300.
- (58) Metzger, R. M.; Panetta, C. A. *NATO ASI Ser.* **1991**, *B248*, 611.
- (59) Metzger, R. M.; Panetta, C. A. *Mater. Res. Soc. Symp. Proc. Ser.* **1990**, *210*, 531.
- (60) Metzger, R. M.; Panetta, C. A. *New J. Chem.* **1991**, *15*, 209.
- (61) Metzger, R. M.; Panetta, C. A. *NATO ASI Ser.* **1991**, *B253*, 779.
- (62) Metzger, R. M. *Am. Inst. Phys. Conf. Proc.* **1992**, *262*, 85.
- (63) Metzger, R. M. In *Electricity and Magnetism in Biology and Medicine*; Blank, M., Ed.; San Francisco Press: San Francisco, 1993; pp 175–178.
- (64) Metzger, R. M. *Am. Chem. Soc. Adv. Chem. Ser.* **1994**, *240*, 81–129.
- (65) Metzger, R. M. *Mater. Sci. Eng.* **1995**, *C3*, 277–285.
- (66) Metzger, R. M. In *Hyper-Structured Molecules I: Chemistry, Physics, and Applications*; Sasabe, H., Ed.; Gordon & Breach: Amsterdam, 1999; pp 19–33.
- (67) Metzger, R. M.; Cava, M. P. *Ann. N.Y. Acad. Sci.* **1998**, *852*, 95.
- (68) Metzger, R. M. *Adv. Mater. Opt. Electron.* **1998**, *8*, 229.
- (69) Metzger, R. M. *Mol. Cryst. Liq. Cryst. Sci. Technol.* **1999**, *A337*, 37.
- (70) Metzger, R. M. *J. Mater. Chem.* **1999**, *9*, 2027.
- (71) Metzger, R. M. *J. Mater. Chem.* **2000**, *10*, 55.
- (72) Metzger, R. M. *Synth. Met.* **2000**, *109*, 23.
- (73) Metzger, R. M. *Acc. Chem. Res.* **1999**, *32*, 950.
- (74) Metzger, R. M.; Chen, B.; Baldwin, J. W. *Am. Chem. Soc. Symp. Proc.* **2001**, *798*, 50.
- (75) Metzger, R. M. *Mater. Res. Soc. Symp. Proc.* **2000**, *582*, H12.2.
- (76) Metzger, R. M. *Adv. Mater. Opt. Electron.* **1999**, *9*, 253.
- (77) Metzger, R. M. *Synth. Met.* **2001**, *124*, 107.
- (78) Panetta, C. A.; Baghdadchi, J.; Metzger, R. M. *Mol. Cryst. Liq. Cryst.* **1984**, *107*, 103.
- (79) Metzger, R. M.; Panetta, C. A.; Heimer, N. E.; Bhatti, A. M.; Torres, E.; Blackburn, G. F.; Tripathy, S. K.; Samuelson, L. A. *J. Mol. Electron.* **1986**, *2*, 119.
- (80) Metzger, R. M.; Schumaker, R. R.; Cava, M. P.; Laidlaw, R. K.; Panetta, C. A.; Torres, E. *Langmuir* **1988**, *4*, 298.
- (81) Torres, E.; Panetta, C. A.; Metzger, R. M. *J. Org. Chem.* **1987**, *52*, 2944.
- (82) Laidlaw, R. K.; Miura, Y.; Grant, J. L.; Cooray, L.; Clark, M.; Kispert, L. D.; Metzger, R. M. *J. Chem. Phys.* **1987**, *87*, 4967.
- (83) Miura, Y.; Torres, E.; Panetta, C. A.; Metzger, R. M. *J. Org. Chem.* **1988**, *53*, 439.
- (84) Miura, Y.; Laidlaw, R. K.; Panetta, C. A.; Metzger, R. M. *Acta Crystallogr.* **1988**, *C44*, 2007.
- (85) Laidlaw, R. K.; Miura, Y.; Panetta, C. A.; Metzger, R. M. *Acta Crystallogr.* **1988**, *C44*, 2009.
- (86) Laidlaw, R. K.; Baghdadchi, J.; Panetta, C. A.; Miura, Y.; Torres, E.; Metzger, R. M. *Acta Crystallogr.* **1988**, *B44*, 645.
- (87) Miura, Y.; Panetta, C. A.; Metzger, R. M. *J. Liq. Chromatogr.* **1988**, *11*, 245.
- (88) Metzger, R. M.; Laidlaw, R. K.; Torres, E.; Panetta, C. A. *J. Cryst. Spectrosc. Res.* **1989**, *19*, 475.
- (89) Metzger, R. M.; Wiser, D. C.; Laidlaw, R. K.; Takassi, M. A.; Mattern, D. L.; Panetta, C. A. *Langmuir* **1990**, *6*, 350.
- (90) Metzger, R. M.; Panetta, C. A. *Synth. Met.* **1991**, *42*, 1407.
- (91) Panetta, C. A.; Heimer, N. E.; Hussey, C. L.; Metzger, R. M. *Synlett* **1991**, 301.
- (92) Wu, X.-L.; Shamsuzzoha, M.; Metzger, R. M.; Ashwell, G. J. *Synth. Met.* **1993**, *57*, 3836.
- (93) Wang, P.; Singleton, J. L.; Wu, X.-L.; Shamsuzzoha, M.; Metzger, R. M.; Panetta, C. A.; Heimer, N. E. *Synth. Met.* **1993**, *57*, 3824.
- (94) Nadizadeh, H.; Mattern, D. L.; Singleton, J.; Wu, X.-L.; Metzger, R. M. *Chem. Mater.* **1994**, *6*, 268.
- (95) Metzger, R. M.; Tachibana, H.; Wu, X.; Höpfner, U.; Chen, B.; Lakshminantham, M. V.; Cava, M. P. *Synth. Met.* **1997**, *85*, 1359.
- (96) Scheib, S.; Cava, M. P.; Baldwin, J. W.; Metzger, R. M. *J. Org. Chem.* **1998**, *63*, 1198.
- (97) Metzger, R. M.; Chen, B.; Vuillaume, D.; Höpfner, U.; Baldwin, J. W.; Kawai, T.; Tachibana, H.; Sakurai, H.; Lakshminantham, M. V.; Cava, M. P. *Mater. Res. Soc. Proc.* **1998**, *488*, 335.

- (98) Metzger, R. M.; Chen, B.; Vuillaume, D.; Lakshmikantham, M. V.; Höpfner, U.; Kawai, T.; Baldwin, J. W.; Wu, X.; Tachibana, H.; Sakurai, H.; Cava, M. P. *Thin Solid Films* **1998**, 327–329, 326.
- (99) Scheib, S.; Cava, M. P.; Baldwin, J. W.; Metzger, R. M. *Thin Solid Films* **1998**, 327–329, 100.
- (100) Hughes, T. V.; Mokijewski, B.; Chen, B.; Lakshmikantham, M. V.; Cava, M. P.; Metzger, R. M. *Langmuir* **1999**, 15, 6925.
- (101) Kwon, O.; McKee, M. L.; Metzger, R. M. *Chem. Phys. Lett.* **1999**, 313, 321.
- (102) Peterson, I. R.; Vuillaume, D.; Metzger, R. M. *J. Phys. Chem. A* **2001**, 105, 4702.
- (103) Metzger, R. M. *Mater. Res. Soc. Symp. Proc.* **2001**, 636, D7.8/JJ9.8.1.
- (104) Krzeminski, C.; Delerue, C.; Allan, G.; Vuillaume, D.; Metzger, R. M. *Phys. Rev.* **2001**, B64, 085405.
- (105) Xu, T.; Morris, T. A.; Szulcowski, G. J.; Amaresh, R. R.; Gao, Y.; Street, S. C.; Kispert, L. D.; Metzger, R. M.; Terenziani, F. *J. Phys. Chem. B* **2002**, 106, 10374.
- (106) Roth, S.; Burghard, M.; Fischer, C. M. In *Molecular Electronics*; Jortner, J., Ratner, M., Eds.; Blackwell Science: Oxford, UK, 1997; pp 255–280.
- (107) Roth, S.; Blumentritt, S.; Burghard, M.; Fischer, C. M.; Müller-Schwannecke, C.; Muster, J.; Phillip, G. *NATO ASI Ser.* **1997**, E341, 109.
- (108) Tour, J. M.; Rawlett, A. M.; Kozaki, M.; Yao, Y.; Jagessar, R. C.; Dirk, S. M.; Price, D. W.; Reed, M. A.; Zhou, C.-W.; Chen, J.; Wang, W.; Campbell, I. *Chem. Eur. J.* **2001**, 7, 5118.
- (109) Compton, R. N.; Cooper, C. D. *J. Chem. Phys.* **1977**, 66, 4325.
- (110) Jin, C.; Haufler, R. E.; Hettich, R. L.; Bashick, C. M.; Compton, R. N.; Puzosky, A. A.; Demyanenko, A. V.; Tuinman, A. A. *Science* **1994**, 263, 68.
- (111) Batley, M.; Lyons, L. E. *Mol. Cryst.* **1968**, 3, 357.
- (112) Chen, W.; Cava, M. P.; Takassi, M. A.; Metzger, R. M. *J. Am. Chem. Soc.* **1988**, 110, 7903.
- (113) Gleiter, R.; Schmidt, E.; Cowan, D. O.; Ferraris, J. P. *J. Electron Spectrosc.* **1973**, 2, 207.
- (114) Lichtenberger, D. L.; Johnston, R. L.; Hinkelmann, K.; Suzuki, T.; Wudl, F. *J. Am. Chem. Soc.* **1990**, 112, 3302.
- (115) Pysch, E. S.; Yang, N. C. *J. Am. Chem. Soc.* **1963**, 85, 2155.
- (116) Clar, E.; Robertson, J. M.; Schloegl, R.; Schmidt, W. *J. Am. Chem. Soc.* **1981**, 103, 1320.
- (117) Cooper, C. D.; Naff, W. T.; Compton, R. N. *J. Chem. Phys.* **1975**, 63, 2752.
- (118) Wacks, M. E.; Dibeler, V. H. *J. Chem. Phys.* **1959**, 31, 1557.
- (119) Wacks, M. E. *J. Chem. Phys.* **1964**, 41, 1661.
- (120) Acker, D. S.; Hertler, W. R. *J. Am. Chem. Soc.* **1962**, 84, 3370.
- (121) Kini, A. M.; Cowan, D. O.; Gerson, F.; Möckel, R. *J. Am. Chem. Soc.* **1985**, 107, 556.
- (122) Peover, M. E. *Trans. Faraday Soc.* **1962**, 58, 2370.
- (123) Lyons, L. E.; Palmer, L. D. *Aust. J. Chem.* **1976**, 29, 1919.
- (124) Wheland, R. C.; Gilsson, J. L. *J. Am. Chem. Soc.* **1976**, 98, 3916.
- (125) Emge, T. J.; Maxfield, McR.; Cowan, D. O.; Kistenmacher, T. J. *Mol. Cryst. Liq. Cryst.* **1981**, 65, 161.
- (126) Aumüller, A.; Hünig, S. *Liebigs Ann. Chem.* **1986**, 165.
- (127) By analogy to TCNQ.
- (128) Kuder, J. K.; Pochan, J. M.; Turner, S. R.; Hinman, D. F. *J. Electrochem. Soc.* **1978**, 125, 1750.
- (129) Chen, E. C. M.; Wentworth, W. E. *J. Chem. Phys.* **1975**, 63, 3183.
- (130) Eiggins, B. R. *Chem. Commun.* **1969**, 1267.
- (131) Kebarle, P.; Chowdhury, S. *Chem. Rev.* **1987**, 87, 513.
- (132) Peover, M. E. *J. Chem. Soc.* **1962**, 4540.
- (133) Ashraf, M.; Headridge, J. B. *Talanta* **1969**, 16, 1439.
- (134) Allemand, P. M.; Koch, A.; Wudl, F.; Rubin, Y.; Diederich, F.; Alvarez, M. M.; Anz, S. J.; Whetten, R. L. *J. Am. Chem. Soc.* **1991**, 113, 1050.
- (135) Yang, S. H.; Pettiette, C. L.; Conceicao, J.; Chesnovsky, O.; Smalley, R. E. *Chem. Phys. Lett.* **1987**, 139, 233.
- (136) Marcus, R. A. *J. Chem. Phys.* **1956**, 24, 966.
- (137) Marcus, R. A. *Angew. Chem., Int. Ed. Engl.* **1993**, 32, 1111.
- (138) Marcus, R. A.; Sutin, N. *Biochim. Biophys. Acta* **1985**, 811, 265.
- (139) Hoffmann, R. *Acc. Chem. Res.* **1971**, 4, 1.
- (140) Moser, C. C.; Keske, J. M.; Warncke, K.; Faris, R. S.; Dutton, P. L. *Nature* **1992**, 355, 796.
- (141) McConnell, H. M. *J. Chem. Phys.* **1961**, 35, 508.
- (142) Calcaterra, L. T.; Closs, G. L.; Miller, J. R. *J. Am. Chem. Soc.* **1983**, 105, 670.
- (143) Schottky, W. *Z. Phys.* **1942**, 118, 539.
- (144) Liu, Y.; Xu, Y.; Wu, J.; Zhu, D. *Solid State Commun.* **1995**, 95, 695.
- (145) Liu, Y.; Xu, Y.; Zhu, D. *Synth. Met.* **1997**, 90, 143.
- (146) Mujica, V.; Ratner, M. A.; Nitzan, A. *Chem. Phys.* **2002**, 281, 147.
- (147) Chabincyn, M. L.; Chen, X.; Holmlin, R. E.; Jacobs, H.; Skulason, H.; Frisbie, C. D.; Mujica, V.; Ratner, M. A.; Rampi, M. A.; Whitesides, G. M. *J. Am. Chem. Soc.* **2002**, 124, 11731.
- (148) Roth, S.; Blumentritt, S.; Burghard, M.; Fischer, C. M.; Philipp, G.; Müller-Schwannecke, C. *Synth. Met.* **1997**, 86, 2415.
- (149) Datta, S. *Electronic Transport in Mesoscopic Systems*; Cambridge University Press: Cambridge, UK, 1995.
- (150) Imry, Y.; Landauer, R. *Rev. Mod. Phys.* **1999**, 71, S306.
- (151) de Picciotto, R.; Stormer, H. L.; Pfeiffer, L. N.; Baldwin, K. W.; West, K. W. *Nature* **2001**, 411, 51.
- (152) Stabel, A.; Herwig, P.; Müllen, K.; Rabe, J. P. *Angew. Chem., Int. Ed. Engl.* **1995**, 34, 1609.
- (153) Hall, L. E.; Reimers, J. R.; Hush, N. S.; Silverbrook, K. *J. Chem. Phys.* **2000**, 112, 1510.
- (154) Davis, W. B.; Wasiliewski, M. R.; Ratner, M. A.; Mujica, V.; Nitzan, A. *J. Phys. Chem. A* **1997**, 101, 6158–6164.
- (155) Ohm, G. S. *Die galvanische Kette, Mathematisch Bearbeitet*; T. H. Riemann: Berlin, 1827.
- (156) Binnig, G.; Rohrer, H.; Gerber, Ch.; Weibel, E. *Appl. Phys. Lett.* **1981**, 40, 178.
- (157) Binnig, G.; Quate, C. F.; Berger, C. *Phys. Rev. Lett.* **1986**, 56, 930.
- (158) Wickramasinghe, H. K. Scanned-Probe Microscopes. *Sci. Am.* **1989**, Oct, 98–105.
- (159) Vettiger, P.; Despont, M.; Drechsler, U.; Dürig, U.; Häberle, W.; Lutwyche, M. I.; Rothuizen, H. E.; Stutz, R.; Widmer, R.; Binnig, G. K. *IBM J. Res. Dev.* **2000**, 44, 323.
- (160) Allara, D. L.; Dunbar, T. D.; Weiss, P. S.; Bumm, L. A.; Cygan, M. T.; Tour, J. M.; Reinert, W. A.; Yao, Y.; Kozaki, M.; Jones, L., II. *Ann. N.Y. Acad. Sci.* **1998**, 852, 349.
- (161) Meinhard, J. E. *J. Appl. Phys.* **1964**, 35, 3059.
- (162) Pietro, W. J. *Adv. Mater.* **1994**, 6, 239.
- (163) Hamm, S.; Wachtel, H. *J. Chem. Phys.* **1994**, 103, 10689.
- (164) Polymeropoulos, E. E.; Möbius, D.; Kuhn, H. *Thin Solid Films* **1980**, 68, 173.
- (165) Sugi, M.; Sakai, K.; Saito, M.; Kawabata, Y.; Iizima, S. *Thin Solid Films* **1985**, 132, 69.
- (166) Fischer, C. M.; Burghard, M.; Roth, S.; v. Klitzing, K. *Europhys. Lett.* **1994**, 28, 129.
- (167) Fischer, C. M.; Burghard, M.; Roth, S. *Synth. Met.* **1995**, 71, 1975.
- (168) Schmelzer, M.; Burghard, M.; Fischer, C. M.; Roth, S.; Göpel, W. *Synth. Met.* **1995**, 71, 2087.
- (169) Fischer, C. M.; Burghard, M.; Roth, S. *Synth. Met.* **1996**, 76, 237.
- (170) (a) Fujihira, M.; Nishiyama, K.; Yamada, H. *Thin Solid Films* **1986**, 132, 77. (b) Fujihira, M.; Yamada, H. *Thin Solid Films* **1988**, 160, 125. (c) Fujihira, M.; Sakomura, M. *Thin Solid Films* **1989**, 179, 471. (d) Fujihira, M.; Sakomura, M.; Kamei, T. *Thin Solid Films* **1989**, 180, 43. (e) Fujihira, M. *Mol. Cryst. Liq. Cryst.* **1990**, 183, 59. (f) Sakomura, M.; Fujihira, M. *Thin Solid Films* **1994**, 243, 616. (g) Fujihira, M.; Sakomura, M.; Aoki, D.; Koike, A. *Thin Solid Films* **1996**, 273, 168. (h) Sakomura, M.; Fujihira, M. *Thin Solid Films* **1996**, 273, 181. (i) Sakomura, M.; Fujihira, M. *Chem. Lett.* **1998**, 701. (j) Sakomura, M.; Oono, T.; Fujihira, M. *Thin Solid Films* **1998**, 327–329, 708. (k) Sakomura, M.; Fujihira, M. *Thin Solid Films* **1998**, 327–329, 718. (l) Sakomura, M.; Lin, S.; Moore, T. A.; Moore, A. L.; Gust, D.; Fujihira, M. *J. Phys. Chem. A* **2002**, 106, 2218. (m) Sakomura, M.; Oono, T.; Sakon, R.; Fujihira, M. *Ultramicroscopy* **2002**, 91, 215.
- (171) Choi, J.-W.; Jung, G.-Y.; Oh, S. Y.; Lee, W. H.; Shin, D. M. *Thin Solid Films* **1996**, 284–285, 876.
- (172) Choi, J.-W.; Kim, M. J.; Chung, S. W.; Oh, S. Y.; Lee, W. H.; Shin, D. M. *Mol. Cryst. Liq. Cryst.* **1996**, A280, 367.
- (173) Choi, J.-W.; Kim, M. J.; Chung, S. W.; Oh, S. Y.; Shin, D. M.; Lee, W. H. *Mol. Cryst. Liq. Cryst.* **1997**, A294, 217.
- (174) Choi, J.-W.; Chung, W. S.; Oh, S. Y.; Lee, W. H.; Shin, D. M. *Thin Solid Films* **1998**, 327–329, 671.
- (175) Choi, J.-W.; Nam, Y.-S.; Lee, W.-H.; Kim, D.; Fujihira, M. *Appl. Phys. Lett.* **2001**, 79, 1570.
- (176) Choi, J.-W.; Nam, Y.-S.; Park, S.-J.; Lee, W.-H.; Kim, D.; Fujihira, M. *Biosens. Bioelectron.* **2001**, 16, 819.
- (177) Choi, J.-W.; Nam, Y.-S.; Kong, B.-S.; Lee, W.-H.; Park, K.-M.; Fujihira, M. *J. Biotechnol.* **2002**, 94, 225.
- (178) Sato, Y.; Itoigawa, H.; Uosaki, K. *Bull. Chem. Soc. Jpn.* **1993**, 66, 1032.
- (179) Alleman, K. S.; Weber, K.; Creager, S. E. *J. Phys. Chem.* **1996**, 100, 17050.
- (180) Abuña, H. D.; Denisevich, P.; Umaña, M.; Meyer, T. J.; Murray, R. W. *J. Am. Chem. Soc.* **1981**, 103, 1.
- (181) Denisevich, P.; Willman, K. W.; Murray, R. W. *J. Am. Chem. Soc.* **1981**, 103, 4727.
- (182) Pickup, P. G.; Kutner, W.; Leidner, C. R.; Murray, R. W. *J. Am. Chem. Soc.* **1984**, 106, 1991.
- (183) Chidsey, C. E. D.; Murray, R. W. *Science* **1986**, 231, 25.
- (184) Smith, D. K.; Lane, G. A.; Wrighton, M. S. *J. Am. Chem. Soc.* **1986**, 108, 3522.
- (185) Smith, D. K.; Tender, L. M.; Lane, G. A.; Licht, S.; Wrighton, M. S. *J. Am. Chem. Soc.* **1989**, 111, 1099.
- (186) Palmore, G. T. R.; Smith, D. K.; Wrighton, M. S. *J. Phys. Chem. B* **1997**, 101, 2437.
- (187) Oh, S.-K.; Baker, L. A.; Crooks, R. M. *Langmuir* **2002**, 18, 6981.
- (188) Berchmans, S.; Ramalechume, C.; Lakshmi, V.; Yegnaraman, V. *J. Mater. Chem.* **2002**, 12, 2538.

- (189) Pomerantz, M.; Aviram, A.; McCorkle, R. A.; Li, L.; Aschott, A. G. *Science* **1992**, *255*, 1115.
- (190) Dhirani, A.; Lin, P.-H.; Guyot-Sionnest, P.; Zehner, R. W.; Sita, L. R. *J. Chem. Phys.* **1997**, *106*, 5249.
- (191) (a) Langer, J. J.; Martynski, M. *Synth. Met.* **1999**, *102*, 1160. (b) Langer, J. J.; Martynski, M. *Synth. Met.* **1999**, *107*, 1. (c) Langer, J. J.; Martynski, M. *Adv. Mater. Opt. Electron* **1999**, *9*, 15.
- (192) Baghdadchi, J.; Panetta, C. A. *J. Org. Chem.* **1983**, *48*, 3852.
- (193) Hertler, W. R. *J. Org. Chem.* **1976**, *41*, 1412.
- (194) Heimer, N. E. Unpublished results.
- (195) Torres, E.; Heimer, N. E.; Clark, B. J.; Hussey, C. L. *J. Org. Chem.* **1991**, *56*, 3737.
- (196) Aviram, A.; Joachim, C.; Pomerantz, M. *Chem. Phys. Lett.* **1988**, *146*, 490.
- (197) Aviram, A.; Joachim, C.; Pomerantz, M. *Chem. Phys. Lett.* **1989**, *160*, 469.
- (198) Aumüller, A.; Hünig, S. *Angew. Chem., Int. Ed. Engl.* **1984**, *23*, 447.
- (199) Aumüller, A.; Hünig, S. *Liebigs Ann. Chem.* **1986**, 142.
- (200) Hussey, C. L.; Baghdadchi, J.; Panetta, C. A.; Metzger, R. M. Unpublished results.
- (201) Mann, B.; Kuhn, H. *J. Appl. Phys.* **1971**, *42*, 4398.
- (202) Handy, R. M.; Scala, L. C. *J. Electrochem. Soc.* **1966**, *113*, 109.
- (203) Tredgold, R. H.; Vickers, A. J.; Allen, R. A. *J. Phys.* **1984**, *D17*, L5.
- (204) Roberts, G. G.; Vincett, P. S.; Barlow, W. A. *J. Phys.* **1978**, *C11*, 2077.
- (205) Geddes, N. J.; Sambles, J. R.; Jarvis, D. J.; Parker, W. G.; Sandman, D. J. *Appl. Phys. Lett.* **1990**, *56*, 1916.
- (206) Geddes, N. J.; Sambles, J. R.; Jarvis, D. J.; Parker, W. G.; Sandman, D. J. *J. Appl. Phys.* **1992**, *71*, 756.
- (207) Bell, N. A.; Broughton, R. A.; Brooks, J. S.; Jones, T. A.; Thorpe, S. C.; Ashwell, G. J. *J. Chem. Soc., Chem. Commun.* **1990**, 325.
- (208) Metzger, R. M.; Heimer, N. E.; Ashwell, G. J. *Mol. Cryst. Liq. Cryst.* **1984**, *107*, 133.
- (209) Saito, G.; Chong, C.-H.; Makihara, M.; Otsuka, A.; Yamochi, H. *J. Am. Chem. Soc.* **2003**, *125*, 1134.
- (210) Ashwell, G. J.; Paxton, G. A. N. *Aust. J. Chem.* **2002**, *55*, 199.
- (211) Reichardt, C. *Solvents and Solvent Effects in Organic Chemistry*, 2nd ed.; VCH: Weinheim, Germany, 1990.
- (212) Broo, A.; Zerner, M. C. *Chem. Phys.* **1996**, *196*, 423.
- (213) Ashwell, G. J.; Jeffries, G.; Dawnay, E. J. C.; Kuczynski, A. P.; Lynch, D. E.; Yu, G.; Bucknall, D. G. *J. Mater. Chem.* **1995**, *5*, 975.
- (214) Vuillaume, D. Private communication.
- (215) Lakshminantham, M. V.; Baldwin, J. W. Unpublished results.
- (216) Jaiswal, A.; Amaresh, R. R.; Lakshminantham, M. V.; Honciuc, A.; Cava, M. P.; Metzger, R. M. *Langmuir*, in press.
- (217) Ashwell, G. J. In *Organic Materials for Nonlinear Optics*; Ashwell, G. J., Bloor, D., Eds.; Royal Society of Chemistry: Cambridge, 1993; p 31.
- (218) Fujitsuka, M.; Ito, O.; Metzger, R. M. Unpublished results.
- (219) Okazaki, N.; Sambles, J. R. In *Extended Abstracts of the International Symposium on Organic Molecular Electronics*, Nagoya, Japan, 2000; pp 66–67.
- (220) Okazaki, N.; Sambles, J. R.; Jory, M. J.; Ashwell, G. J. *Appl. Phys. Lett.* **2002**, *81*, 2300.
- (221) (a) Philipp, G.; Müller-Schwanneke, C.; Burghard, M.; Roth, S.; v. Klitzing, K. *J. Appl. Phys.* **1999**, *85*, 3374. (b) Xu, T.; Morris, T. A.; Szulcowski, G. J.; Metzger, R. M.; Szablewski, M. *J. Mater. Chem.* **2002**, *12*, 3167.
- (222) Zhou, C.; Deshpande, M. R.; Reed, M. A.; Jones, L., II; Tour, J. M. *Appl. Phys. Lett.* **1997**, *71*, 611.
- (223) Chen, J.; Wang, J. W.; Reed, M. A.; Rawlett, A. M.; Price, D. W.; Tour, J. M. *Appl. Phys. Lett.* **2000**, *77*, 1224.
- (224) Brady, A. C.; Hodder, B.; Martin, A. S.; Sambles, J. R.; Ewels, C. P.; Jones, R.; Briddon, P. R.; Musa, A. M.; Panetta, C. A.; Mattern, D. L. *J. Mater. Chem.* **1999**, *9*, 2271.
- (225) Ashwell, G. J.; Gandolfo, D. S. *J. Mater. Chem.* **2001**, *11*, 246.
- (226) Ashwell, G. J.; Gandolfo, D. S. *J. Mater. Chem.* **2002**, *12*, 411.
- (227) Ashwell, G. J.; Gandolfo, D. S.; Hamilton, R. *J. Mater. Chem.* **2002**, *12*, 416.
- (228) (a) Ng, M.-K.; Yu, L. *Angew. Chem., Int. Ed.* **2002**, *41*, 3598. (b) Ng, M.-K.; Lee, D.-C.; Yu, L. *J. Am. Chem. Soc.* **2002**, *124*, 11862.
- (229) Hu, W.; Liu, Y.; Xu, Y.; Liu, S.; Zhou, S.; Zhu, D. *Synth. Met.* **1999**, *104*, 19.
- (230) Zhou, S.; Liu, Y.; Qiu, W.; Xu, Y.; Huang, X.; Li, Y.; Jiang, L.; Zhu, D. *Adv. Funct. Mater.* **2002**, *12*, 65.
- (231) Zhang, Y. J.; Li, Y.; Liu, Q.; Jin, J.; Ding, B.; Song, Y.; Jiang, L.; Du, X.; Zhao, Y.; Li, T. *J. Synth. Met.* **2002**, *128*, 43.
- (232) Cingolani, R.; Rinaldi, R.; Maruccio, G.; Biasco, A. *Physica* **2002**, *E13*, 1229.
- (233) Pickholz, M.; dos Santos, M. C. *J. Mol. Struct. (THEOCHEM)* **1998**, *432*, 89.
- (234) Kuznetsov, A. M.; Ulstrup, J. *J. Chem. Phys.* **2002**, *116*, 2149.
- (235) Kosov, D. S. *J. Chem. Phys.* **2002**, *116*, 6368.
- (236) Emberly, E. G.; Kirczenow, G. *Phys. Rev.* **2001**, *B64*, 235412.
- (237) Taylor, J.; Brandbyge, M.; Stokbro, K. *Phys. Rev. Lett.* **2002**, *89*, 138301.
- (238) Seminario, J. M.; Zacarias, A. G.; Tour, J. M. *J. Am. Chem. Soc.* **2000**, *122*, 3015.
- (239) Nitzan, A. *J. Phys. Chem.* **2001**, *A105*, 2677.
- (240) Majumder, C.; Biere, T.; Mizuseki, H.; Kawazoe, Y. *J. Chem. Phys.* **2002**, *117*, 7669.
- (241) Majumder, C.; Biere, T.; Mizuseki, H.; Kawazoe, Y. *J. Phys. Chem. A* **2002**, *106*, 7911.
- (242) Pati, R.; Karna, S. P. *J. Chem. Phys.* **2001**, *115*, 1703.
- (243) Karzaki, Y.; Cornil, J.; Brédas, J. L. *J. Am. Chem. Soc.* **2001**, *123*, 10076.
- (244) Aviram, A.; Freise, M. J.; Seiden, P. E.; Young, W. R. U.S. Patent 3,953,874, April 27, 1976.
- (245) Sandman, D. J.; Geddes, N. J.; Sambles, J. R.; Parker, W. G. U.S. Patent 5,057,878, October 15, 1991.
- (246) Sandman, D. J.; Geddes, N. J.; Sambles, J. R.; Parker, W. G. U.S. Patent 5,152,805, October 6, 1992.
- (247) Metzger, R. M.; Chen, B. U.S. Patent 6,169,291, January 2, 2001.
- (248) Reed, M. A. U.S. Patent 5,475,341, Decemer 12, 1995.
- (249) Ellenbogen, J. C. U.S. Patent 6,339,227, January 15, 2002.
- (250) Metzger, R. M. Submitted to *Nanotechnology*.
- (251) Heath, J. R.; Kuekes, P. J.; Snider, G. S.; Williams, R. S. *Science* **1998**, *280*, 1716.

CR020413D